Jordan Journal of PHYSICS

An International Peer-Reviewed Research Journal

Volume 9, No. 1, 2016, 1437 H

Jordan Journal of Physics (*JJP*): An International Peer-Reviewed Research Journal funded by the Scientific Research Support Fund, Ministry of Higher Education and Scientific Research, Jordan, and published biannually by the Deanship of Research and Graduate Studies, Yarmouk University, Irbid, Jordan.

Manuscripts should be submitted to:

Prof. Nehad M. Tashtoush
Editor-in-Chief, Jordan Journal of Physics
Deanship of Research and Graduate Studies
Yarmouk University-Irbid-Jordan
Tel. 00 962 2 7211111 Ext. 2075
E-mail: *jjp@yu.edu.jo*
Website: *http://Journals.yu.edu.jo/jjp*

Jordan Journal of
PHYSICS
An International Peer-Reviewed Research Journal

Volume 9, No. 1, 2016, 1437 H

The Hashemite Kingdom of Jordan

Yarmouk University

Jordan Journal of PHYSICS

An International Peer-Reviewed Research Journal
Funded by the Scientific Research Support Fund

Volume 9, No. 1, 2016, 1437 H

Instructions to Authors

Instructions to authors concerning manuscript organization and format apply to hardcopy submission by mail, and also to electronic online submission via the Journal homepage website (http://jjp.yu.edu.jo).

Manuscript Submission

1- **E-mail to** : jjp@yu.edu.jo

2- **Online**: Follow the instructions at the journal homepage website.

Original *Research Articles*, *Communications* and *Technical Notes* are subject to critical review by minimum of two competent referees. Authors are encouraged to suggest names of competent reviewers. *Feature Articles* in active Physics research fields, in which the author's own contribution and its relationship to other work in the field constitute the main body of the article, appear as a result of an invitation from the Editorial Board, and will be so designated. The author of a *Feature Article* will be asked to provide a clear, concise and critical status report of the field as an introduction to the article. *Review Articles* on active and rapidly changing Physics research fields will also be published. Authors of *Review Articles* are encouraged to submit two-page proposals to the Editor-in-Chief for approval. Manuscripts submitted in *Arabic* should be accompanied by an Abstract and Keywords in English.

Organization of the Manuscript

Manuscripts should be typed double spaced on one side of A4 sheets (21.6 x 27.9 cm) with 3.71 cm margins, using Microsoft Word 2000 or a later version thereof. The author should adhere to the following order of presentation: Article Title, Author(s), Full Address and E-mail, Abstract, PACS and Keywords, Main Text, Acknowledgment. Only the first letters of words in the Title, Headings and Subheadings are capitalized. Headings should be in **bold** while subheadings in *italic* fonts.

Title Page: Includes the title of the article, authors' first names, middle initials and surnames and affiliations. The affiliation should comprise the department, institution (university or company), city, zip code and state and should be typed as a footnote to the author's name. The name and complete mailing address, telephone and fax numbers, and e-mail address of the author responsible for correspondence (designated with an asterisk) should also be included for official use. The title should be carefully, concisely and clearly constructed to highlight the emphasis and content of the manuscript, which is very important for information retrieval.

Abstract: A one paragraph abstract not exceeding 200 words is required, which should be arranged to highlight the purpose, methods used, results and major findings.

Keywords: A list of 4-6 keywords, which expresses the precise content of the manuscript for indexing purposes, should follow the abstract.

PACS: Authors should supply one or more relevant PACS-2006 classification codes, (available at http://www.aip.org/pacs/pacs06/pacs06-toc.html)

Introduction: Should present the purpose of the submitted work and its relationship to earlier work in the field, but it should not be an extensive review of the literature (e.g., should not exceed 1 ½ typed pages).

Experimental Methods: Should be sufficiently informative to allow competent reproduction of the experimental procedures presented; yet concise enough not to be repetitive of earlier published procedures.

Results: should present the results clearly and concisely.

Discussion: Should be concise and focus on the interpretation of the results.

Conclusion: Should be a brief account of the major findings of the study not exceeding one typed page.

Acknowledgments: Including those for grant and financial support if any, should be typed in one paragraph directly preceding the References.

References: References should be typed double spaced and numbered sequentially in the order in which they are cited in the text. References should be cited in the text by the appropriate Arabic numerals, enclosed in square brackets. Titles of journals are abbreviated according to list of scientific periodicals. The style and punctuation should conform to the following examples:

1. Journal Article:

a) Heisenberg, W., Z. Phys. 49 (1928) 619.
b) Bednorz, J. G. and Müller, K. A., Z. Phys. B64 (1986) 189
c) Bardeen, J., Cooper, L.N. and Schrieffer, J. R., Phys. Rev. 106 (1957) 162.
d) Asad, J. H., Hijjawi, R. S., Sakaji, A. and Khalifeh, J. M., Int. J. Theor. Phys. 44(4) (2005), 3977.

2. Books with Authors, but no Editors:

a) Kittel, C., "Introduction to Solid State Physics", 8^{th} Ed. (John Wiley and Sons, New York, 2005), chapter 16.
b) Chikazumi, S., C. D. Graham, JR, "Physics of Ferromagnetism", 2^{nd} Ed. (Oxford University Press, Oxford, 1997).

3. Books with Authors and Editors:

a) Allen, P. B. "Dynamical Properties of Solids", Ed. (1), G. K. Horton and A. A. Maradudin (North-Holland, Amsterdam, 1980), p137.
b) Chantrell, R. W. and O'Grady, K., "Magnetic Properities of Fine Particles" Eds. J. L. Dormann and D. Fiorani (North-Holland, Amsterdam, 1992), p103.

4. Technical Report:

Purcell, J. "The Superconducting Magnet System for the 12-Foot Bubble Chamber", report ANL/HEP6813, Argonne Natt. Lab., Argonne, III, (1968).

5. Patent:

Bigham, C. B., Schneider, H. R., US patent 3 925 676 (1975).

6. Thesis:

Mahmood, S. H., Ph.D. Thesis, Michigan State University, (1986), USA (Unpublished).

7. Conference or Symposium Proceedings:

Blandin, A. and Lederer, P. Proc. Intern. Conf. on Magnetism, Nottingham (1964), P.71.

8. Internet Source:

Should include authors' names (if any), title, internet website, URL, and date of access.

9. Prepublication online articles (already accepted for publication):

Should include authors' names (if any), title of digital database, database website, URL, and date of access.

For other types of referenced works, provide sufficient information to enable readers to access them.

Tables: Tables should be numbered with Arabic numerals and referred to by number in the Text (e.g., Table 1). Each table should be typed on a separate page with the legend above the table, while explanatory footnotes, which are indicated by superscript lowercase letters, should be typed below the table.

Illustrations: Figures, drawings, diagrams, charts and photographs are to be numbered in a consecutive series of Arabic numerals in the order in which they are cited in the text. Computer-generated illustrations and good-quality digital photographic prints are accepted. They should be black and white originals (not photocopies) provided on separate pages and identified with their corresponding numbers. Actual size graphics should be provided, which need no further manipulation, with lettering (Arial or Helvetica) not smaller than 8 points, lines no thinner than 0.5 point, and each of uniform density. All colors should be removed from graphics except for those graphics to be considered for publication in color. If graphics are to be submitted digitally, they should conform to the following minimum resolution requirements: 1200 dpi for black and white line art, 600 dpi for grayscale art, and 300 dpi for color art. All graphic files must be saved as TIFF images, and all illustrations must be submitted in the actual size at which they should appear in the journal. Note that good quality hardcopy original illustrations are required for both online and mail submissions of manuscripts.

Text Footnotes: The use of text footnotes is to be avoided. When their use is absolutely necessary, they should be typed at the bottom of the page to which they refer, and should be cited in the text by a superscript asterisk or multiples thereof. Place a line above the footnote, so that it is set off from the text.

Supplementary Material: Authors are encouraged to provide all supplementary materials that may facilitate the review process, including any detailed mathematical derivations that may not appear in whole in the manuscript.

Revised Manuscript and Computer Disks

Following the acceptance of a manuscript for publication and the incorporation of all required revisions, authors should submit an original and one more copy of the final disk containing the complete manuscript typed double spaced in Microsoft Word for Windows 2000 or a later version thereof. All graphic files must be saved as PDF, JPG, or TIFF images.

Allen, P.B., "…………….", in: Horton, G.K., and Muradudin, A. A., (eds.), "Dynamical…….", (North……..), pp….

Reprints

Twenty (20) reprints free of charge are provided to the corresponding author. For orders of more reprints, a reprint order form and prices will be sent with the article proofs, which should be returned directly to the Editor for processing.

Copyright

Submission is an admission by the authors that the manuscript has neither been previously published nor is being considered for publication elsewhere. A statement transferring copyright from the authors to Yarmouk University is required before the manuscript can be accepted for publication. The necessary form for such transfer is supplied by the Editor-in-Chief. Reproduction of any part of the contents of a published work is forbidden without a written permission by the Editor-in-Chief.

Disclaimer

Opinions expressed in this Journal are those of the authors and neither necessarily reflects the opinions of the Editorial Board or the University, nor the policy of the Higher Scientific Research Committee or the Ministry of Higher Education and Scientific Research. The publisher shoulders no responsibility or liability whatsoever for the use or misuse of the information published by JJP.

Indexing

JJP is currently applying for indexing and abstracting to all related International Services.

Jordan Journal of
PHYSICS
An International Peer-Reviewed Research Journal

Volume 9, No. 1, 2016, 1437 H

Table of Contents:

Volume 9, Number 1, 2016. pp. 1-30

Jordan Journal of Physics

ARTICLE

About the Cosmological Constant, Acceleration Field, Pressure Field and Energy

Sergey G. Fedosin

Sviazeva Str. 22-79, Perm, 614088, Russia.

Received on: 12/9/2015; Accepted on: 26/11/2015

Abstract: Based on the condition of relativistic energy uniqueness, the calibration of the cosmological constant was performed. This allowed to obtain the corresponding equation for the metric and to determine the generalized momentum, the relativistic energy, momentum and mass of the system, as well as the expressions for the kinetic and potential energies. The scalar curvature at an arbitrary point of the system equaled zero, if the matter is absent at this point; the presence of a gravitational or electromagnetic field is enough for the space-time curvature. Four-potentials of the acceleration field and pressure field, as well as tensor invariants determining the energy density of these fields, were introduced into the Lagrangian in order to describe the system's motion more precisely. The structure of the Lagrangian used is completely symmetrical in form with respect to the four-potentials of gravitational, electromagnetic, acceleration and pressure fields. The stress-energy tensors of the gravitational, acceleration and pressure fields are obtained in explicit form. Each of them can be expressed through the corresponding field vector and additional solenoidal vector. A description of the equations of acceleration and pressure fields is provided.

Keywords: Cosmological constant, Acceleration field, Pressure field, Covariant theory of gravitation.

1. Introduction

The most popular application of the cosmological constant Λ in the general theory of relativity (GTR) is that this quantity represents the manifestation of the vacuum energy [1-2]. There is another approach to the cosmological constant interpretation, according to which this quantity represents the energy possessed by any solitary particle in the absence of external fields. In this case, including Λ into the Lagrangian seems quite appropriate, since the Lagrangian contains such energy components, which should fully describe the properties of any system consisting of particles and fields.

Earlier in [3-4], we used such calibration of the cosmological constant, which allowed to maximally simplify the equation for the metric. The disadvantage of this approach was that the relativistic energy of the system could not be determined uniquely, since the expression for the energy included the scalar curvature. In this paper, we use another universal calibration of the cosmological constant, which is suitable for any particle and system of particles and fields. As a result, the energy is independent of both the scalar curvature and the cosmological constant.

In GTR, the gravitational field as a separate object is not included in the Lagrangian and the role of a field is played by the metric itself. A known problem arising from such an approach is that in GTR there is no stress-energy tensor of the gravitational field.

In contrast, in the covariant theory of gravitation, the Lagrangian is used containing

Corresponding Author: Sergey G. Fedosin **Email**: intelli@list.ru

the term with the energy of the particles in the gravitational field and the term with the energy of the gravitational field as such. Thus, the gravitational field is included in the Lagrangian in the same way as the electromagnetic field. In this case, the metric of the curved spacetime is used to specify the equations of motion as compared to the case of such a weak field, the limit of which is the special theory of relativity. In the weak field limit, a simplified metric is used, which almost does not depend on the coordinates and time. This is enough in many cases, for example, in case of describing the motion of planets. However, generally, in case of strong fields and for studying the subtle effects, the use of metric becomes necessary.

We will note that the term with the particle energy in the Lagrangian can be written in different ways. In [5-6], this term contains the invariant $c\rho_0\sqrt{g_{\mu\nu}u^\mu u^\nu}$, where ρ_0 is the mass density in the co-moving reference frame and u^μ is four-velocity. The corresponding quantity in [7] has the form $\rho_0 c^2$. In [3] and [8], instead of it the product $c\sqrt{g_{\mu\nu}J^\mu J^\nu}$ is used, where J^μ is mass four-current. In this paper, we have chosen another form of the mentioned invariant – in the form $u_\mu J^\mu$. The reason for this choice is the fact that we consider the mass four-current $J^\mu = \rho_0 u^\mu$ to be the fullest representative of the properties of matter particles containing both the mass density and the four-velocity. The mass four-current can be considered as the four-potential of the matter field. All the other four-vectors in the Lagrangian are four-potentials of the respective fields and are written with covariant indices. With the help of these four-potentials, tensor invariants are calculated which characterize the energy of the respective field in the Lagrangian.

Action and its variations in the principle of least action

The action function

We use the following expression as the action function for continuously distributed matter in the gravitational and electromagnetic fields in an arbitrary frame of reference:

$$S=\int L\,dt=\int\begin{pmatrix} k(R-2\Lambda)-\frac{1}{c}D_\mu J^\mu+\frac{c}{16\pi G}\Phi_{\mu\nu}\Phi^{\mu\nu}-\frac{1}{c}A_\mu j^\mu-\frac{c\varepsilon_0}{4}F_{\mu\nu}F^{\mu\nu}- \\ -\frac{1}{c}u_\mu J^\mu-\frac{c}{16\pi\eta}u_{\mu\nu}u^{\mu\nu}-\frac{1}{c}\pi_\mu J^\mu-\frac{c}{16\pi\sigma}f_{\mu\nu}f^{\mu\nu} \end{pmatrix}\sqrt{-g}\,d\Sigma, \qquad (1)$$

where:

L – the Lagrange function or Lagrangian,

dt – the differential of the coordinate time of the used reference frame,

k – a coefficient to be determined,

R – the scalar curvature,

Λ – the cosmological constant,

$J^\mu = \rho_0 u^\mu$ – the four-vector of gravitational (mass) current,

ρ_0 – the mass density in the reference frame associated with the particle,

$u^\mu = \frac{c\,dx^\mu}{ds}$ – the four-velocity of a point particle, dx^μ – four-displacement, ds – interval,

c – the speed of light as a measure of the propagation velocity of electromagnetic and gravitational interactions,

$D_\mu = \left(\frac{\psi}{c}, -\mathbf{D}\right)$ – the four-potential of the gravitational field, described by the scalar potential ψ and the vector potential $\mathbf{D}$ of this field,

G – the gravitational constant,

$\Phi_{\mu\nu} = \nabla_\mu D_\nu - \nabla_\nu D_\mu = \partial_\mu D_\nu - \partial_\nu D_\mu$ – the gravitational tensor (the tensor of gravitational field strengths),

$\Phi^{\alpha\beta} = g^{\alpha\mu} g^{\nu\beta}\Phi_{\mu\nu}$ – definition of the gravitational tensor with contravariant indices by means of the metric tensor $g^{\alpha\mu}$,

$A_\mu = \left(\frac{\varphi}{c}, -\mathbf{A} \right)$ – the four-potential of the electromagnetic field, which is set by the scalar potential φ and the vector potential $\mathbf{A}$ of this field,

$j^\mu = \rho_{0q} u^\mu$ – the four-vector of the electromagnetic (charge) current,

ρ_{0q} – the charge density in the reference frame associated with the particle,

ε_0 – the vacuum permittivity,

$F_{\mu\nu} = \nabla_\mu A_\nu - \nabla_\nu A_\mu = \partial_\mu A_\nu - \partial_\nu A_\mu$ – the electromagnetic tensor (the tensor of electromagnetic field strengths),

$u_\mu = g_{\mu\nu} u^\nu$ – the four-velocity with a covariant index, expressed through the metric tensor and the four-velocity with a contravariant index; it is convenient to consider the covariant four-velocity locally averaged over the particle system as the four-potential of the acceleration field $u_\mu = \left(\frac{\vartheta}{c}, -\mathbf{U} \right)$, where ϑ and $\mathbf{U}$ denote the scalar and vector potentials, respectively,

$u_{\mu\nu} = \nabla_\mu u_\nu - \nabla_\nu u_\mu = \partial_\mu u_\nu - \partial_\nu u_\mu$ – the acceleration tensor calculated through the derivatives of the four-potential of the acceleration field,

η – a function of coordinates and time,

$\pi_\mu = \frac{p_0}{\rho_0 c^2} u_\mu = \left(\frac{\wp}{c}, -\mathbf{\Pi} \right)$ – the four-potential of the pressure field, consisting of the scalar potential $\wp$ and the vector potential $\mathbf{\Pi}$, p_0 is the pressure in the reference frame associated with the particle, the relation $\frac{p_0}{\rho_0 c^2}$ specifies the equation of the matter state,

$f_{\mu\nu} = \nabla_\mu \pi_\nu - \nabla_\nu \pi_\mu = \partial_\mu \pi_\nu - \partial_\nu \pi_\mu$ – the tensor of the pressure field,

σ – a function of coordinates and time,

$\sqrt{-g}\, d\Sigma = \sqrt{-g}\, c\, dt\, dx^1 dx^2 dx^3$ – the invariant four-volume, expressed through the differential of the time coordinate $dx^0 = c\, dt$, through the product $dx^1 dx^2 dx^3$ of differentials of the spatial coordinates and through the square root $\sqrt{-g}$ of the determinant g of the metric tensor, taken with a negative sign.

Action function (1) consists of almost the same terms as those which were considered in [3]. The difference is that now we replace the term with the energy density of particles with four terms located at the end of (1). It is natural to assume that each term is included in (1) relatively independently of the other terms, describing the state of the system in one way or another. The value of the four-potential u_μ of the set of matter units or point particles of the system defines the four-field of the system's velocities, and the product $u_\mu J^\mu$ in (1) can be regarded as the energy of interaction of the mass current J^μ with the field of velocities. Similarly, D_μ is the four-potential of the gravitational field, and the product $D_\mu J^\mu$ defines the energy of interaction of the mass current with the gravitational field. The electromagnetic field is specified by the four-potential A_μ, the source of the field is the electromagnetic current j^μ, and the product of these quantities $A_\mu j^\mu$ is the density of the energy of interaction of a moving charged matter unit with the electromagnetic field. The invariant of the gravitational field in the form of the tensor product $\Phi_{\mu\nu}\Phi^{\mu\nu}$ is associated with the gravitational field energy and cannot be equal to zero even outside bodies. The same holds for the electromagnetic field invariant $F_{\mu\nu}F^{\mu\nu}$. This follows from the properties of long-range action of the specified fields. As for the field of velocities u_μ, the field should be used to describe the motion of the matter particles. Accordingly, the field of accelerations in the form of the tensor $u_{\mu\nu}$ and the energy of this field associated with the invariant $u_{\mu\nu}u^{\mu\nu}$ refer to the accelerated motion of particles and are calculated for those spatial points within the system's volume where the matter is located.

The last two terms in (1) are associated with the pressure in the matter, and the product $\pi_\mu J^\mu$ characterizes the interaction of the pressure field with the mass four-current, and the invariant $f_{\mu\nu} f^{\mu\nu}$ is part of the stress-energy tensor of the pressure field.

We will also note the difference of four-currents J^μ and j^μ – all particles of the system make contribution to the mass current J^μ, and only charged particles make contribution to the electromagnetic current j^μ. This results in difference of the fields' influence – the gravitational field influences any particles and the electromagnetic field influences only the charged particles or the matter, in which by the field can sufficiently divide with its influence the charges of opposite signs from each other. The field of velocities u_μ, as well as the mass current J^μ, are associated with all the particles of the system. Therefore, the product $u_\mu J^\mu$ describes that part of the particles' energy, which stays if we somehow "turn off " in the system under consideration all the macroscopic gravitational and electromagnetic fields and remove the pressure, without changing the field of velocities u_μ or the mass current $J^\mu = \rho_0 u^\mu$.

Variations of the action function

We will vary the action function S in (1) term by term, then the total variation δS will be the sum of variations of individual terms. In total, there are 9 terms inside the integral in (1). If we consider the quantity Λ a constant (a cosmological constant), then according to [7-9] the variation of the first term in the action function (1) is equal to:

$$\delta S_1 = \int \begin{pmatrix} -kR^{\alpha\beta} + \frac{k}{2} R g^{\alpha\beta} - \\ -k\Lambda g^{\alpha\beta} \end{pmatrix} \delta g_{\alpha\beta} \sqrt{-g}\, d\Sigma, \tag{2}$$

where:

$R^{\alpha\beta}$ is the Ricci tensor,

$\delta g_{\alpha\beta}$ is the variation of the metric tensor.

According to [3], the variations of terms 2 and 3 in the action function are as follows:

$$\delta S_2 = \int \begin{pmatrix} -\frac{1}{c} \Phi_{\beta\sigma} J^\sigma \xi^\beta - \frac{1}{c} J^\beta \delta D_\beta \\ -\frac{1}{2c} D_\mu J^\mu g^{\alpha\beta} \delta g_{\alpha\beta} \end{pmatrix} \sqrt{-g}\, d\Sigma, \tag{3}$$

$$\delta S_3 = \int \begin{pmatrix} -\frac{c}{4\pi G} \nabla_\alpha \Phi^{\alpha\beta} \delta D_\beta - \\ -\frac{1}{2c} U^{\alpha\beta} \delta g_{\alpha\beta} \end{pmatrix} \sqrt{-g}\, d\Sigma, \tag{4}$$

where:

ξ^β is the variation of coordinates, which results in the variation of the mass four-current J^μ and in the variation of the electromagnetic four-current j^μ,

δD_β is the variation of the four-potential of the gravitational field,

and $U^{\alpha\beta}$ denotes the stress-energy tensor of the gravitational field:

$$\left.\begin{aligned} U^{\alpha\beta} &= \frac{c^2}{4\pi G} \left(g^{\alpha\nu} \Phi_{\kappa\nu} \Phi^{\kappa\beta} - \frac{1}{4} g^{\alpha\beta} \Phi_{\mu\nu} \Phi^{\mu\nu} \right) \\ &= -\frac{c^2}{4\pi G} \left(\Phi^\alpha{}_\kappa \Phi^{\kappa\beta} + \frac{1}{4} g^{\alpha\beta} \Phi_{\mu\nu} \Phi^{\mu\nu} \right). \end{aligned}\right\} \tag{5}$$

Variations of terms 4 and 5 in the action function according to [6-7] and [10] are as follows:

$$\delta S_4 = \int \begin{pmatrix} -\frac{1}{c} F_{\beta\sigma} j^\sigma \xi^\beta - \frac{1}{c} j^\beta \delta A_\beta \\ -\frac{1}{2c} A_\mu j^\mu g^{\alpha\beta} \delta g_{\alpha\beta} \end{pmatrix} \sqrt{-g}\, d\Sigma, \tag{6}$$

$$\delta S_5 = \int \begin{pmatrix} c\varepsilon_0 \nabla_\alpha F^{\alpha\beta}\, \delta A_\beta - \\ -\frac{1}{2c} W^{\alpha\beta} \delta g_{\alpha\beta} \end{pmatrix} \sqrt{-g}\, d\Sigma, \tag{7}$$

where δA_β is the variation of the four-potential of the electromagnetic field and $W^{\alpha\beta}$ denotes the stress-energy tensor of the electromagnetic field:

$$\left.\begin{aligned} W^{\alpha\beta} &= \varepsilon_0 c^2 \left(-g^{\alpha\nu} F_{\kappa\nu} F^{\kappa\beta} + \frac{1}{4} g^{\alpha\beta} F_{\mu\nu} F^{\mu\nu} \right) \\ &= \varepsilon_0 c^2 \left(F^{\alpha}_{\ \kappa} F^{\kappa\beta} + \frac{1}{4} g^{\alpha\beta} F_{\mu\nu} F^{\mu\nu} \right). \end{aligned}\right\} \tag{8}$$

Variations of the other terms in the action function (1) are defined in Appendices A-D and have the following form:

$$\delta S_6 = \int \begin{pmatrix} -\frac{1}{c} u_{\beta\sigma} J^{\sigma} \xi^{\beta} - \frac{1}{c} J^{\beta} \delta u_{\beta} \\ -\frac{1}{2c} u_{\mu} J^{\mu} g^{\alpha\beta} \delta g_{\alpha\beta} \end{pmatrix} \sqrt{-g}\, d\Sigma, \tag{9}$$

$$\delta S_7 = \int \begin{pmatrix} \frac{c}{4\pi\eta} \nabla_{\alpha} u^{\alpha\beta} \delta u_{\beta} - \\ -\frac{1}{2c} B^{\alpha\beta} \delta g_{\alpha\beta} \end{pmatrix} \sqrt{-g}\, d\Sigma, \tag{10}$$

where δu_{β} is the variation of the four-potential of the acceleration field and $B^{\alpha\beta}$ denotes the stress-energy tensor of the field of accelerations:

$$B^{\alpha\beta} = \frac{c^2}{4\pi\eta} \left(-g^{\alpha\nu} u_{\kappa\nu} u^{\kappa\beta} + \frac{1}{4} g^{\alpha\beta} u_{\mu\nu} u^{\mu\nu} \right). \tag{11}$$

$$\delta S_8 = \int \begin{pmatrix} -\frac{1}{c} f_{\beta\sigma} J^{\sigma} \xi^{\beta} - \frac{1}{c} J^{\beta} \delta \pi_{\beta} \\ -\frac{1}{2c} \pi_{\mu} J^{\mu} g^{\alpha\beta} \delta g_{\alpha\beta} \end{pmatrix} \sqrt{-g}\, d\Sigma. \tag{12}$$

$$\delta S_9 = \int \begin{pmatrix} \frac{c}{4\pi\sigma} \nabla_{\alpha} f^{\alpha\beta} \delta \pi_{\beta} - \\ -\frac{1}{2c} P^{\alpha\beta} \delta g_{\alpha\beta} \end{pmatrix} \sqrt{-g}\, d\Sigma, \tag{13}$$

where the stress-energy tensor of the pressure field is given as:

$$P^{\alpha\beta} = \frac{c^2}{4\pi\sigma} \left(-g^{\alpha\nu} f_{\kappa\nu} f^{\kappa\beta} + \frac{1}{4} g^{\alpha\beta} f_{\mu\nu} f^{\mu\nu} \right). \tag{14}$$

In variation, in order to simplify (10), the special case is considered, when η is a constant, which does not vary by definition. According to its meaning, η depends on the parameters of the system under consideration and can therefore have different values. The same should be said about σ.

The Motion Equations of the Field, Particles and Metric

According to the principle of least action, we should sum up all the variations of the individual terms of the action function and equate the result to zero. The sum of variations (2), (3), (4), (6), (7), (9), (10), (12) and (13) gives the total variation of the action function:

$$\left.\begin{aligned} \delta S &= \delta S_1 + \delta S_2 + \delta S_3 + \delta S_4 + \delta S_5 \\ &+ \delta S_6 + \delta S_7 + \delta S_8 + \delta S_9 = 0. \end{aligned}\right\} \tag{15}$$

The field equations

When the system moves in spacetime, the variations $\delta g_{\alpha\beta}$, ξ^{β}, δD_{β}, δA_{β}, δu_{β} and $\delta \pi_{\beta}$ do not vanish, since it is supposed that they can occur only at the beginning and the end of the process, when the conditions of motion are precisely fixed. Consequently, the sum of the terms, which is located before these variations, should vanish. For example, the variation δA_{β} occurs only in δS_4 according to (6) and in δS_5 from (7), then from (15) it follows that:

$$\int \left(-\frac{1}{c} j^{\beta} + c\varepsilon_0 \nabla_{\alpha} F^{\alpha\beta} \right) \delta A_{\beta} \sqrt{-g}\, d\Sigma = 0.$$

From this, we obtain the equation of the electromagnetic field with the field sources as:

$$\nabla_{\alpha} F^{\alpha\beta} = \frac{1}{c^2 \varepsilon_0} j^{\beta} \quad \text{or} \quad \nabla_{\beta} F^{\alpha\beta} = -\mu_0 j^{\alpha}, \tag{16}$$

where $\mu_0 = \frac{1}{c^2 \varepsilon_0}$ is the vacuum permeability.

The second equation of the electromagnetic field follows from the definition of the electromagnetic tensor in terms of the electromagnetic four-potential and from the antisymmetry properties of this tensor:

$$\nabla_\sigma F_{\mu\nu} + \nabla_\nu F_{\sigma\mu} + \nabla_\mu F_{\nu\sigma} = 0$$

or $\varepsilon^{\alpha\beta\gamma\delta} \nabla_\gamma F_{\alpha\beta} = 0$, (17)

where $\varepsilon^{\alpha\beta\gamma\delta}$ is a Levi-Civita symbol or a completely antisymmetric unit tensor.

The variation δD_β is present only in (3) and (4), so that according to (15) we obtain:

$$\int \left(-\frac{1}{c} J^\beta - \frac{c}{4\pi G} \nabla_\alpha \Phi^{\alpha\beta} \right) \delta D_\beta \sqrt{-g}\, d\Sigma = 0.$$

The equation of gravitational field with the field sources follows from this as:

$$\nabla_\alpha \Phi^{\alpha\beta} = -\frac{4\pi G}{c^2} J^\beta \text{ or } \nabla_\beta \Phi^{\alpha\beta} = \frac{4\pi G}{c^2} J^\alpha . \qquad (18)$$

If we take into account the definition of the gravitational tensor: $\Phi_{\mu\nu} = \nabla_\mu D_\nu - \nabla_\nu D_\mu = \partial_\mu D_\nu - \partial_\nu D_\mu$ and take the covariant derivative of this tensor with subsequent cyclic interchange of the indices, the following equations are solved identically:

$$\nabla_\sigma \Phi_{\mu\nu} + \nabla_\nu \Phi_{\sigma\mu} + \nabla_\mu \Phi_{\nu\sigma} = 0$$

or $\varepsilon^{\alpha\beta\gamma\delta} \nabla_\gamma \Phi_{\alpha\beta} = 0$. (19)

Equation (19) without the sources and equation (18) with the sources define a complete set of gravitational field equations in the covariant theory of gravitation.

Consider now the rule for the difference of the second covariant derivatives with respect to the covariant derivative of the electromagnetic four-potential $\nabla^\alpha A^\beta$:

$$(\nabla_\alpha \nabla_\beta - \nabla_\beta \nabla_\alpha) \nabla^\alpha A^\beta =$$
$$-R^{\alpha}_{\mu,\alpha\beta} \nabla^\mu A^\beta - R^{\beta}_{\mu,\alpha\beta} \nabla^\alpha A^\mu$$
$$= R^{\beta}_{\mu,\alpha\beta} (\nabla^\mu A^\alpha - \nabla^\alpha A^\mu) = -R_{\mu\alpha} F^{\mu\alpha}.$$

With the rule in mind, the application of the covariant derivative ∇_α to (16) and (18) gives the following:

$$\nabla_\alpha \nabla_\beta F^{\alpha\beta} = \nabla_\alpha \nabla_\beta \nabla^\alpha A^\beta - \nabla_\alpha \nabla_\beta \nabla^\beta A^\alpha$$
$$= -R_{\mu\alpha} F^{\mu\alpha} = -\mu_0 \nabla_\alpha j^\alpha.$$

$$R_{\mu\alpha} \Phi^{\mu\alpha} = -\frac{4\pi G}{c^2} \nabla_\alpha J^\alpha .$$

This shows that field tensors $F^{\mu\alpha}$ and $\Phi^{\mu\alpha}$ lead to the divergence of the corresponding four-currents in a curved space-time. Mixed curvature tensor $R^{\beta}_{\mu,\alpha\beta}$ and Ricci tensor $R_{\mu\alpha}$ vanish only in Minkowski space. In this case, the covariant derivatives become the partial derivatives and the continuity equations for the gravitational and electromagnetic four-currents in the special theory of relativity are obtained:

$$\partial_\alpha j^\alpha = 0, \; \partial_\alpha J^\alpha = 0. \qquad (20)$$

We will note that in order to simplify the equations for the four-potential of fields, we can use expressions which are called gauge conditions:

$$\nabla_\beta D^\beta = \nabla^\mu D_\mu = 0, \nabla_\beta A^\beta = \nabla^\mu A_\mu = 0. \qquad (21)$$

The acceleration field equations

The variation of four-potential δu_β is included in (9) and (10). Therefore, according to (15), we obtain:

$$\int \left(-\frac{1}{c} J^\beta + \frac{c}{4\pi\eta} \nabla_\alpha u^{\alpha\beta} \right) \delta u_\beta \sqrt{-g}\, d\Sigma = 0 .$$

$$\nabla_\alpha u^{\alpha\beta} = \frac{4\pi\eta}{c^2} J^\beta \text{, or } \nabla_\beta u^{\alpha\beta} = -\frac{4\pi\eta}{c^2} J^\alpha . \qquad (22)$$

If we compare (18) and (22), it turns out that the presence of the four-vector of mass current J^α not only leads to the occurrence of space-time gradient of the gravitational field in the system under consideration, but also is generally accompanied by changes in time or by four-velocity gradients of the particles that constitute this system. Besides, the covariant four-velocities of the whole set of particles forms the velocity field u_β, the derivatives of which define the acceleration field and are described by the tensor $u_{\mu\nu}$. As an example of a system, where it can be clearly observed, we can take a rotating partially-charged collapsing gas-dust cloud, held by gravity. An ordered acceleration field occurs in the cloud due to the rotational acceleration and contains the centripetal and tangential acceleration.

Due to its definition in the form of a four-rotor of u_β, the following relations hold for acceleration tensor $u_{\mu\nu}$:

$$\nabla_\sigma u_{\mu\nu} + \nabla_\nu u_{\sigma\mu} + \nabla_\mu u_{\nu\sigma} = 0$$
$$\text{or } \varepsilon^{\alpha\beta\gamma\delta} \nabla_\gamma u_{\alpha\beta} = 0. \qquad (23)$$

As we can see, the structure of equations (22) and (23) for the acceleration field is similar to the structure of equations for the strengths of gravitational and electromagnetic fields.

In the local geodetic reference frame, the derivatives of the metric tensor and the curvature tensor become equal to zero, the covariant derivative becomes a partial derivative and the equations take the simplest form. We will go over to this reference frame and apply the derivative ∂^ν to (23) and make substitution for the first and third terms using (22):

$$0 = \partial_\sigma \partial^\nu u_{\mu\nu} + \partial^\nu \partial_\nu u_{\sigma\mu} + \partial_\mu \partial^\nu u_{\nu\sigma}$$
$$= \partial_\sigma \left(-\frac{4\pi\eta}{c^2} J_\mu \right) + \square u_{\sigma\mu} + \partial_\mu \left(\frac{4\pi\eta}{c^2} J_\sigma \right).$$

$$\square u_{\sigma\mu} = \partial_\sigma \left(\frac{4\pi\eta}{c^2} J_\mu \right) - \partial_\mu \left(\frac{4\pi\eta}{c^2} J_\sigma \right).$$

If we apply definition $u_{\sigma\mu} = \partial_\sigma u_\mu - \partial_\mu u_\sigma$ to four-d'Alembertian $\square u_{\sigma\mu}$, where $\square = \partial^\nu \partial_\nu$ is the d'Alembert operator, it will give:

$$\square u_{\sigma\mu} = \square (\partial_\sigma u_\mu - \partial_\mu u_\sigma) = \partial_\sigma \square u_\mu - \partial_\mu \square u_\sigma.$$

Comparing with the previous expression, we find the wave equation for the four-potential u_μ:

$$\square u_\mu = \frac{4\pi\eta}{c^2} J_\mu.$$

On the other hand, after lowering the acceleration tensor indices, we have from (22):

$$\frac{4\pi\eta}{c^2} J_\mu = \partial^\nu u_{\nu\mu} = \partial^\nu (\partial_\nu u_\mu - \partial_\mu u_\nu)$$
$$= \square u_\mu - \partial_\mu \partial^\nu u_\nu.$$

Comparing this equation with equation for $\square u_\mu$ leads to the expression:

$$\partial^\nu u_\nu = \partial_\mu u^\mu = \varsigma,$$

where ς is some constant.

In an arbitrary reference frame, we should specify the obtained expressions, since in contrast to permutations of partial derivatives, in case of permutation of the covariant derivatives from the sequence $\nabla_\mu \nabla_\nu$ to the sequence $\nabla_\nu \nabla_\mu$, some additional terms appear. In particular, if we use the relation:

$$\nabla^\nu u_\nu = \nabla_\mu u^\mu = 0, \qquad (24)$$

then after substituting the expression $u^{\alpha\beta} = \nabla^\alpha u^\beta - \nabla^\beta u^\alpha$ in (22), the wave equation can be written as follows:

$$\left. \begin{aligned} & g^{\rho\nu} \partial_\rho \partial_\nu u^\alpha \\ & + g^{\rho\nu} \begin{pmatrix} \Gamma^\alpha_{\nu s} \partial_\rho u^s - \Gamma^s_{\rho\nu} \partial_s u^\alpha \\ + \Gamma^\alpha_{s\rho} \partial_\nu u^s + u^s \partial_s \Gamma^\alpha_{\nu\rho} \end{pmatrix} \\ & = \frac{4\pi\eta}{c^2} J^\alpha. \end{aligned} \right\} \qquad (25)$$

In the curved space, operator $\nabla_\nu \nabla^\nu$ acts differently on scalars, four-vectors and four-tensors, and it usually contains the Ricci tensor. Due to condition (24), the Ricci tensor is absent in (25), but the terms with the Christoffel symbols remain.

Equation (24) is a gauge condition for the four-potential u_ν, which is similar by its meaning to gauge conditions (21) for the electromagnetic and gravitational four-potentials. Both (24) and (25) will hold on condition that $\eta = const$.

In Appendix E, it will be shown that the acceleration tensor $u_{\mu\nu}$ includes the vector components $\mathbf{S}$ and $\mathbf{N}$, based on which, according to (E6), we can build a four-vector of particles' acceleration.

The pressure field equations

To obtain the pressure field equations, we need to choose in (15) those terms which contain the variation $\delta\pi_\beta$. This variation is present in (12) and (13), which gives the following:

$$\int \left(-\frac{1}{c} J^\beta + \frac{c}{4\pi\sigma} \nabla_\alpha f^{\alpha\beta} \right) \delta\pi_\beta \sqrt{-g}\, d\Sigma = 0.$$

$$\nabla_\alpha f^{\alpha\beta} = \frac{4\pi\sigma}{c^2} J^\beta \quad \text{or} \quad \nabla_\beta f^{\alpha\beta} = -\frac{4\pi\sigma}{c^2} J^\alpha . \qquad (26)$$

It follows from (26) that the mass four-current generates the pressure field in bodies, which can be described by the pressure tensor $f^{\alpha\beta}$. The same relations hold for this tensor as for the tensors of other fields:

$$\nabla_\sigma f_{\mu\nu} + \nabla_\nu f_{\sigma\mu} + \nabla_\mu f_{\nu\sigma} = 0$$

or $\varepsilon^{\alpha\beta\gamma\delta} \nabla_\gamma f_{\alpha\beta} = 0$. (27)

The wave equation for the four-potential of the pressure field follows from (26):

$$\left. \begin{aligned} & g^{\rho\nu} \partial_\rho \partial_\nu \pi^\alpha + \\ & g^{\rho\nu} \begin{pmatrix} \Gamma^\alpha_{\nu s} \partial_\rho \pi^s - \Gamma^s_{\rho\nu} \partial_s \pi^\alpha \\ + \Gamma^\alpha_{s\rho} \partial_\nu \pi^s + \pi^s \partial_s \Gamma^\alpha_{\nu\rho} \end{pmatrix} \\ & = \frac{4\pi\sigma}{c^2} J^\alpha . \end{aligned} \right\} \qquad (28)$$

Equation (28) will be valid if there is gauge condition of the pressure four-potential:

$$\nabla^\nu \pi_\nu = \nabla_\mu \pi^\mu = 0 . \qquad (29)$$

The properties of the pressure field are described in Appendix F, where it is shown that the pressure tensor $f_{\mu\nu}$ contains two vector components $\mathbf{C}$ and $\mathbf{I}$, which determine the energy and the pressure force, as well as the pressure energy flux.

The equations of motion of particles

The variation ξ^β that leads to the equations of motion of the particles is present in (3), (6), (9) and (12). For this variation, it follows from (15):

$$\int \begin{pmatrix} -\frac{1}{c} \Phi_{\beta\sigma} J^\sigma - \frac{1}{c} F_{\beta\sigma} j^\sigma - \\ -\frac{1}{c} u_{\beta\sigma} J^\sigma - \frac{1}{c} f_{\beta\sigma} J^\sigma \end{pmatrix} \xi^\beta \sqrt{-g}\, d\Sigma = 0 ,$$

$$-u_{\beta\sigma} J^\sigma = \Phi_{\beta\sigma} J^\sigma + F_{\beta\sigma} j^\sigma + f_{\beta\sigma} J^\sigma .$$

The left side of the equation can be transformed, considering the expression $J^\sigma = \rho_0 u^\sigma$ for the four-vector of mass current density and the definition of the acceleration tensor $u_{\beta\sigma} = \nabla_\beta u_\sigma - \nabla_\sigma u_\beta$:

$$\left. \begin{aligned} & -u_{\beta\sigma} J^\sigma = -\rho_0 u^\sigma \left(\nabla_\beta u_\sigma - \nabla_\sigma u_\beta \right) \\ & = \rho_0 u^\sigma \nabla_\sigma u_\beta = \rho_0 \frac{D u_\beta}{D\tau} . \end{aligned} \right\} \qquad (30)$$

We used the relation $u^\sigma \nabla_\beta u_\sigma = 0$, which follows from the equation $\nabla_\beta (u^\sigma u_\sigma) = \nabla_\beta (c^2) = 0$ and the operator of proper-time-derivative as operator of the derivative with respect to the proper time $u^\sigma \nabla_\sigma = \frac{D}{D\tau}$, where D is a symbol of four-differential in curved spacetime and τ is the proper time [11]. Taking (30) into account, the equation of motion takes the form:

$$\rho_0 \frac{D u_\beta}{D\tau} = \Phi_{\beta\sigma} J^\sigma + F_{\beta\sigma} j^\sigma + f_{\beta\sigma} J^\sigma . \qquad (31)$$

We will note that the equations of field motion (16) – (19), of the acceleration field (22) and (23), of the pressure field (26) and (27) and the equation of the particles' motion (31) are differential equations, which are valid at any point volume of spacetime in the system under consideration. In particular, if the mass density ρ_0 in some point volume is zero, then all the terms in (31) will be zero.

The quantity $\frac{D u_\beta}{D\tau}$ at the left side of (31) is the four-acceleration of a point particle, while the proper time differential $D\tau = d\tau$ is associated with the interval by relation: $ds = c\, d\tau$ and the relation: $Du_\beta = dx^\sigma \nabla_\sigma u_\beta$ holds. The first two terms at the right side of (31) are the densities of the gravitational and electromagnetic four-forces, respectively. It can be shown (see for example [3], [12]) that for four-forces exerted by the field on the particle, there are alternative expressions in terms of the stress-energy tensors (5) and (8):

$$\Phi_{\beta\sigma} J^\sigma = -\nabla^k U_{\beta k} , \quad F_{\beta\sigma} j^\sigma = -\nabla^k W_{\beta k} . \qquad (32)$$

Similarly, the left side of (31) with regard to (30) is expressed in terms of stress-energy tensor of the acceleration field (11) as:

$$\rho_0 \frac{Du_\beta}{D\tau} = -u_{\beta\sigma} J^\sigma = \nabla^k B_{\beta k} . \qquad (33)$$

To prove (33), we should expand the tensor $B_{\beta k}$ with the help of definition (11), apply the covariant derivative ∇^k to the tensor products and then use equations (22) and (23). Equation (33) shows that the four-acceleration of the particle can be described by either the acceleration tensor $u_{\beta\sigma}$ or the tensor $B_{\beta k}$.

For the pressure field, we can write the same as for other fields:

$$f_{\beta\sigma} J^\sigma = -\nabla^k P_{\beta k} . \qquad (34)$$

In (34), the pressure four-force is associated with the covariant derivative of the stress-energy tensor of the pressure field.

From (31) – (34) it follows that:

$$\nabla^k (B_{\beta k} + U_{\beta k} + W_{\beta k} + P_{\beta k}) = 0$$

or $\nabla_\beta (B^{\alpha\beta} + U^{\alpha\beta} + W^{\alpha\beta} + P^{\alpha\beta}) = 0 . \qquad (35)$

In Minkowski space $u_\beta = (\gamma \mathrm{c}, -\gamma \mathbf{v})$, where $\gamma = \frac{1}{\sqrt{1 - v^2/c^2}}$ is present, four-differentials D become ordinary differentials d, $D\tau = d\tau = dt/\gamma$, and the motion equation (31) falls into the scalar and vector equations, while the vector equation contains the total gravitational force with regard to the torsion field, the electromagnetic Lorentz force and the pressure force:

$$\rho_0 c^2 \frac{d\gamma}{dt} = \rho_0 \mathbf{v} \cdot \mathbf{\Gamma} + \rho_{0q} \mathbf{v} \cdot \mathbf{E} + \rho_0 \mathbf{v} \cdot \mathbf{C} , \qquad (36)$$

$$\left. \begin{aligned} & \rho_0 \frac{d(\gamma \mathbf{v})}{dt} = \rho_0 \left(\mathbf{\Gamma} + [\mathbf{v} \times \mathbf{\Omega}] \right) \\ & + \rho_{0q} \left(\mathbf{E} + [\mathbf{v} \times \mathbf{B}] \right) + \rho_0 \left(\mathbf{C} + [\mathbf{v} \times \mathbf{I}] \right), \end{aligned} \right\} \qquad (37)$$

where $\mathbf{v}$ is the velocity of a point particle, $\mathbf{\Gamma}$ is the gravitational field strength, ρ_{0q} is the charge density, $\mathbf{E}$ is the electric field strength, $\mathbf{C}$ is the pressure field strength, $\mathbf{\Omega}$ is the torsion field vector, $\mathbf{B}$ is the magnetic field induction and $\mathbf{I}$ is the solenoidal vector of the pressure field.

If during the time dt the density ρ_0 does not change, it can be put under the derivative's sign. Then, at the left side of (36) the quantity $\frac{dE_r}{dt}$ appears, where $E_r = \frac{\rho_0 c^2}{\sqrt{1 - v^2/c^2}}$ is the relativistic energy density. Similarly, at the left side of (37) the quantity $\frac{d\mathbf{J}}{dt}$ appears, where $\mathbf{J} = \frac{\rho_0 \mathbf{v}}{\sqrt{1 - v^2/c^2}}$ is the mass three-current density.

The equations for the metric

Let us consider action variations (2), (3), (4), (6), (7), (9), (10), (12) and (13), which contain the variation $\delta g_{\alpha\beta}$. The sum of all the terms in (15) with the variation $\delta g_{\alpha\beta}$ must be zero:

$$\int \begin{pmatrix} -kR^{\alpha\beta} + \frac{k}{2} R g^{\alpha\beta} - k\Lambda g^{\alpha\beta} - \frac{1}{2c} D_\mu J^\mu g^{\alpha\beta} - \frac{1}{2c} U^{\alpha\beta} - \frac{1}{2c} A_\mu j^\mu g^{\alpha\beta} \\ -\frac{1}{2c} W^{\alpha\beta} - \frac{1}{2c} u_\mu J^\mu g^{\alpha\beta} - \frac{1}{2c} B^{\alpha\beta} - \frac{1}{2c} \pi_\mu J^\mu g^{\alpha\beta} - \frac{1}{2c} P^{\alpha\beta} \end{pmatrix} \delta g_{\alpha\beta} \sqrt{-g}\, d\Sigma = 0 .$$

$$\begin{aligned} & -2ckR^{\alpha\beta} + ckR g^{\alpha\beta} - 2ck\Lambda g^{\alpha\beta} = \\ & = D_\mu J^\mu g^{\alpha\beta} + U^{\alpha\beta} + A_\mu j^\mu g^{\alpha\beta} + W^{\alpha\beta} + u_\mu J^\mu g^{\alpha\beta} + B^{\alpha\beta} + \pi_\mu J^\mu g^{\alpha\beta} + P^{\alpha\beta} . \end{aligned} \qquad (38)$$

The equation for the metric (38) allows to determine the metric tensor $g^{\alpha\beta}$ by the known quantities characterizing the matter and field. If we take the covariant derivative ∇_β in this equation, the left side of the equation vanishes on condition $\Lambda = const$. Taking (35) into account, we obtain:

$$\nabla_{\beta}\begin{pmatrix} D_{\mu} J^{\mu} g^{\alpha\beta} + A_{\mu} j^{\mu} g^{\alpha\beta} + \\ +u_{\mu} J^{\mu} g^{\alpha\beta} + \pi_{\mu} J^{\mu} g^{\alpha\beta} \end{pmatrix} = 0,$$

$$D_{\mu} J^{\mu} + A_{\mu} j^{\mu} + u_{\mu} J^{\mu} + \pi_{\mu} J^{\mu} = \chi, \qquad (39)$$

where χ is a function of time and coordinates and the scalar invariant with respect to coordinate transformations.

If we expand the scalar products of vectors using the expressions:

$$D_{\mu} J^{\mu} = c\rho_0 \frac{dt}{ds} D_{\mu} \frac{dx^{\mu}}{dt} = c\rho_0 \frac{dt}{ds}(\psi - \mathbf{v}\cdot\mathbf{D}),$$

$$A_{\mu} j^{\mu} = c\rho_{0q} \frac{dt}{ds}(\varphi - \mathbf{v}\cdot\mathbf{A}), \qquad (40)$$

$$\pi_{\mu} J^{\mu} = c\rho_0 \frac{dt}{ds}(\wp - \mathbf{v}\cdot\mathbf{\Pi}),$$

then (39) can be written as:

$$\left.\begin{array}{l} c\rho_0 \dfrac{dt}{ds}(\psi - \mathbf{v}\cdot\mathbf{D}) + c\rho_{0q} \dfrac{dt}{ds}(\varphi - \mathbf{v}\cdot\mathbf{A}) \\ +\rho_0 c^2 + c\rho_0 \dfrac{dt}{ds}(\wp - \mathbf{v}\cdot\mathbf{\Pi}) = \chi. \end{array}\right\} \qquad (41)$$

If the system's matter and charges are divided into small pieces and scattered to infinity, then there the external field potentials become equal to zero, since interparticle interaction tends to be zero, and at $\mathbf{v} = 0$ we obtain the following:

$$(\rho_0 \psi_0 + \rho_{0q} \varphi_0 + \rho_0 c^2 + p_0)_{\infty} = \chi. \qquad (42)$$

Consequently, χ is associated with the particle's proper scalar potentials ψ_0 and φ_0, the mass density ρ_0 and the pressure p_0 in the particle located at infinity. Expression (41) can be considered as the differential law of conservation of mass-energy: the greater the velocity $\mathbf{v}$ of a point particle is, and the greater the gravitational field potentials ψ and $\mathbf{D}$, the electromagnetic field potentials φ and $\mathbf{A}$ and the pressure field potentials $\wp$ and $\mathbf{\Pi}$ are, the more the mass density ρ_0 differs from its value at infinity. For example, if a point particle falls into the gravitational field with the potential ψ, then the change in the particle's energy is described by the term $c\frac{dt}{ds}\rho_0 \psi$. According to (41), such energy change can be compensated by the change in the rest energy of the particle due to the change ρ_0. Since the gravitational field potential ψ is always negative, then the mass density ρ_0 and the pressure inside the point particle should increase due to the field potential.

This is possible, if we remember that the whole procedure of deriving the motion equations of particles, field and metric from the principle of least action is based on the fact that the mass and charge of the matter unit at varying of the coordinates remain constant, despite of the change in the charge density, mass density and its volume [7]. If the mass of a simple system in the form of a point particle and the fields associated with it is proportional to χ, then according to (41) the mass of such a system remains unchanged, despite of the change in the fields, mass density ρ_0 and pressure p_0. Conservation of the mass-energy of each particle with regard to the mass-energy of the fields leads to conservation of the mass-energy of an arbitrary system including a multitude of particles and the fields surrounding them. We will remind that this article refers to the continuously distributed matter, so that each point particle or a unit of this matter may have its own mass density ρ_0 and its value χ.

We will now return to (38) and take the contraction of tensors by means of multiplying the equation by $g_{\alpha\beta}$, taking into account the relation $g_{\alpha\beta} g^{\alpha\beta} = 4$, and then dividing all by 2:

$$\left.\begin{array}{l} ckR - 4ck\Lambda = \\ \quad 2D_{\mu} J^{\mu} + 2A_{\mu} j^{\mu} + 2u_{\mu} J^{\mu} + 2\pi_{\mu} J^{\mu} \end{array}\right\}, \qquad (43)$$

where $R = g_{\alpha\beta} R^{\alpha\beta}$ is the scalar curvature, and it was taken into account that the contractions of tensors $U^{\alpha\beta}$, $W^{\alpha\beta}$, $B^{\alpha\beta}$ and $P^{\alpha\beta}$ are equal to zero.

In case if the cosmological constant Λ were known, based on (43), we could find the scalar curvature R.

In order to simplify equation (38) in [3] and [4], we introduced the gauge for Λ, at which the following equation would hold, if we additionally take into account the term with the pressure $\pi_\mu J^\mu$:

$$2ck\Lambda = -u_\mu J^\mu - D_\mu J^\mu - A_\mu j^\mu - \pi_\mu J^\mu . \quad (44)$$

In the gauge (44), the equation for the metric (38) takes the following form, provided that $-2ck = \frac{c^4}{8\pi G\beta}$, where β is a constant of order of unity:

$$\left. \begin{aligned} & R^{\alpha\beta} - \frac{1}{2} R\, g^{\alpha\beta} = \\ & \quad \frac{8\pi G\beta}{c^4}\left(U^{\alpha\beta} + W^{\alpha\beta} + B^{\alpha\beta} + P^{\alpha\beta}\right). \end{aligned} \right\} (45)$$

We will note that if from the right side of (45) we exclude the stress-energy tensor of the gravitational field $U^{\alpha\beta}$, replace the tensor $B^{\alpha\beta}$ by the stress-energy tensor of the matter in the form $\phi^{\alpha\beta} = \rho_0 u^\alpha u^\beta$ and neglect the tensor $P^{\alpha\beta}$, then at $\beta = 1$ we will obtain a typical equation for the metric used in the general theory of relativity:

$$R^{\alpha\beta} - \frac{1}{2} R\, g^{\alpha\beta} = \frac{8\pi G}{c^4}\left(W^{\alpha\beta} + \phi^{\alpha\beta}\right). \quad (46)$$

The equation for the metric (38) and expression (39) must hold in the covariant theory of gravitation, provided that $\Lambda = const$. If in (39) we remove the term $D_\mu J^\mu$, then we will obtain an expression suitable for use in the general theory of relativity. In this case, given that $u_\mu J^\mu = \rho_0 c^2$, instead of (39), we obtain the following:

$$A_\mu j^\mu + \rho_0 c^2 + \pi_\mu J^\mu = \chi . \quad (47)$$

If in (47) we equate the term with the energy of particles in the electromagnetic field (in the case when the field is zero) to zero, then the sum of the rest energy density and the pressure energy of each uncharged point particle must be unchanged. It follows that the pressure change must be accompanied by a change in the mass density. If the system contains the electromagnetic field with the four-potential A_μ acting on the four-currents j^μ generating them, then in the general case there must be an inverse correlation of the rest energy, pressure energy and the energy of charges in the electromagnetic field.

Indeed, in the general theory of relativity, the mass density determines the rest energy density and spacetime metric, which represents the gravitational field. In (47), the energy of charges in the electromagnetic field is specified by the term $A_\mu j^\mu$, and the mass density and hence the metric are associated with this energy at a constant χ. On the other hand, the metric is obtained from (46). Therefore, the occurrence of the electromagnetic field influences the metric in two relations — in (47) the mass density and the corresponding metric change, as well as in the equation for the metric (46) the stress-energy tensor of the matter $\phi^{\alpha\beta}$ changes, while the stress-energy tensor of the electromagnetic field $W^{\alpha\beta}$ also makes contribution to the metric.

A well-known paradox of general theory of relativity is associated with all of this — the electromagnetic field influences the density, the mass of the bodies as the source of gravitation and the metric, while the gravitational field itself (i.e., metric) does not influence the electrical charges of the bodies, which are the sources of the electromagnetic field. Thus the gravitational and electromagnetic fields are unequal relative to each other, despite the similarity of field equations and the same character of long-range action. Above, we pointed out the fact that the mass four-current leads to the gravitational field gradients, and the addition of the charge to this mass current generates additional electromagnetic (charge) four-current and the corresponding electromagnetic field gradients, depending on the sign of the charge. From this, we can see that the gravitational field looks like a fundamental, basic and indestructible field and the electromagnetic field manifests as some superstructure and the result of charge separation in the initially neutral matter.

If we consider (44) to be valid, then from comparison with (39), we see that the equation $2ck\Lambda = -\chi$ must be satisfied. Thus, when Λ is considered as a cosmological constant, we can use it to achieve simplification of the equation for the metric (38) and bring it to the form of (45). At the same time, the relation (39) is symmetrical with respect to the contribution of the gravitational and electromagnetic fields to the density, in spite of the difference in fields. We will remind that in the equation of motion (31), both fields also make symmetrical contributions to the four-acceleration of a point charge.

Although the gauge for Λ in the form of (44) seems the simplest and simplifies some of the equations, in Section 7 the necessity and convenience of another gauge will be shown.

Hamiltonian

In this and the next sections, we rely on the standard approach of analytical mechanics. As the coordinates, it is convenient to choose a set of Cartesian coordinates: $x^0 = ct$, $x^1 = x$, $x^2 = y$, $x^3 = z$.

Let us consider action (1) and express the Lagrangian from it:

$$L = \int \left(-u_\mu J^\mu - D_\mu J^\mu - A_\mu j^\mu - \pi_\mu J^\mu \right) \sqrt{-g}\, dx^1 dx^2 dx^3 + \int \begin{pmatrix} c\,k\,R - 2c\,k\,\Lambda + \dfrac{c^2}{16\pi G} \Phi_{\mu\nu} \Phi^{\mu\nu} - \dfrac{1}{4\mu_0} F_{\mu\nu} F^{\mu\nu} \\ - \dfrac{c^2}{16\pi \eta} u_{\mu\nu} u^{\mu\nu} - \dfrac{c^2}{16\pi\sigma} f_{\mu\nu} f^{\mu\nu} \end{pmatrix} \sqrt{-g}\, dx^1 dx^2 dx^3 . \qquad (48)$$

The integration in (48) is carried out over the infinite three-dimensional volume of space and over all the material particles of the system. We assume that the scalar curvature R depends on the metric tensor, and the metric tensor $g_{\mu\nu}$, the field tensors $\Phi_{\mu\nu}$, $F_{\mu\nu}$, $u_{\mu\nu}$, $f_{\mu\nu}$, the mass density ρ_0, the charge density ρ_{0q} and the pressure p_0 are functions of the coordinates t, x, y, z and do not depend on the particle velocities. Then, the Lagrangian in its general form (48) depends on the coordinates, as well as on the four-potential of pressure π_μ and four-potentials of the gravitational and electromagnetic fields D_μ and A_μ.

We will divide the first integral in the Lagrangian (48) into the sum of particular integrals, each of which describes the state of one of the set N_p of the system's particles. We will also take into account that the Lagrangian depends on the three-dimensional velocities of the particles $\overset{n}{\mathbf{v}} = \left(\dfrac{dx}{dt}, \dfrac{dy}{dt}, \dfrac{dz}{dt} \right) = (\dot{x}, \dot{y}, \dot{z})$, where $n = 1, 2, 3, \ldots N_p$ specifies the particle's number, while the velocity of any particle is part of only one corresponding particular integral. If we denote by L_f the second integral in (48), which is associated with the energies of fields inside and outside the fixed physical system and is independent of the particles' velocities, then we can write for the Lagrangian:

$$L = L(t, x, y, z, \overset{n}{\mathbf{v}}, D_\mu, A_\mu, \pi_\mu) = \sum_{n=1}^{N_p} \overset{n}{L} + L_f = \overset{n}{L}_n + L_f ,$$

where $\overset{n}{L} = \int \begin{pmatrix} -u_\mu J^\mu - D_\mu J^\mu \\ -A_\mu j^\mu - \pi_\mu J^\mu \end{pmatrix} \sqrt{-g}\, dx^1 dx^2 dx^3$ is a particular Lagrangian of an arbitrary particle.

We will introduce now the Hamiltonian H of the system as a function of generalized three-dimensional momenta $\overset{n}{\mathbf{P}}$ of the particles: $H = H(t, x, y, z, \overset{n}{\mathbf{P}}, D_\mu, A_\mu, \pi_\mu)$. Under the system's generalized momentum, we mean the sum of the generalized momenta of the whole set of particles:

$$\mathbf{P} = \sum_{n=1}^{N_p} \overset{n}{\mathbf{P}} = \overset{n}{\mathbf{P}}_n = \overset{1}{\mathbf{P}} + \overset{2}{\mathbf{P}} + \overset{3}{\mathbf{P}} + \ldots + \overset{N_p}{\mathbf{P}} .$$

To find the Hamiltonian, we will apply the Legendre transformations to the system of particles:

$$H = \sum_{n=1}^{N_p} \left(\overset{n}{\mathbf{P}} \cdot \overset{n}{\mathbf{v}} \right) - L = \left(\overset{n}{\mathbf{P}} \cdot \overset{n}{\mathbf{v}} \right)_n - L , \qquad (49)$$

provided that:

$$\mathbf{P} = \sum_{n=1}^{N_p} \frac{\partial L}{\partial \overset{n}{\mathbf{v}}} = \sum_{n=1}^{N_p} \frac{\partial \overset{n}{L}}{\partial \overset{n}{\mathbf{v}}}. \tag{50}$$

The equality in (50) gives the definition of the generalized momentum $\mathbf{P}$, and we can see that the generalized momentum of an arbitrary particle equals $\overset{n}{\mathbf{P}} = \frac{\partial \overset{n}{L}}{\partial \overset{n}{\mathbf{v}}}$. On the other hand, the equations $\overset{n}{\mathbf{P}} = \frac{\partial \overset{n}{L}}{\partial \overset{n}{\mathbf{v}}}$ allow to express the velocity $\overset{n}{\mathbf{v}}$ of an arbitrary particle through the generalized momentum $\overset{n}{\mathbf{P}}$. Then, we can substitute these velocities in (49) and determine H only through $\overset{n}{\mathbf{P}}$.

In order to find $\frac{\partial \overset{n}{L}}{\partial \overset{n}{\mathbf{v}}}$ in (50), in each particular Lagrangian $\overset{n}{L}$, we should express J^{μ} and j^{μ} in terms of the velocity $\overset{n}{\mathbf{v}}$ and interval ds:

$$J^{\mu} = c\rho_0 \frac{dx^{\mu}}{ds} = c\rho_0 \frac{dt}{ds}\frac{dx^{\mu}}{dt},$$

$$j^{\mu} = c\rho_{0q} \frac{dt}{ds}\frac{dx^{\mu}}{dt}, \tag{51}$$

while $dx^{\mu} = (cdt, d\mathbf{r})$, and we introduce the notation $\frac{dx^{\mu}}{dt} = (c, \frac{d\mathbf{r}}{dt}) = (c, \overset{n}{\mathbf{v}}) = (c, \overset{n}{v^i})$, where the four-dimensional quantity $\frac{dx^{\mu}}{dt}$ is not a real four-vector. With regard to the definition of the four-potential of the acceleration field $u_{\mu} = \left(\frac{\vartheta}{c}, -\mathbf{U}\right)$, for each particle we obtain:

$$u_{\mu} J^{\mu} = c\rho_0 \frac{dt}{ds}\left(\vartheta - \overset{n}{\mathbf{v}} \cdot \overset{n}{\mathbf{U}}\right). \tag{52}$$

In (48), the unit of volume of the system in any particular integral can be expressed in terms of the unit of volume in the reference frame K_p associated with the particle in the following way:

$$\sqrt{-g}\, dx^1 dx^2 dx^3 = \frac{ds}{cdt}\left(\sqrt{-g}\, dx^1 dx^2 dx^3\right)_0. \tag{53}$$

From this formula in the weak-field limit in Minkowski space, when $ds = cdt/\gamma$, it follows that the volume of a moving particle is decreased in comparison with the volume of a particle at rest. Given that $ds = c\,d\tau$, where τ is the proper time in the reference frame K_p of the particle, the equality of four-volumes in different reference frames follows from (53):

$$\int \sqrt{-g}\, cdt\, dx^1 dx^2 dx^3 = \int \left(\sqrt{-g}\, c\, d\tau\, dx^1 dx^2 dx^3\right)_0.$$

This equation reflects the fact that the four-volume is a four-invariant.

Under the above conditions, (40), (51), (52) and (53) can be written for the Lagrangian (48) as follows:

$$\left.\begin{aligned} L = \sum_{n=1}^{N_p} \int^{n} & \begin{pmatrix} -\rho_0\left(\vartheta - \overset{n}{\mathbf{v}} \cdot \overset{n}{\mathbf{U}}\right) - \rho_0(\psi - \overset{n}{\mathbf{v}} \cdot \overset{n}{\mathbf{D}}) \\ -\rho_{0q}(\varphi - \overset{n}{\mathbf{v}} \cdot \overset{n}{\mathbf{A}}) - \rho_0(\wp - \overset{n}{\mathbf{v}} \cdot \overset{n}{\mathbf{\Pi}}) \end{pmatrix} \left(\sqrt{-g}\, dx^1 dx^2 dx^3\right)_0 \\ + \int & \begin{pmatrix} ckR - 2ck\Lambda + \frac{c^2}{16\pi G}\Phi_{\mu\nu}\Phi^{\mu\nu} - \frac{1}{4\mu_0}F_{\mu\nu}F^{\mu\nu} - \\ -\frac{c^2}{16\pi\eta}u_{\mu\nu}u^{\mu\nu} - \frac{c^2}{16\pi\sigma}f_{\mu\nu}f^{\mu\nu} \end{pmatrix} \sqrt{-g}\, dx^1 dx^2 dx^3, \end{aligned}\right\} \tag{54}$$

as well as after partial volume integration:

$$
\left.
\begin{array}{l}
L=-\sum_{n=1}^{N_p}\left(\begin{array}{l}\overset{n}{m}\left(\vartheta-\overset{n}{\mathbf{v}}\cdot\overset{n}{\mathbf{U}}\right)+\overset{n}{m}\,(\psi-\overset{n}{\mathbf{v}}\cdot\overset{n}{\mathbf{D}})\\ +\overset{n}{q}\,(\varphi-\overset{n}{\mathbf{v}}\cdot\overset{n}{\mathbf{A}})+\overset{n}{m}\,(\wp-\overset{n}{\mathbf{v}}\cdot\overset{n}{\mathbf{\Pi}})\end{array}\right)\\
+\int\left(\begin{array}{l}c\,k\,R-2c\,k\,\Lambda+\dfrac{c^2}{16\pi G}\Phi_{\mu\nu}\Phi^{\mu\nu}-\dfrac{1}{4\mu_0}F_{\mu\nu}F^{\mu\nu}-\\ -\dfrac{c^2}{16\pi\eta}u_{\mu\nu}u^{\mu\nu}-\dfrac{c^2}{16\pi\sigma}f_{\mu\nu}f^{\mu\nu}\end{array}\right)\sqrt{-g}\,dx^1dx^2dx^3,
\end{array}
\right\} \qquad (55)
$$

where $\overset{n}{m}=\int\rho_0\left(\sqrt{-g}\,dx^1dx^2dx^3\right)_0$ is the mass of an arbitrary particle, $\overset{n}{q}=\int\rho_{0q}\left(\sqrt{-g}\,dx^1dx^2dx^3\right)_0$ is the particle's charge. In (55), the scalar and vector field potentials are averaged over the particle's volume, which means that they are the effective potentials at the location of the particle.

In operations with three-vectors, it is convenient to write vectors in the form of components or projections on the spatial axes of the coordinate system using, for example, instead of the velocity $\mathbf{v}$, the quantity v^i, where $i=1,2,3$. Then, $v^1=v_x$, $v^2=v_y$, $v^3=v_z$, and the velocity derivative can be represented as: $\frac{\partial}{\partial\mathbf{v}}=\frac{\partial}{\partial v^i}$. For the gravitational vector potential in particular, we obtain: $\mathbf{D}=(D_x,D_y,D_z)$ $=(D_1,D_2,D_3)$.

With this in mind, from (55) and (50), we find:

$$
\mathbf{P}=P_i=\sum_{n=1}^{N_p}\frac{\partial\overset{n}{L}}{\partial\overset{n}{v}{}^i}
=\sum_{n=1}^{N_p}\left(\overset{n}{m}\,\overset{n}{U}_i+\overset{n}{m}\,\overset{n}{D}_i+\overset{n}{q}\,\overset{n}{A}_i+\overset{n}{m}\,\overset{n}{\Pi}_i\right),
$$

$$
\overset{n}{\mathbf{P}}=\overset{n}{m}\,\overset{n}{U}_i+\overset{n}{m}\,\overset{n}{D}_i+\overset{n}{q}\,\overset{n}{A}_i+\overset{n}{m}\,\overset{n}{\Pi}_i\,. \qquad (56)
$$

Based on this, we find for the sums of the scalar products of three-vectors by summing over the index i:

$$
\left.
\begin{array}{l}
\sum_{n=1}^{N_p}\left(\overset{n}{\mathbf{P}}\cdot\overset{n}{\mathbf{v}}\right)=\\
\sum_{n=1}^{N_p}\left(\begin{array}{l}\overset{n}{m}\,\overset{n}{U}_i\,\overset{n}{v}{}^i+\overset{n}{m}\,\overset{n}{D}_i\,\overset{n}{v}{}^i\\ +\overset{n}{q}\,\overset{n}{A}_i\,\overset{n}{v}{}^i+\overset{n}{m}\,\overset{n}{\Pi}_i\,\overset{n}{v}{}^i\end{array}\right),
\end{array}
\right\} \qquad (57)
$$

From (49), taking (55) and (57) into account, we have:

$$
\left.
\begin{array}{l}
H=\sum_{n=1}^{N_p}\left(\overset{n}{m}\,\vartheta+\overset{n}{m}\,\psi+\overset{n}{q}\,\varphi+\overset{n}{m}\,\wp\right)\\
-\int\left(\begin{array}{l}c\,k\,R-2c\,k\,\Lambda+\dfrac{c^2}{16\pi G}\Phi_{\mu\nu}\Phi^{\mu\nu}-\dfrac{1}{4\mu_0}F_{\mu\nu}F^{\mu\nu}-\\ -\dfrac{c^2}{16\pi\eta}u_{\mu\nu}u^{\mu\nu}-\dfrac{c^2}{16\pi\sigma}f_{\mu\nu}f^{\mu\nu}\end{array}\right)\sqrt{-g}\,dx^1dx^2dx^3.
\end{array}
\right\} \qquad (58)
$$

In (58), the Hamiltonian contains the scalar curvature R and the cosmological constant Λ. As it will be shown in Section 6 about the energy, this Hamiltonian represents the relativistic energy of the system. To make the picture complete, we could also express the quantity $\vartheta=cg_{0\mu}u^\mu$ in (58) through the generalized momentum P_i. We have described this procedure in [4].

For continuously distributed matter, the masses and charges of the particles in (58) can be expressed through the corresponding integrals: $\overset{n}{m} = \int^{n} \rho_0 \left(\sqrt{-g}\, dx^1 dx^2 dx^3 \right)_0$, $\overset{n}{q} = \int^{n} \rho_{0q} \left(\sqrt{-g}\, dx^1 dx^2 dx^3 \right)_0$. Also, taking (53) into account, in which we can substitute the expression $\frac{c\,dt}{ds} = \frac{u^0}{c}$, where u^0 denotes the time component of the four-velocity of an arbitrary particle, from (58) we find:

$$\left.\begin{aligned} H &= \frac{1}{c} \int \left(\rho_0 \vartheta + \rho_0 \psi + \rho_{0q} \varphi + \rho_0 \wp \right) u^0 \sqrt{-g}\, dx^1 dx^2 dx^3 \\ &- \int \begin{pmatrix} c\,k\,R - 2c\,k\,\Lambda + \frac{c^2}{16\pi G} \Phi_{\mu\nu} \Phi^{\mu\nu} - \frac{1}{4\mu_0} F_{\mu\nu} F^{\mu\nu} - \\ - \frac{c^2}{16\pi\eta} u_{\mu\nu} u^{\mu\nu} - \frac{c^2}{16\pi\sigma} f_{\mu\nu} f^{\mu\nu} \end{pmatrix} \sqrt{-g}\, dx^1 dx^2 dx^3. \end{aligned}\right\} \qquad (59)$$

Hamilton's equations

Assuming that the Hamiltonian depends on the generalized three-momenta of particles $\overset{n}{\mathbf{P}}$: $H = H(t, \overset{n}{\mathbf{r}}, \overset{n}{\mathbf{P}}, D_\mu, A_\mu, \pi_\mu)$ and the Lagrangian depends on three-velocity of particles $\overset{n}{\mathbf{v}}$: $L = L(t, \overset{n}{\mathbf{r}}, \overset{n}{\mathbf{v}}, D_\mu, A_\mu, \pi_\mu)$, where $\overset{n}{\mathbf{r}} = (x, y, z)$ is a three-dimensional radius-vector of the particle with the number n, we will take differentials of L and H, as well as the differentials of both sides of equation (49):

$$\left.\begin{aligned} DL &= \frac{\partial L}{\partial t} Dt + \sum_{n=1}^{N_p} \frac{\partial L}{\partial \overset{n}{\mathbf{r}}} D\overset{n}{\mathbf{r}} + \sum_{n=1}^{N_p} \frac{\partial L}{\partial \overset{n}{\mathbf{v}}} D\overset{n}{\mathbf{v}} \\ &+ \frac{\partial L}{\partial D_\mu} DD_\mu + \frac{\partial L}{\partial A_\mu} DA_\mu + \frac{\partial L}{\partial \pi_\mu} D\pi_\mu . \end{aligned}\right\} \qquad (60)$$

$$\left.\begin{aligned} DH &= \frac{\partial H}{\partial t} Dt + \sum_{n=1}^{N_p} \frac{\partial H}{\partial \overset{n}{\mathbf{r}}} D\overset{n}{\mathbf{r}} \\ &+ \sum_{n=1}^{N_p} \frac{\partial H}{\partial \overset{n}{\mathbf{P}}} D\overset{n}{\mathbf{P}} + \frac{\partial H}{\partial D_\mu} DD_\mu \\ &+ \frac{\partial H}{\partial A_\mu} DA_\mu + \frac{\partial H}{\partial \pi_\mu} D\pi_\mu . \end{aligned}\right\} \qquad (61)$$

$$DH = \sum_{n=1}^{N_p} \left(D\overset{n}{\mathbf{P}} \cdot \overset{n}{\mathbf{v}} \right) + \sum_{n=1}^{N_p} \left(\overset{n}{\mathbf{P}} \cdot D\overset{n}{\mathbf{v}} \right) - DL . \qquad (62)$$

Substituting (60) and (61) into (62), we find:

$$\frac{\partial H}{\partial t} = -\frac{\partial L}{\partial t}, \quad \frac{\partial H}{\partial \overset{n}{\mathbf{r}}} = -\frac{\partial L}{\partial \overset{n}{\mathbf{r}}}, \quad \frac{\partial H}{\partial D_\mu} = -\frac{\partial L}{\partial D_\mu},$$
$$\frac{\partial H}{\partial A_\mu} = -\frac{\partial L}{\partial A_\mu}, \quad \frac{\partial H}{\partial \pi_\mu} = -\frac{\partial L}{\partial \pi_\mu}, \quad \frac{\partial H}{\partial \overset{n}{\mathbf{P}}} = \overset{n}{\mathbf{v}},$$
$$\frac{\partial L}{\partial \overset{n}{\mathbf{v}}} = \overset{n}{\mathbf{P}}. \qquad (63)$$

The last equation in (63) leads to (50) and gives the expression (56) for the generalized momentum $\overset{n}{\mathbf{P}}$ of an arbitrary particle of the system in an explicit form.

We will now apply the principle of least action to the Lagrangian in the form $L = L(t, \overset{n}{\mathbf{r}}, \overset{n}{\mathbf{v}}, D_\mu, A_\mu, \pi_\mu)$, equating the action variation to zero, when the particle moves from the time point t_1 to the time point t_2.

$$\left.\begin{aligned} \delta S &= \delta \int_{t_1}^{t_2} L(t, \overset{n}{\mathbf{r}}, \overset{n}{\mathbf{v}}, D_\mu, A_\mu, \pi_\mu)\, dt \\ &= \int_{t_1}^{t_2} \begin{pmatrix} \sum_{n=1}^{N_p} \frac{\partial L}{\partial \overset{n}{\mathbf{r}}} \delta \overset{n}{\mathbf{r}} + \sum_{n=1}^{N_p} \frac{\partial L}{\partial \overset{n}{\mathbf{v}}} \delta \overset{n}{\mathbf{v}} \\ + \frac{\partial L}{\partial D_\mu} \delta D_\mu + \frac{\partial L}{\partial A_\mu} \delta A_\mu \\ + \frac{\partial L}{\partial \pi_\mu} \delta \pi_\mu \end{pmatrix} dt = 0. \end{aligned}\right\} \qquad (64)$$

In (64), it was assumed that the time variation is equal to zero: $\delta t = 0$. Partial derivatives with variations δD_μ, δA_μ and $\delta \pi_\mu$ lead to field equations (16), (18) and (26). If we take into account the definition of velocity in the second term in the integral (64): $\overset{n}{\mathbf{v}} = \frac{d\overset{n}{\mathbf{r}}}{dt}$, then the integral for this term is taken by parts. Then, for the first and second terms in the integral (64), we have the following:

$$\left.\begin{aligned} &\sum_{n=1}^{N_p}\int_{t_1}^{t_2}\left(\frac{\partial L}{\partial \overset{n}{\mathbf{r}}}\delta\overset{n}{\mathbf{r}}dt+\frac{\partial L}{\partial \overset{n}{\mathbf{v}}}d\,\delta\overset{n}{\mathbf{r}}\right)= \\ &\sum_{n=1}^{N_p}\frac{\partial L}{\partial \overset{n}{\mathbf{v}}}\delta\overset{n}{\mathbf{r}}\Bigg|_{t_1}^{t_2}+\sum_{n=1}^{N_p}\int_{t_1}^{t_2}\left(\frac{\partial L}{\partial \overset{n}{\mathbf{r}}}-\frac{d}{dt}\frac{\partial L}{\partial \overset{n}{\mathbf{v}}}\right)\delta\overset{n}{\mathbf{r}}\,dt. \end{aligned}\right\} \quad (65)$$

When varying the action, the variations $\delta\overset{n}{\mathbf{r}}$ are equal to zero only at the beginning and at the end of the motion; that is at t_1 and t_2. Therefore, for vanishing of the variation δS, it is necessary that the quantity in brackets inside the integral (65) would be equal to zero. This leads to the well-known Lagrange equations of motion:

$$\frac{\partial L}{\partial \overset{n}{\mathbf{r}}}=\frac{d}{dt}\frac{\partial L}{\partial \overset{n}{\mathbf{v}}}. \qquad (66)$$

According to (63), $\frac{\partial L}{\partial \overset{n}{\mathbf{v}}}=\overset{n}{\mathbf{P}}$, as well as $\frac{\partial H}{\partial \overset{n}{\mathbf{r}}}=-\frac{\partial L}{\partial \overset{n}{\mathbf{r}}}$. Let us substitute this in (66):

$$\frac{\partial H}{\partial \overset{n}{\mathbf{r}}}=-\frac{d\overset{n}{\mathbf{P}}}{dt}. \qquad (67)$$

Equation (67) together with equation $\frac{\partial H}{\partial \overset{n}{\mathbf{P}}}=\overset{n}{\mathbf{v}}$ from (63) represent the standard Hamiltonian equations describing the motion of an arbitrary particle of the system in the gravitational and electromagnetic fields and in the pressure field. According to (67), the rate of change of the generalized momentum of the particle by the coordinate time is equal to the generalized force, which is found as the gradient with respect to the particle's coordinates of the relativistic energy of the system taken with the opposite sign. These equations are widely used; not only in the general theory of relativity, but also in other areas of theoretical physics. We have checked these equations in [4] in the framework of the covariant theory of gravitation by direct substitution of the Hamiltonian.

The system's energy

We will consider a closed system which is in the state of some stationary motion. An example would be a charged ball rotating around its center of mass, which forms the system under consideration together with its gravitational and electromagnetic fields and the internal pressure. In such a system, the energy should be conserved as a consequence of lack of energy losses to the environment and taking into account the homogeneity of time; i.e., the equivalence of the time points for the system's state.

The system's Lagrangian, taking the fields' energy into account, has the form of (55). Due to the stationary motion, we can assume that within the system's volume the metric tensor $g_{\mu\nu}$, the scalar curvature R, the four-potentials of the field D_μ, A_μ and of the pressure π_μ do not depend on time. But, since any point particle moves with the ball, then its location and velocity are changed, being defined by the radius vector $\mathbf{r}$ and velocity $\mathbf{v}$, respectively. We may assume that the Lagrangian of the system does not depend explicitly on time and is a function of the form: $L = L(\overset{n}{\mathbf{r}},\overset{n}{\mathbf{v}})$. Now, we will take the time derivative of the Lagrangian, as it is done for example in [13], not only for one but for a set of particles, and will apply (66):

$$\begin{aligned} \frac{dL}{dt} &= \frac{1}{dt}\sum_{n=1}^{N_p}\left(\frac{\partial L}{\partial \overset{n}{\mathbf{r}}}d\overset{n}{\mathbf{r}}+\frac{\partial L}{\partial \overset{n}{\mathbf{v}}}d\overset{n}{\mathbf{v}}\right) \\ &= \sum_{n=1}^{N_p}\left(\frac{\partial L}{\partial \overset{n}{\mathbf{r}}}\overset{n}{\mathbf{v}}+\frac{\partial L}{\partial \overset{n}{\mathbf{v}}}\frac{d\overset{n}{\mathbf{v}}}{dt}\right) \\ &= \sum_{n=1}^{N_p}\left(\overset{n}{\mathbf{v}}\frac{d}{dt}\frac{\partial L}{\partial \overset{n}{\mathbf{v}}}+\frac{\partial L}{\partial \overset{n}{\mathbf{v}}}\frac{d\overset{n}{\mathbf{v}}}{dt}\right) \\ &= \frac{d}{dt}\sum_{n=1}^{N_p}\left(\overset{n}{\mathbf{v}}\frac{\partial L}{\partial \overset{n}{\mathbf{v}}}\right). \end{aligned}$$

$$\frac{d}{dt}\left(\sum_{n=1}^{N_p}\left(\overset{n}{\mathbf{v}}\frac{\partial L}{\partial \overset{n}{\mathbf{v}}}\right)-L\right)=0.$$

The quantity in the brackets is not time-dependent and is constant. This gives the definition of relativistic energy as a conserved quantity for a closed system at stationary motion:

$$E=\sum_{n=1}^{N_p}\left(\overset{n}{\mathbf{v}}\frac{\partial L}{\partial \overset{n}{\mathbf{v}}}\right)-L. \tag{68}$$

With regard to (63) and (49), we find the following:

$$E=\sum_{n=1}^{N_p}\left(\overset{n}{\mathbf{P}}\cdot\overset{n}{\mathbf{v}}\right)-L=H. \tag{69}$$

It turns out that the relativistic energy can be expressed in a covariant form, since according to (69) the formula for the energy coincides with the formula for the Hamiltonian in (49).

To calculate the relativistic energy of the system with the matter, which is continuously distributed over the volume, it is convenient to pass from the mass and charge of the particle to the corresponding densities inside the particle. According to (59), we obtain:

$$\left.\begin{array}{l} E=\dfrac{1}{c}\displaystyle\int\left(\rho_0\vartheta+\rho_0\psi+\rho_{0q}\varphi+\rho_0\wp\right)u^0\sqrt{-g}\,dx^1dx^2dx^3 \\ -\displaystyle\int\left(\begin{array}{l} c\,k\,R-2c\,k\,\Lambda+\dfrac{c^2}{16\pi G}\Phi_{\mu\nu}\Phi^{\mu\nu}-\dfrac{1}{4\mu_0}F_{\mu\nu}F^{\mu\nu}- \\ -\dfrac{c^2}{16\pi\eta}u_{\mu\nu}u^{\mu\nu}-\dfrac{c^2}{16\pi\sigma}f_{\mu\nu}f^{\mu\nu}\end{array}\right)\sqrt{-g}\,dx^1dx^2dx^3. \end{array}\right\} \tag{70}$$

Using expression (70), we can find the invariant energy E_0 of the system, for which we should use the frame of reference of the center of mass and calculate the integral. In addition, at a known velocity $\mathbf{v}$ of the center of mass of the system in an arbitrary reference frame K, we can calculate the momentum of the system in K. This can be clarified as follows. We will define the invariant mass of the system taking the mass-energy of the fields into account using the relation: $m_0=\frac{E_0}{c^2}$, where c is the speed of light as a measure of the velocity of propagation of electromagnetic and gravitational interactions. If the four-displacement in K has the form: $d\hat{x}^\mu=(cdt,dx,dy,dz)=(cdt,d\mathbf{r})=dt(c,\mathbf{v})$, then, for the four-velocity of the system in K, we can write: $\hat{u}^\mu=\frac{cd\hat{x}^\mu}{ds}=\frac{cdt}{ds}\frac{d\hat{x}^\mu}{dt}=\frac{cdt}{ds}(c,\mathbf{v})$. The four-vector $p^\mu=m_0\hat{u}^\mu=\frac{cdt}{ds}(m_0c,\,m_0\mathbf{v})=\left(\frac{E}{c},\,\mathbf{p}\right)$ defines the four-momentum, which contains the relativistic energy $E=\frac{cdt}{ds}m_0c^2=\frac{cdt}{ds}E_0$ and relativistic momentum $\mathbf{p}=\frac{cdt}{ds}m_0\mathbf{v}=\frac{cdt}{ds}\frac{E_0}{c^2}\mathbf{v}$. This gives the formula for determining the momentum through the energy: $\mathbf{p}=\frac{E}{c^2}\mathbf{v}$, and, correspondingly, for the four-momentum: $p^\mu=\left(\frac{E}{c},\,\mathbf{p}\right)=\left(\frac{E}{c},\,\frac{E}{c^2}\mathbf{v}\right)$.

In the reference frame K', in which the system is at rest $\mathbf{v}=0$, $\mathbf{p}=0$, $dt=d\tau$, and then $E=E_0$, and also $(p^\mu)_{\mathbf{v}=0}=\left(\frac{E_0}{c},0,0,0\right)$; that is in the four-momentum in the reference frame K', only the time component is non-zero.

If we multiply the four-momentum by the speed of light, we will obtain the four-vector of the form $H^\mu=cp^\mu=\left(E,\,c\mathbf{p}\right)=\left(E,\,\frac{E}{c}\mathbf{v}\right)$, the time component of which is the relativistic energy, equal in value to the Hamiltonian. Thus, we find the four-vector, which in [4] was called the Hamiltonian four-vector.

The Cosmological Constant Gauge and the Resulting Consequences

We will make transformations and substitute (43) and (39) in (70):

$$\left.\begin{array}{l} E=\frac{1}{c}\int\left(\rho_0\vartheta+\rho_0\psi+\rho_{0q}\varphi+\rho_0\wp\right)u^0\sqrt{-g}\,dx^1dx^2dx^3 \\ -\int\begin{pmatrix} 2ck\Lambda+2\chi+\frac{c^2}{16\pi G}\Phi_{\mu\nu}\Phi^{\mu\nu}-\frac{1}{4\mu_0}F_{\mu\nu}F^{\mu\nu} \\ -\frac{c^2}{16\pi\eta}u_{\mu\nu}u^{\mu\nu}-\frac{c^2}{16\pi\sigma}f_{\mu\nu}f^{\mu\nu}\end{pmatrix}\sqrt{-g}\,dx^1dx^2dx^3. \end{array}\right\} \qquad (71)$$

If we choose the condition for the cosmological constant in the form:

$$2ck\Lambda+2\chi=0, \qquad (72)$$

then the relativistic energy (71) is uniquely defined, since the dependence on the constants Λ and χ disappears:

$$\left.\begin{array}{l} E=\frac{1}{c}\int\left(\rho_0\vartheta+\rho_0\psi+\rho_{0q}\varphi+\rho_0\wp\right)u^0\sqrt{-g}\,dx^1dx^2dx^3 \\ -\int\begin{pmatrix} \frac{c^2}{16\pi G}\Phi_{\mu\nu}\Phi^{\mu\nu}-\frac{1}{4\mu_0}F_{\mu\nu}F^{\mu\nu} \\ -\frac{c^2}{16\pi\eta}u_{\mu\nu}u^{\mu\nu}-\frac{c^2}{16\pi\sigma}f_{\mu\nu}f^{\mu\nu}\end{pmatrix}\sqrt{-g}\,dx^1dx^2dx^3. \end{array}\right\} \qquad (73)$$

We will remind that the quantities Λ and χ can have their own values for each particle of matter. But on condition of (72), the expression for the relativistic energy (73) becomes universal for any particle in an arbitrary system of particles and their fields.

From (72) and (39), the following equation is obtained:

$$\left.\begin{array}{l} 2ck\Lambda=-2D_\mu J^\mu-2A_\mu j^\mu \\ \quad -2u_\mu J^\mu-2\pi_\mu J^\mu. \end{array}\right\} \qquad (74)$$

In order to estimate the value of the cosmological constant Λ, it is convenient to divide all of the system's matter into small pieces, scatter them apart to infinity and leave them motionless. Then, the vector potentials of the fields and pressure become equal to zero and the relation remains:

$$ck\Lambda=(-\rho_0\psi_0-\rho_{0q}\varphi_0-\rho_0c^2-p_0)_\infty .$$

It follows that Λ, just like χ in (42), is associated with the rest energy, with the pressure energy and with the proper energy of the fields of the system under consideration.

If in some volume there are no particles and the mass density ρ_0 and the charge density ρ_{0q} are zero, then in this volume there must remain the relativistic energy of the external fields:

$$E_{rf}=-\int\begin{pmatrix}\frac{c^2}{16\pi G}\Phi_{\mu\nu}\Phi^{\mu\nu} \\ -\frac{1}{4\mu_0}F_{\mu\nu}F^{\mu\nu}\end{pmatrix}\sqrt{-g}\,dx^1dx^2dx^3 . \qquad (75)$$

Based on (73), we can express the energy of a small body at rest. For simplicity, we will assume that the body does not rotate as a whole and there is no motion of the matter and charges inside it (an ideal solid body without the intrinsic magnetic field and the torsion field). Under such conditions, the coordinate time of the system becomes approximately equal to the proper time of the body: $dt\approx d\tau$. Since the interval $ds=c\,d\tau$, then we obtain: $ds\approx c\,dt$. Since there is no spatial motion in any part of the body, we can write:

$$\vartheta=c\,g_{0\mu}u^\mu=g_{0\mu}\frac{c^2dx^\mu}{ds}$$

$$=g_{0\mu}\frac{c^2}{ds}(c\,dt,0,0,0)=g_{00}\frac{c^3dt}{ds}=c^2g_{00}.$$

$$u^0=\frac{c\,dx^0}{ds}\approx c .$$

With this in mind, we obtain from (73):

$$\left.\begin{aligned} E_0 &= \int \left(g_{00} \rho_0 c^2 + \rho_0 \psi + \rho_{0q} \varphi + \rho_0 \wp \right) \sqrt{-g}\, dx^1 dx^2 dx^3 - \\ &- \int \begin{pmatrix} \frac{c^2}{16\pi G} \Phi_{\mu\nu} \Phi^{\mu\nu} - \frac{1}{4\mu_0} F_{\mu\nu} F^{\mu\nu} \\ - \frac{c^2}{16\pi\eta} u_{\mu\nu} u^{\mu\nu} - \frac{c^2}{16\pi\sigma} f_{\mu\nu} f^{\mu\nu} \end{pmatrix} \sqrt{-g}\, dx^1 dx^2 dx^3 . \end{aligned}\right\} \quad (76)$$

In the weak field limit in (76), we can use $g_{00} \approx 1$, $\sqrt{-g} \approx 1$. The tensor product $u_{\mu\nu} u^{\mu\nu}$ in the absence of matter motion inside the ideal solid body vanishes. Using (F5) and (F6), we can write:

$$\mathbf{C} = -\nabla \left(\frac{p_0}{\rho_0} \right), \ \mathbf{I} = 0,$$

$$\frac{c^2}{16\pi\sigma} f_{\mu\nu} f^{\mu\nu} = -\frac{1}{8\pi\sigma} (C^2 - c^2 I^2) = -\frac{1}{8\pi\sigma} \left[\nabla \left(\frac{p_0}{\rho_0} \right) \right]^2 .$$

Besides, in [4] it was found that in the weak field for a motionless body in the form of a ball with uniform density of mass and charge, the following relations hold for the body's proper fields:

$$\left.\begin{aligned} & -\frac{c^2}{16\pi G} \Phi_{\mu\nu} \Phi^{\mu\nu} = \frac{1}{8\pi G} \Gamma^2 , \\ & \frac{1}{4\mu_0} F_{\mu\nu} F^{\mu\nu} = -\frac{\varepsilon_0}{2} E^2 , \\ & \int \left(\frac{1}{2} \rho_0 \psi \right) dx^1 dx^2 dx^3 = \int \left(-\frac{1}{8\pi G} \Gamma^2 \right) dx^1 dx^2 dx^3 , \\ & \int \left(\frac{1}{2} \rho_{0q} \varphi \right) dx^1 dx^2 dx^3 = \int \left(\frac{\varepsilon_0}{2} E^2 \right) dx^1 dx^2 dx^3 . \end{aligned}\right\} \quad (77)$$

According to (77), the potential energy of the ball's matter in the proper gravitational field which is associated with the scalar potential ψ is twice the potential energy associated with the field strength $\mathbf{\Gamma}$. The same is true for the electromagnetic field with the potential φ and the strength $\mathbf{E}$ both in the case of uniform arrangement of charges in the ball's volume and in case of their location on the surface only. Substituting (77) into (76) in the framework of the special theory of relativity gives the invariant energy of the system in the form of a fixed solid spherical body with uniform density of mass and charge, taking into account the energy of their proper potential fields:

$$\left(E_0 \right)_{SR} = \int \begin{pmatrix} \rho_0 c^2 + \frac{1}{2} \rho_0 \psi \\ + \frac{1}{2} \rho_{0q} \varphi + p_0 \\ - \frac{1}{8\pi\sigma} \left[\nabla \left(\frac{p_0}{\rho_0} \right) \right]^2 \end{pmatrix} dx^1 dx^2 dx^3 . \quad (78)$$

This calculation is apparently incomplete, since in reality inside any body there are particles, which cannot be as motionless as the body itself is. Therefore, in (78), in addition to the pressure and its gradient within the body, it is necessary to add the kinetic energy of motion of all the particles which constitute the body.

The metric

Substituting (74) and (39) into (43), we find the expression for the scalar curvature R:

$$\left.\begin{aligned} ckR &= -2D_\mu J^\mu - 2A_\mu j^\mu \\ &\quad - 2u_\mu J^\mu - 2\pi_\mu J^\mu \\ &= -2\chi , \end{aligned}\right\} \quad (79)$$

while $ck = -\frac{c^4}{16\pi G\beta}$, where β is a constant of the order of unity.

As it can be seen, the scalar curvature is zero in the whole space outside the body. The equation $R=0$ does not mean, however, that the spacetime is flat as in the special theory of relativity, since the curvature of spacetime is determined by the components of the Riemann curvature tensor.

We will now substitute (74) into the equation for the metric (38):

$$\left.\begin{aligned}&-2ck\,R^{\alpha\beta}+ck\,R\,g^{\alpha\beta}=\\&-D_{\mu}J^{\mu}\,g^{\alpha\beta}+U^{\alpha\beta}-A_{\mu}j^{\mu}\,g^{\alpha\beta}+W^{\alpha\beta}\\&-u_{\mu}J^{\mu}\,g^{\alpha\beta}+B^{\alpha\beta}-\pi_{\mu}J^{\mu}\,g^{\alpha\beta}+P^{\alpha\beta},\end{aligned}\right\}\quad(80)$$

that also can be written using (39) as follows:

$$\left.\begin{aligned}&-2ck\,R^{\alpha\beta}+ck\,R\,g^{\alpha\beta}=\\&\quad U^{\alpha\beta}+W^{\alpha\beta}+B^{\alpha\beta}+P^{\alpha\beta}-\chi g^{\alpha\beta}.\end{aligned}\right\}\quad(81)$$

If we take the covariant derivative of (81), the left side of the equation vanishes due to the property of the Einstein tensor located there. The right side, with regard to the equation of motion (35) and provided that the metric tensor $g^{\alpha\beta}$ in covariant differentiation behaves as a constant and χ is a constant, vanishes too.

In (80), we can use (79) to replace the scalar curvature:

$$\left.\begin{aligned}-2ck\,R^{\alpha\beta}=\,&D_{\mu}J^{\mu}\,g^{\alpha\beta}+U^{\alpha\beta}\\&+A_{\mu}j^{\mu}\,g^{\alpha\beta}+W^{\alpha\beta}\\&+u_{\mu}J^{\mu}\,g^{\alpha\beta}+B^{\alpha\beta}\\&+\pi_{\mu}J^{\mu}\,g^{\alpha\beta}+P^{\alpha\beta}.\end{aligned}\right\}\quad(82)$$

If we sum up (80) and (82) and divide the result by 2, we will obtain the following equation for the metric:

$$\left.\begin{aligned}&R^{\alpha\beta}-\frac{1}{4}R\,g^{\alpha\beta}=\\&\quad-\frac{1}{2ck}(B^{\alpha\beta}+U^{\alpha\beta}+W^{\alpha\beta}+P^{\alpha\beta}),\end{aligned}\right\}\quad(83)$$

while with regard to (79) $\nabla_{\beta}R=0$, according to (35) $\nabla_{\beta}(B^{\alpha\beta}+U^{\alpha\beta}+W^{\alpha\beta}+P^{\alpha\beta})=0$ and $\nabla_{\beta}\left(R^{\alpha\beta}-\frac{1}{2}R\,g^{\alpha\beta}\right)=0$ as the property of the Einstein tensor.

In empty space according to (83), the curvature tensor $R^{\alpha\beta}$ depends only on the stress-energy tensors of the gravitational and electromagnetic fields $U^{\alpha\beta}$ and $W^{\alpha\beta}$, so these fields change the curvature of spacetime outside the bodies. We will note that in equation (83), the cosmological constant Λ and the tensor product of the type $D_{\mu}J^{\mu}\,g^{\alpha\beta}$ are missing. This fact makes determination of the metric tensor components much easier.

If we compare (83) with the Einstein equation (46), then two major differences will be found out — at the right side of (83) stress-energy tensors $U^{\alpha\beta}$, $B^{\alpha\beta}$ and $P^{\alpha\beta}$ are present, and in addition the coefficient in front of the scalar curvature R is two times less than in (46).

The Energy Components

In Newtonian mechanics, the relations for the Lagrangian and the total energy are known: $L=E_k-U$, $E_t=E_k+U$, where E_k denotes the kinetic energy, which depends only on the velocity, and U denotes the potential energy of the system, depending both on the coordinates and the velocity. In relativistic physics, instead of individual scalar functions and three-dimensional vectors, four-vectors and four-tensors are used, in which the scalar functions and three-dimensional vectors are combined into one whole. In addition, instead of the negative total energy E_t, the positive relativistic energy E is usually used. While we have already determined the energy E in (73), then for the Lagrangian (54) we should additionally replace the scalar curvature R with the help of (79) and the cosmological constant Λ with the help of (74). Taking the relation: $\left(\sqrt{-g}\,dx^1dx^2dx^3\right)_0=\frac{u^0}{c}\sqrt{-g}\,dx^1dx^2dx^3$ into account this will give the following:

$$\left.\begin{aligned} L &= \frac{1}{c}\sum_{n=1}^{N_p}\int^{n}\begin{pmatrix} -\rho_0\left(\vartheta-\overset{n}{\mathbf{v}}\cdot\overset{n}{\mathbf{U}}\right)-\rho_0(\psi-\overset{n}{\mathbf{v}}\cdot\overset{n}{\mathbf{D}}) \\ -\rho_{0q}(\varphi-\overset{n}{\mathbf{v}}\cdot\overset{n}{\mathbf{A}})-\rho_0(\wp-\overset{n}{\mathbf{v}}\cdot\overset{n}{\mathbf{\Pi}}) \end{pmatrix} u^0\sqrt{-g}\,dx^1dx^2dx^3 \\ &+\int\begin{pmatrix} \frac{c^2}{16\pi G}\Phi_{\mu\nu}\Phi^{\mu\nu}-\frac{1}{4\mu_0}F_{\mu\nu}F^{\mu\nu} \\ -\frac{c^2}{16\pi\eta}u_{\mu\nu}u^{\mu\nu}-\frac{c^2}{16\pi\sigma}f_{\mu\nu}f^{\mu\nu} \end{pmatrix}\sqrt{-g}\,dx^1dx^2dx^3, \end{aligned}\right\} \tag{84}$$

Calculating the energy E_V, which is associated with the four-dimensional motion, as a half-sum of the relativistic energy (73) and the Lagrangian (84), we find:

$$\left.\begin{aligned} E_V &= \frac{1}{2}(E+L) \\ &= \frac{1}{2c}\sum_{n=1}^{N_p}\int^{n}\left(\rho_0\overset{n}{\mathbf{v}}\cdot\overset{n}{\mathbf{U}}+\rho_0\overset{n}{\mathbf{v}}\cdot\overset{n}{\mathbf{D}}+\rho_{0q}\overset{n}{\mathbf{v}}\cdot\overset{n}{\mathbf{A}}+\rho_0\overset{n}{\mathbf{v}}\cdot\overset{n}{\mathbf{\Pi}}\right)u^0\sqrt{-g}\,dx^1dx^2dx^3. \end{aligned}\right\} \tag{85}$$

where $\overset{n}{\mathbf{v}}$ is three-velocity vector of the particle with the number n.

If in (57) we replace the masses $\overset{n}{m}$ and charges $\overset{n}{q}$ by the corresponding integrals in the form: $\overset{n}{m}=\int^{n}\rho_0\left(\sqrt{-g}\,dx^1dx^2dx^3\right)_0$, $\overset{n}{q}=\int^{n}\rho_{0q}\left(\sqrt{-g}\,dx^1dx^2dx^3\right)_0$, and transform the volume units in the form $\left(\sqrt{-g}\,dx^1dx^2dx^3\right)_0=\frac{u^0}{c}\sqrt{-g}\,dx^1dx^2dx^3$, then we obtain the relation $E_V=\frac{1}{2}\sum_{n=1}^{N_p}\left(\overset{n}{\mathbf{P}}\cdot\overset{n}{\mathbf{v}}\right)$. As we can see, the kinetic energy E_V of the system in the reference frame of the center of mass vanishes only when the velocities $\overset{n}{\mathbf{v}}$ of all the system's particles at the same time vanish.

We will determine the potential energy U_P as a half-difference of the relativistic energy (73) and the Lagrangian (84):

$$\left.\begin{aligned} U_P &= \frac{1}{2}(E-L)=\frac{1}{c}\int\left(\rho_0\vartheta+\rho_0\psi+\rho_{0q}\varphi+\rho_0\wp\right)u^0\sqrt{-g}\,dx^1dx^2dx^3 \\ &-\frac{1}{2c}\sum_{n=1}^{N_p}\int^{n}\begin{pmatrix} \rho_0\overset{n}{\mathbf{v}}\cdot\overset{n}{\mathbf{U}}+\rho_0\overset{n}{\mathbf{v}}\cdot\overset{n}{\mathbf{D}} \\ +\rho_{0q}\overset{n}{\mathbf{v}}\cdot\overset{n}{\mathbf{A}}+\rho_0\overset{n}{\mathbf{v}}\cdot\overset{n}{\mathbf{\Pi}} \end{pmatrix}u^0\sqrt{-g}\,dx^1dx^2dx^3 \\ &-\int\left(\frac{c^2}{16\pi G}\Phi_{\mu\nu}\Phi^{\mu\nu}-\frac{1}{4\mu_0}F_{\mu\nu}F^{\mu\nu}-\frac{c^2}{16\pi\eta}u_{\mu\nu}u^{\mu\nu}-\frac{c^2}{16\pi\sigma}f_{\mu\nu}f^{\mu\nu}\right)\sqrt{-g}\,dx^1dx^2dx^3. \end{aligned}\right\} \tag{86}$$

For a solid body in the limit of the special theory of relativity, when $\sqrt{-g}=1$, $u^0=c\overset{n}{\gamma}$, $\overset{n}{\gamma}=\frac{1}{\sqrt{1-\overset{n}{v}{}^2/c^2}}$, the expression for the kinetic energy (85) of the system is as follows:

$$(E_V)_{SR} = \frac{1}{2} \sum_{n=1}^{N_p} \int^{n} \begin{pmatrix} \rho_0 \overset{n}{\mathbf{v}} \cdot \overset{n}{\mathbf{U}} + \rho_0 \overset{n}{\mathbf{v}} \cdot \overset{n}{\mathbf{D}} \\ + \rho_{0q} \overset{n}{\mathbf{v}} \cdot \overset{n}{\mathbf{A}} + \rho_0 \overset{n}{\mathbf{v}} \cdot \overset{n}{\mathbf{\Pi}} \end{pmatrix} \overset{n}{\gamma} dx^1 dx^2 dx^3. \qquad (87)$$

The main part of the kinetic energy is proportional to the square of the velocity, and vector potentials of all fields, including the velocity field and pressure field, make contribution to this part of the energy.

For the potential energy (86) of a solid body in the limit of special theory of relativity, the tensor product $u_{\mu\nu} u^{\mu\nu}$ according to (E8) tends to zero. We will also take into account the values of other tensor products:

$$\frac{c^2}{16\pi G} \Phi_{\mu\nu} \Phi^{\mu\nu} = -\frac{1}{8\pi G} \left(\Gamma^2 - c^2 \Omega^2 \right),$$

$$\frac{c^2 \varepsilon_0}{4} F_{\mu\nu} F^{\mu\nu} = -\frac{\varepsilon_0}{2} (E^2 - c^2 B^2),$$

$$\frac{c^2}{16\pi \sigma} f_{\mu\nu} f^{\mu\nu} = -\frac{1}{8\pi \sigma} (C^2 - c^2 I^2).$$

It gives the following:

$$\begin{aligned} (U_P)_{SR} = & \int \left(\rho_0 \vartheta + \rho_0 \psi + \rho_{0q} \varphi + \rho_0 \wp \right) \overset{n}{\gamma} \, dx^1 dx^2 dx^3 \\ & - \frac{1}{2} \sum_{n=1}^{N_p} \int^{n} \left(\rho_0 \overset{n}{\mathbf{v}} \cdot \overset{n}{\mathbf{U}} + \rho_0 \overset{n}{\mathbf{v}} \cdot \overset{n}{\mathbf{D}} + \rho_{0q} \overset{n}{\mathbf{v}} \cdot \overset{n}{\mathbf{A}} + \rho_0 \overset{n}{\mathbf{v}} \cdot \overset{n}{\mathbf{\Pi}}) \right) \overset{n}{\gamma} dx^1 dx^2 dx^3 \\ & + \int \left(\frac{1}{8\pi G} \left(\Gamma^2 - c^2 \Omega^2 \right) - \frac{\varepsilon_0}{2} (E^2 - c^2 B^2) - \frac{1}{8\pi \sigma} (C^2 - c^2 I^2) \right) dx^1 dx^2 dx^3. \end{aligned}$$

The potential energy depends also on the velocity. If $\overset{n}{\mathbf{v}} = 0$ for all material particles of the system, then the potential energy of the system remains, taking the field energy into account:

$$\left. \begin{aligned} (U_P)_{SR} = & \int \left(\rho_0 c^2 + \rho_0 \psi + \rho_{0q} \varphi + \rho_0 \wp \right) dx^1 dx^2 dx^3 \\ & + \int \left(\frac{1}{8\pi G} \left(\Gamma^2 - c^2 \Omega^2 \right) - \frac{\varepsilon_0}{2} (E^2 - c^2 B^2) - \frac{1}{8\pi \sigma} (C^2 - c^2 I^2) \right) dx^1 dx^2 dx^3. \end{aligned} \right\} \qquad (88)$$

In the absence of external fields and internal motions in the fixed system, in (88) the fields Ω, B, I become equal to zero. As a result, with regard to (77), the potential energy becomes equal to the relativistic energy (78) for a fixed ideal solid body.

Conclusions

We have presented the Lagrangian of the system as consisting of one term for the curvature and four pairs of terms of identical form for each of the four fields: gravitational and electromagnetic fields, acceleration field and pressure field. As a result, for each field we have obtained equations coinciding in form with each other. The spacetime is also represented by its proper tensor metric field $g_{\alpha\beta}$. The mass four-current J^{μ} interacts with the specified fields, gaining energy in them. Moreover, the electromagnetic field changes the energy of electromagnetic four-current j^{μ}. However, the fields also have their proper energy and momentum, which are part of the tensors $U^{\alpha\beta}$ (5), $W^{\alpha\beta}$ (8), $B^{\alpha\beta}$ (11) and $P^{\alpha\beta}$ (14), respectively.

The similarity of field equations implies the necessity of gauge; not only of the four-potentials of the gravitational and electromagnetic fields, but also of the four-potentials of the acceleration field and pressure field, as well as of the mass four-current J^{μ} and electromagnetic four-current j^{μ}. From the standpoint of physics, the meaning of such gauges is that the source of divergence of the three-velocity vector of small volume may be the time changes in the particle's energy in any fields which are present in the given volume.

This may be the particle's energy in the velocity field, the energy in the pressure field or the energy in the gravitational or electromagnetic fields.

In contrast to the standard approach, we do not use any of the variety of known forms of stress-energy tensors of matter. Instead, the energy and momentum of the matter are described based on the acceleration field, the acceleration field tensor and the stress-energy tensor of the acceleration field. The contribution of pressure to the system's energy and momentum, respectively, is described through the pressure field with the help of the pressure field tensor and the stress-energy tensor of the pressure field. In this case, the acceleration field and the pressure field, as well as the electromagnetic and gravitational fields, are regarded as the four-dimensional vector fields with their own four-potentials.

Representation of the gravitational field as a vector field is performed within the covariant theory of gravitation [3-4], in contrast to the general theory of relativity, where gravitation is described indirectly through the spacetime geometry and is considered as a metric tensor field. We consider as an advantage of our approach the fact that the energy and momentum of the gravitational field at each point are uniquely determined with the help of the stress-energy tensor of the gravitational field; whereas, in the general theory of relativity, we have to restrict ourselves only to the corresponding pseudotensor, such as the Landau-Lifshitz stress-energy pseudotensor [13].

In order to uniquely identify the relativistic energy of a particle or a matter unit, we used a special gauge of the cosmological constant, giving this constant the meaning of the rest energy of the particle with "turned-off" external fields and influences. This led to the expression for the relativistic energy of the system (73) and to the equation for the metric (83), the right side of which is the sum of four stress-energy tensors of the fields.

In the absence of the cosmological constant in the Lagrangian (1), it would be impossible to perform the specified calibration, the physical system's energy would be uncertain and the presented theory would remain unfinished. In our approach, the cosmological constant does not reflect the energy density of the empty cosmic space, or the so-called dark energy, but rather the energy density of the matter scattered in space. Given that $-2ck=\frac{c^4}{8\pi G\beta}$, where β is a constant of the order of unity, it follows from (74) that $\Lambda \approx \frac{16\pi G\rho_0\beta}{c^2}$. Substituting here the standard estimate of the cosmological constant $\Lambda \approx 10^{-52}$ m^{-2}, we find the corresponding mass density: $\rho_0 \approx 3\times 10^{-27}$ kg/m. This density is sufficiently close to the density of cosmic matter, averaged over the entire space.

It can be noted that our expression for the relativistic energy and the equation for the metric differ substantially from those obtained in the general theory of relativity. For the energy it follows from the fact that instead of the stress-energy tensor of matter we use the stress-energy tensors of the acceleration field and the pressure field, while the gravitational field is directly included in the energy, and not indirectly through the metric.

Let us take the Einstein equation for the metric with the cosmological constant from [14]. In the general case, the right-hand side of this equation contains the stress-energy tensor of the electromagnetic field $W^{\alpha\beta}$ and the stress-energy tensor of matter $\phi^{\alpha\beta}$:

$$\left.\begin{array}{l} R^{\alpha\beta}-\frac{1}{2}R\,g^{\alpha\beta}+\Lambda\,g^{\alpha\beta}= \\ \quad \frac{8\pi G}{c^4}\left(W^{\alpha\beta}+\phi^{\alpha\beta}\right). \end{array}\right\} \qquad (89)$$

The simplest form of the stress-energy tensor of matter without taking the pressure into account is the expression in terms of the mass density and the four-velocity: $\phi^{\alpha\beta}=\rho_0 u^\alpha u^\beta$. Contraction (89) with the metric tensor $g_{\alpha\beta}$ gives the following:

$$\Lambda=\frac{8\pi G\phi}{4c^4}+\frac{R}{4},$$

where $\phi=g_{\alpha\beta}\phi^{\alpha\beta}$.

After substituting Λ in (89), the equation for the metric is transformed as follows:

$$\left.\begin{array}{l} R^{\alpha\beta}-\frac{1}{4}R\,g^{\alpha\beta}= \\ \quad \frac{8\pi G}{c^4}\left(W^{\alpha\beta}+\phi^{\alpha\beta}-\frac{\phi}{4}g^{\alpha\beta}\right). \end{array}\right\} \quad (90)$$

Now, equation for the metric (90) in the general theory of relativity can be compared with our equation for the metric (83). The main difference is that in (83) all the tensors at the right side act the same way, and in contraction with the metric tensor they vanish. But, it is not the case in (90) – if the expression $g_{\alpha\beta}W^{\alpha\beta}=0$ is valid for the electromagnetic stress-energy tensor, then for the stress-energy tensor of matter the relation $g_{\alpha\beta}\phi^{\alpha\beta}=0$ does not hold, so that in (90) one more term $-\frac{\phi}{4}g^{\alpha\beta}$ is needed. As a result, in the general theory of relativity, not only the gravitational field is represented in a special way, through the metric tensor, which differs from the method of introducing the electromagnetic field into the equation for the metric, but also the stress-energy tensor of matter $\phi^{\alpha\beta}$ is asymmetric with respect to the metric, in contrast to the stress-energy tensor of the electromagnetic field $W^{\alpha\beta}$.

Appendix A. Variation of the sixth term in the action function

We need to find the variation for the sixth term in (1):

$$\delta S_6=-\frac{1}{c}\int\delta\left(u_\mu J^\mu\sqrt{-g}\right)d\Sigma. \quad (A1)$$

We will need the expressions for variation of the metric tensor and the four-vector of the mass current, which can be found, for example, in [7], [9] and [14]:

$$\delta g^{\mu\nu}=-g^{\mu\alpha}g^{\nu\beta}\delta g_{\alpha\beta},$$

$$\delta\sqrt{-g}=\frac{\sqrt{-g}}{2}g^{\alpha\beta}\delta g_{\alpha\beta}. \quad (A2)$$

$$\left.\begin{array}{l} \delta J^\beta=\nabla_\sigma\left(J^\sigma\xi^\beta-J^\beta\xi^\sigma\right) \\ \quad =\frac{1}{\sqrt{-g}}\partial_\sigma\left[\sqrt{-g}\left(J^\sigma\xi^\beta-J^\beta\xi^\sigma\right)\right]. \end{array}\right\} \quad (A3)$$

In view of (A2) and (A3), we have the following:

$$\left.\begin{array}{l} \delta\left(u_\mu J^\mu\sqrt{-g}\right) \\ \quad =u_\mu\sqrt{-g}\,\delta J^\mu+u_\mu J^\mu\delta\sqrt{-g} \\ \qquad +J^\mu\sqrt{-g}\,\delta u_\mu \\ \quad =u_\mu\,\partial_\sigma\left[\sqrt{-g}\left(J^\sigma\xi^\mu-J^\mu\xi^\sigma\right)\right] \\ \qquad +\frac{1}{2}u_\mu J^\mu g^{\alpha\beta}\sqrt{-g}\,\delta g_{\alpha\beta} \\ \qquad +J^\mu\sqrt{-g}\,\delta u_\mu. \end{array}\right\} \quad (A4)$$

We will transform the first term in (A4) with the help of functions' product differentiation by parts:

$$\begin{array}{l} u_\mu\,\partial_\sigma\left[\sqrt{-g}\left(J^\sigma\xi^\mu-J^\mu\xi^\sigma\right)\right]= \\ \quad \partial_\sigma\left[u_\mu\sqrt{-g}\left(J^\sigma\xi^\mu-J^\mu\xi^\sigma\right)\right] \\ \qquad -\sqrt{-g}\left(J^\sigma\xi^\mu-J^\mu\xi^\sigma\right)\partial_\sigma u_\mu. \end{array}$$

In action variation, the term with the divergence can be neglected; the remaining term can be transformed as follows:

$$\begin{array}{l} -\sqrt{-g}\left(J^\sigma\xi^\mu-J^\mu\xi^\sigma\right)\partial_\sigma u_\mu= \\ \quad -(\partial_\sigma u_\mu-\partial_\mu u_\sigma)J^\sigma\xi^\mu\sqrt{-g}= \\ \quad u_{\mu\sigma}J^\sigma\xi^\mu\sqrt{-g}. \end{array}$$

Substituting these results in (A4) and then in (A1), we find:

$$\delta S_6=\int\left(\begin{array}{l} -\frac{1}{c}u_{\beta\sigma}J^\sigma\xi^\beta-\frac{1}{c}J^\beta\delta u_\beta \\ -\frac{1}{2c}u_\mu J^\mu g^{\alpha\beta}\delta g_{\alpha\beta} \end{array}\right)\sqrt{-g}\,d\Sigma.$$

Appendix B. Variation of the seventh term in the action function

Variation for the seventh term in (1) for the special case, when η is a constant, taking into account (A2) will be equal to:

$$\delta S_7 = -\frac{c}{16\pi\eta}\int \delta\left(u_{\mu\nu}u^{\mu\nu}\sqrt{-g}\right) d\Sigma ,$$

$$\left.\begin{aligned} &\delta\left(u_{\mu\nu}u^{\mu\nu}\sqrt{-g}\right) \\ &\quad = \delta\left(u_{\mu\nu}u^{\mu\nu}\right)\sqrt{-g} + u_{\mu\nu}u^{\mu\nu}\delta\sqrt{-g} \\ &\quad = u_{\mu\nu}\delta u^{\mu\nu}\sqrt{-g} + u^{\mu\nu}\delta u_{\mu\nu}\sqrt{-g} \\ &\quad + \frac{1}{2}u_{\mu\nu}u^{\mu\nu}g^{\alpha\beta}\sqrt{-g}\ \delta g_{\alpha\beta} . \end{aligned}\right\} \qquad (B1)$$

Since $u^{\mu\nu} = g^{\mu\alpha}g^{\beta\nu}u_{\alpha\beta}$, the tensor $u_{\alpha\beta}$ is antisymmetric, then using the expression for $\delta g^{\beta\nu}$ from (A2), we find:

$$\begin{aligned} &u_{\mu\nu}\delta u^{\mu\nu}\sqrt{-g} = u_{\mu\nu}\delta\left(g^{\mu\alpha}g^{\beta\nu}u_{\alpha\beta}\right)\sqrt{-g} \\ &= u_{\mu\nu}\begin{bmatrix} g^{\mu\alpha}g^{\beta\nu}\delta u_{\alpha\beta} + g^{\mu\alpha}u_{\alpha\beta}\delta g^{\beta\nu} + \\ + g^{\beta\nu}u_{\alpha\beta}\delta g^{\mu\alpha} \end{bmatrix}\sqrt{-g} \\ &= u^{\alpha\beta}\delta u_{\alpha\beta}\sqrt{-g} + 2u_{\mu\nu}g^{\mu\alpha}u_{\alpha\beta}\sqrt{-g}\ \delta g^{\beta\nu} \\ &= u^{\alpha\beta}\delta u_{\alpha\beta}\sqrt{-g} - 2g^{\nu\beta}u_{\kappa\nu}u^{\kappa\alpha}\sqrt{-g}\ \delta g_{\alpha\beta} . \end{aligned}$$

Substituting this expression in (B1) gives the following:

$$\left.\begin{aligned} &\delta\left(u_{\mu\nu}u^{\mu\nu}\sqrt{-g}\right) = 2u^{\alpha\beta}\delta u_{\alpha\beta}\sqrt{-g} \\ &\quad - 2g^{\nu\beta}u_{\kappa\nu}u^{\kappa\alpha}\sqrt{-g}\ \delta g_{\alpha\beta} \\ &\quad + \frac{1}{2}u_{\mu\nu}u^{\mu\nu}g^{\alpha\beta}\sqrt{-g}\ \delta g_{\alpha\beta} . \end{aligned}\right\} \qquad (B2)$$

We will denote by $B^{\alpha\beta}$ the stress-energy tensor of the acceleration field:

$$B^{\alpha\beta} = \frac{c^2}{4\pi\eta}\begin{pmatrix} -g^{\alpha\nu}u_{\kappa\nu}u^{\kappa\beta} \\ + \frac{1}{4}g^{\alpha\beta}u_{\mu\nu}u^{\mu\nu} \end{pmatrix} . \qquad (B3)$$

Given that $u_{\mu\nu} = \nabla_\mu u_\nu - \nabla_\nu u_\mu = \partial_\mu u_\nu - \partial_\nu u_\mu$, using differentiation by parts, as well as the equation which is valid for the antisymmetric tensor: $\partial_\alpha\left(u^{\alpha\beta}\sqrt{-g}\right) = \sqrt{-g}\,\nabla_\alpha u^{\alpha\beta}$, for the term $2u^{\alpha\beta}\delta u_{\alpha\beta}\sqrt{-g}$ in (B2), we obtain:

$$\begin{aligned} &2u^{\alpha\beta}\delta u_{\alpha\beta}\sqrt{-g} \\ &\quad = 2u^{\alpha\beta}\delta\left(\partial_\alpha u_\beta - \partial_\beta u_\alpha\right)\sqrt{-g} \\ &\quad = 2u^{\alpha\beta}\left(\partial_\alpha \delta u_\beta - \partial_\beta \delta u_\alpha\right)\sqrt{-g} \\ &\quad = 4u^{\alpha\beta}\sqrt{-g}\ \partial_\alpha \delta u_\beta \\ &\quad = 4\,\partial_\alpha\left(u^{\alpha\beta}\sqrt{-g}\ \delta u_\beta\right) - 4\,\partial_\alpha\left(u^{\alpha\beta}\sqrt{-g}\ \right)\delta u_\beta \\ &\quad = 4\,\partial_\alpha\left(u^{\alpha\beta}\sqrt{-g}\ \delta u_\beta\right) - 4\ \nabla_\alpha u^{\alpha\beta}\ \sqrt{-g}\ \delta u_\beta . \end{aligned}$$

The term $4\partial_\alpha\left(u^{\alpha\beta}\sqrt{-g}\,\delta u_\beta\right)$ in the last expression is the divergence, and it can be neglected in the variation of the action function.

Substituting the remaining term in (B2) and then in (B1) and using (B3), we find:

$$\delta S_7 = \int \begin{pmatrix} \frac{c}{4\pi\eta}\nabla_\alpha u^{\alpha\beta}\delta u_\beta - \\ -\frac{1}{2c}B^{\alpha\beta}\delta g_{\alpha\beta} \end{pmatrix}\sqrt{-g}\, d\Sigma.$$

Appendix C. Variation of the eighth term in the action function

Action variation for the eighth term in (1) has the form:

$$\delta S_8 = -\frac{1}{c}\int \delta\left(\pi_\mu J^\mu\sqrt{-g}\right) d\Sigma .$$

Acting like in Appendix A, taking (A2) and (A3) into account, we find:

$$\begin{aligned} &\delta\left(\pi_\mu J^\mu\sqrt{-g}\right) \\ &\quad = \pi_\mu\sqrt{-g}\ \delta J^\mu + \pi_\mu J^\mu\delta\sqrt{-g} + J^\mu\sqrt{-g}\ \delta\pi_\mu \\ &\quad = \pi_\mu\,\partial_\sigma\left[\sqrt{-g}\left(J^\sigma\xi^\mu - J^\mu\xi^\sigma\right)\right] \\ &\qquad + \frac{1}{2}\pi_\mu J^\mu g^{\alpha\beta}\sqrt{-g}\ \delta g_{\alpha\beta} + J^\mu\sqrt{-g}\ \delta\pi_\mu . \end{aligned}$$

$$\pi_\mu \partial_\sigma \left[\sqrt{-g} \left(J^\sigma \xi^\mu - J^\mu \xi^\sigma \right) \right]$$
$$= \partial_\sigma \left[\pi_\mu \sqrt{-g} \left(J^\sigma \xi^\mu - J^\mu \xi^\sigma \right) \right]$$
$$- \sqrt{-g} \left(J^\sigma \xi^\mu - J^\mu \xi^\sigma \right) \partial_\sigma \pi_\mu .$$

In action variation, the term with the divergence is insignificant; the second term is transformed further:

$$-\sqrt{-g} \left(J^\sigma \xi^\mu - J^\mu \xi^\sigma \right) \partial_\sigma \pi_\mu$$
$$= -(\partial_\sigma \pi_\mu - \partial_\mu \pi_\sigma) J^\sigma \xi^\mu \sqrt{-g}$$
$$= f_{\mu\sigma} J^\sigma \xi^\mu \sqrt{-g} .$$

As a result, the variation of the eighth term equals:

$$\delta S_8 = \int \left(\begin{array}{l} -\frac{1}{c} f_{\beta\sigma} J^\sigma \xi^\beta - \frac{1}{c} J^\beta \delta \pi_\beta \\ -\frac{1}{2c} \pi_\mu J^\mu g^{\alpha\beta} \delta g_{\alpha\beta} \end{array} \right) \sqrt{-g}\, d\Sigma .$$

Appendix D. Variation of the ninth term in the action function

In the special case when σ is a constant, for the variation of the ninth term in (1), with regard to (A2), we have:

$$\delta S_9 = -\frac{c}{16\pi\sigma} \int \delta \left(f_{\mu\nu} f^{\mu\nu} \sqrt{-g} \right) d\Sigma ,$$

$$\left. \begin{array}{l} \delta \left(f_{\mu\nu} f^{\mu\nu} \sqrt{-g} \right) \\ \quad = \delta \left(f_{\mu\nu} f^{\mu\nu} \right) \sqrt{-g} + f_{\mu\nu} f^{\mu\nu} \delta \sqrt{-g} \\ \quad = f_{\mu\nu} \delta f^{\mu\nu} \sqrt{-g} + f^{\mu\nu} \delta f_{\mu\nu} \sqrt{-g} \\ \qquad + \frac{1}{2} f_{\mu\nu} f^{\mu\nu} g^{\alpha\beta} \sqrt{-g}\; \delta g_{\alpha\beta} . \end{array} \right\} \quad \text{(D1)}$$

Replacing $f^{\mu\nu} = g^{\mu\alpha} g^{\beta\nu} f_{\alpha\beta}$ and using $\delta g^{\beta\nu}$ in (A2), we transform the first term of the equation and then substitute it in (D1):

$$f_{\mu\nu} \delta f^{\mu\nu} \sqrt{-g}$$
$$= f_{\mu\nu} \delta \left(g^{\mu\alpha} g^{\beta\nu} f_{\alpha\beta} \right) \sqrt{-g}$$
$$= f_{\mu\nu} \left[\begin{array}{l} g^{\mu\alpha} g^{\beta\nu} \delta f_{\alpha\beta} + g^{\mu\alpha} f_{\alpha\beta} \delta g^{\beta\nu} \\ + g^{\beta\nu} f_{\alpha\beta} \delta g^{\mu\alpha} \end{array} \right] \sqrt{-g}$$
$$= f^{\alpha\beta} \delta f_{\alpha\beta} \sqrt{-g} + 2 f_{\mu\nu} g^{\mu\alpha} f_{\alpha\beta} \sqrt{-g}\; \delta g^{\beta\nu}$$
$$= f^{\alpha\beta} \delta f_{\alpha\beta} \sqrt{-g} - 2 g^{\nu\beta} f_{\kappa\nu} f^{\kappa\alpha} \sqrt{-g}\; \delta g_{\alpha\beta} .$$

$$\delta \left(f_{\mu\nu} f^{\mu\nu} \sqrt{-g} \right)$$
$$= 2 f^{\alpha\beta} \delta f_{\alpha\beta} \sqrt{-g}$$
$$- 2 g^{\nu\beta} f_{\kappa\nu} f^{\kappa\alpha} \sqrt{-g}\; \delta g_{\alpha\beta}$$
$$+ \frac{1}{2} f_{\mu\nu} f^{\mu\nu} g^{\alpha\beta} \sqrt{-g}\; \delta g_{\alpha\beta} .$$

We will denote by $P^{\alpha\beta}$ the stress-energy tensor of the pressure field:

$$P^{\alpha\beta} = \frac{c^2}{4\pi\sigma} \left(\begin{array}{l} -g^{\alpha\nu} f_{\kappa\nu} f^{\kappa\beta} \\ + \frac{1}{4} g^{\alpha\beta} f_{\mu\nu} f^{\mu\nu} \end{array} \right) . \qquad \text{(D2)}$$

We will transform the term $2 f^{\alpha\beta} \delta f_{\alpha\beta} \sqrt{-g}$, given that $f_{\mu\nu} = \partial_\mu \pi_\nu - \partial_\nu \pi_\mu$, using differentiation by parts as well as equation $\partial_\alpha \left(f^{\alpha\beta} \sqrt{-g} \right) = \sqrt{-g} \nabla_\alpha f^{\alpha\beta}$ which is valid for the antisymmetric tensor:

$$2 f^{\alpha\beta} \delta f_{\alpha\beta} \sqrt{-g}$$
$$= 2 f^{\alpha\beta} \delta \left(\partial_\alpha \pi_\beta - \partial_\beta \pi_\alpha \right) \sqrt{-g}$$
$$= 2 f^{\alpha\beta} \left(\partial_\alpha \delta\pi_\beta - \partial_\beta \delta\pi_\alpha \right) \sqrt{-g}$$
$$= 4 f^{\alpha\beta} \sqrt{-g}\; \partial_\alpha \delta\pi_\beta$$
$$= 4 \partial_\alpha \left(f^{\alpha\beta} \sqrt{-g}\, \delta\pi_\beta \right)$$
$$- 4 \partial_\alpha \left(f^{\alpha\beta} \sqrt{-g} \right) \delta\pi_\beta$$
$$= 4 \partial_\alpha \left(f^{\alpha\beta} \sqrt{-g}\, \delta p_\beta \right)$$
$$- 4 \nabla_\alpha f^{\alpha\beta} \sqrt{-g}\, \delta\pi_\beta .$$

In the latter equation, the term with the divergence can be neglected, since it does not contribute to the variation of the action function. Substituting the results in (D1), we find the required variation:

$$\delta S_9 = \int \begin{pmatrix} \frac{c}{4\pi\sigma} \nabla_\alpha f^{\alpha\beta} \delta\pi_\beta \\ -\frac{1}{2c} P^{\alpha\beta} \delta g_{\alpha\beta} \end{pmatrix} \sqrt{-g}\, d\Sigma .$$

Appendix E. Acceleration tensor and equations for the acceleration field

By definition, the acceleration field appears as a result of applying the four-rotor to the four-potential:

$$u_{\mu\nu} = \nabla_\mu u_\nu - \nabla_\nu u_\mu = \partial_\mu u_\nu - \partial_\nu u_\mu .$$

The tensor $u_{\mu\nu}$ is antisymmetric and includes various components of accelerations. By its structure, this tensor is similar to the gravitational tensor $\Phi_{\mu\nu}$ and the electromagnetic tensor $F_{\mu\nu}$, each of which consists of two vector components depending on the field potentials and the velocities of the field sources.

In order to better understand the physical meaning of the acceleration field, we will introduce the following notations:

$$u_{0i} = \partial_0 u_i - \partial_i u_0 = \frac{1}{c} S_i ,$$

$$u_{ij} = \partial_i u_j - \partial_j u_i = -N_k , \qquad \text{(E1)}$$

where the indices i, j, k form triples of non-recurring numbers of the form 1,2,3 or 3,1,2 or 2,3,1; three-vectors $\mathbf{S}$ and $\mathbf{N}$ can be written by components:

$$\mathbf{S} = S_i = (S_1, S_2, S_3) = (S_x, S_y, S_z) ;$$
$$\mathbf{N} = N_i = (N_1, N_2, N_3) = (N_x, N_y, N_z) .$$

Then, the tensor $u_{\mu\nu}$ can be represented as follows:

$$u_{\mu\nu} = \begin{pmatrix} 0 & \frac{S_x}{c} & \frac{S_y}{c} & \frac{S_z}{c} \\ -\frac{S_x}{c} & 0 & -N_z & N_y \\ -\frac{S_y}{c} & N_z & 0 & -N_x \\ -\frac{S_z}{c} & -N_y & N_x & 0 \end{pmatrix} . \qquad \text{(E2)}$$

In order to simplify our further arguments, we will consider the case of the flat spacetime; i.e., Minkowski space or the spacetime of the special theory of relativity. The role of the metric tensor in this case is played by the tensor $\eta^{\alpha\beta}$, the non-zero components of which are $\eta^{00} = 1$, $\eta^{11} = \eta^{22} = \eta^{33} = -1$. With its help, we will raise the indices of the acceleration tensor:

$$\left. \begin{array}{l} u^{\alpha\beta} = \eta^{\alpha\mu}\eta^{\nu\beta} u_{\mu\nu} \\ = \begin{pmatrix} 0 & -\frac{S_x}{c} & -\frac{S_y}{c} & -\frac{S_z}{c} \\ \frac{S_x}{c} & 0 & -N_z & N_y \\ \frac{S_y}{c} & N_z & 0 & -N_x \\ \frac{S_z}{c} & -N_y & N_x & 0 \end{pmatrix} \end{array} \right\} . \qquad \text{(E3)}$$

We will expand the four-vector of the mass current: $J^\mu = \rho_0 u^\mu = \rho_0 \left(\gamma c, \gamma \mathbf{v}\right)$, where $\gamma = \frac{1}{\sqrt{1 - v^2/c^2}}$. In equations (22) and (23), we can replace the covariant derivatives ∇_β with the partial derivatives ∂_β. Now, with the help of the vectors $\mathbf{S}$ and $\mathbf{N}$, these equations can be presented as follows:

$$\nabla \cdot \mathbf{S} = 4\pi\eta\gamma\rho_0 , \; \nabla \times \mathbf{N} = \frac{1}{c^2}\frac{\partial \mathbf{S}}{\partial t} + \frac{4\pi\eta\gamma\rho_0 \mathbf{v}}{c^2} ,$$

$$\nabla \cdot \mathbf{N} = 0 , \; \nabla \times \mathbf{S} = -\frac{\partial \mathbf{N}}{\partial t} . \qquad \text{(E4)}$$

The equations (E4), obtained in the framework of the special theory of relativity for the case $\eta = const$, are similar in their form to Maxwell equations in electrodynamics.

If we multiply scalarly the second equation in (E4) by $\mathbf{S}$, multiply scalarly the fourth equation by $-\mathbf{N}$ and sum up the results, we will obtain the following:

$$\left.\begin{aligned} -\nabla\cdot[\mathbf{S}\times\mathbf{N}] = \frac{1}{2c^2}\frac{\partial(S^2+c^2N^2)}{\partial t} \\ +\frac{4\pi\eta\gamma\rho_0\mathbf{v}\cdot\mathbf{S}}{c^2}. \end{aligned}\right\} \quad \text{(E5)}$$

Equation (E5) contains the Poynting's theorem applied to the acceleration field. The meaning of this differential equation is that if in a system the work is done to accelerate the particles, then the power of this work is associated with the divergence of the acceleration field's flux and the change in time of the energy associated with the acceleration field. The relation (E5), in a generally covariant form according to (33), can be written as follows:

$$\nabla_\beta B^{0\beta} = -u^{0\beta} J_\beta .$$

We will now substitute (E2) in (30) and write the scalar and vector relations for the components of the four-acceleration $a_\beta = (a_0, a_i)$:

$$\rho_0 \frac{du_0}{d\tau} = \rho_0 a_0 = -u_{0\sigma} J^\sigma = -\frac{\gamma\rho_0}{c}\mathbf{S}\cdot\mathbf{v} ,$$

$$\left.\begin{aligned} \rho_0 \frac{du_i}{d\tau} = \rho_0 a_i = -u_{i\sigma} J^\sigma \\ = \gamma\rho_0\left(\mathbf{S}+[\mathbf{v}\times\mathbf{N}]\right). \end{aligned}\right\} \quad \text{(E6)}$$

The components of the four-acceleration are obtained from these relations after canceling ρ_0. As we can see, both vectors $\mathbf{S}$ and $\mathbf{N}$ make contribution to the space component a_i of the four-acceleration, the vector $\mathbf{S}$ has the dimension of an ordinary three-acceleration and the dimension of the vector $\mathbf{N}$ is the same as that of the frequency.

If we take into account that the four-potential of the acceleration field $u_\mu = \left(\frac{\vartheta}{c}, -\mathbf{U}\right)$ in the case of one particle can be regarded as the covariant four-velocity, then from (E1) in Minkowski space, it follows:

$$\mathbf{S} = -\nabla\vartheta - \frac{\partial\mathbf{U}}{\partial t} = -c^2\nabla\gamma - \frac{\partial(\gamma\mathbf{v})}{\partial t},$$

$$\mathbf{N} = \nabla\times\mathbf{U} = \nabla\times\left(\gamma\mathbf{v}\right). \quad \text{(E7)}$$

The vector $\mathbf{S}$ is the acceleration field strength and the vector $\mathbf{N}$ is a quantity similar in its meaning to the magnetic field induction in electrodynamics or to the torsion field in the covariant theory of gravitation (the gravitomagnetic field in the general theory of relativity). At the constant velocity $\mathbf{v} = const$, the vectors $\mathbf{S}$ and $\mathbf{N}$ vanish. If there are non-zero time derivatives or spatial gradients of the velocity, then the acceleration field with the components $\mathbf{S}$ and $\mathbf{N}$ and the acceleration tensor $u_{\mu\nu}$ appear. In this case, it is possible to state that the non-zero tensor $u_{\mu\nu}$ in the inertial reference frame leads to the corresponding inertia forces as the consequence of any acceleration of bodies relative to the chosen reference frame.

If we substitute the tensors from (E2) and (E3) into (B3), then the stress-energy tensor of the acceleration field $B^{\alpha\beta}$ will be expressed through the vectors $\mathbf{S}$ and $\mathbf{N}$. In particular, for the tensor invariant $u_{\mu\nu}u^{\mu\nu}$ and the time components of the tensor $B^{\alpha\beta}$, we have:

$$u_{\mu\nu}u^{\mu\nu} = -\frac{2}{c^2}(S^2 - c^2N^2),$$

$$B^{00} = \frac{1}{8\pi\eta}(S^2 + c^2N^2), \; B^{0i} = \frac{c}{4\pi\eta}[\mathbf{S}\times\mathbf{N}]. \quad \text{(E8)}$$

The component B^{00}, after its integration over the volume in the Lorentz reference frame, determines the energy of the acceleration field in the given volume, and the vector $\mathbf{K} = cB^{0i} = \frac{c^2}{4\pi\eta}[\mathbf{S}\times\mathbf{N}]$ is the density of the energy flux of the acceleration field. Therefore, to calculate the energy flux of the acceleration field, the vector $\mathbf{K}$ should also be integrated over the volume.

Appendix F. The pressure tensor and equations for the pressure field

The pressure tensor is built by antisymmetric differentiation of the four-potential π_ν:

$$f_{\mu\nu} = \nabla_\mu \pi_\nu - \nabla_\nu \pi_\mu = \partial_\mu \pi_\nu - \partial_\nu \pi_\mu .$$

We will introduce the following notations:

$$f_{0i} = \partial_0 \pi_i - \partial_i \pi_0 = \frac{1}{c} C_i ,$$

$$f_{ij} = \partial_i \pi_j - \partial_j \pi_i = -I_k , \qquad \text{(F1)}$$

where the indices i, j, k form triples of non-recurring numbers of the form 1,2,3 or 3,1,2 or 2,3,1; the three-vectors $\mathbf{C}$ and $\mathbf{I}$ in the Cartesian coordinates have the components: $\mathbf{C} = C_i = (C_1, C_2, C_3) = (C_x, C_y, C_z)$; $\mathbf{I} = I_i = (I_1, I_2, I_3) = (I_x, I_y, I_z)$.

In the specified notations, the tensor $f_{\mu\nu}$ can be represented by the components:

$$f_{\mu\nu} = \begin{pmatrix} 0 & \frac{C_x}{c} & \frac{C_y}{c} & \frac{C_z}{c} \\ -\frac{C_x}{c} & 0 & -I_z & I_y \\ -\frac{C_y}{c} & I_z & 0 & -I_x \\ -\frac{C_z}{c} & -I_y & I_x & 0 \end{pmatrix}. \qquad \text{(F2)}$$

In Minkowski space, the metric tensor does not depend on the coordinates and time and consists of zeros and ones. In such space, the components of the tensor $f^{\mu\nu}$ repeat the components of the tensor $f_{\mu\nu}$ and differ only in the signs of the time components:

$$f^{\mu\nu} = \begin{pmatrix} 0 & -\frac{C_x}{c} & -\frac{C_y}{c} & -\frac{C_z}{c} \\ \frac{C_x}{c} & 0 & -I_z & I_y \\ \frac{C_y}{c} & I_z & 0 & -I_x \\ \frac{C_z}{c} & -I_y & I_x & 0 \end{pmatrix}. \qquad \text{(F3)}$$

Substituting in equations (26) and (27) the covariant derivatives ∇_β with the partial derivatives ∂_β, we can represent these equations in the form of four equations for the vectors $\mathbf{C}$ and $\mathbf{I}$:

$$\nabla \cdot \mathbf{C} = 4\pi \sigma \gamma \rho_0 ,$$

$$\nabla \times \mathbf{I} = \frac{1}{c^2} \frac{\partial \mathbf{C}}{\partial t} + \frac{4\pi \sigma \gamma \rho_0 \mathbf{v}}{c^2}, \quad \nabla \cdot \mathbf{I} = 0 ,$$

$$\nabla \times \mathbf{C} = -\frac{\partial \mathbf{I}}{\partial t} . \qquad \text{(F4)}$$

We will remind that the equations (F4), obtained in the framework of the special theory of relativity, are valid for the case of $\sigma = const$. Similarly to (E5), we obtain the equation of local pressure energy conservation:

$$\left. \begin{aligned} -\nabla \cdot [\mathbf{C} \times \mathbf{I}] = \frac{1}{2c^2} \frac{\partial (C^2 + c^2 I^2)}{\partial t} \\ + \frac{4\pi \sigma \gamma \rho_0 \mathbf{v} \cdot \mathbf{C}}{c^2} . \end{aligned} \right\}$$

This equation also follows from equation (34) and can be written with the help of the tensor $P^{\alpha\beta}$ according to (D2) as follows:

$$\nabla_\beta P^{0\beta} = -f^{0\beta} J_\beta .$$

Tensor invariant $f_{\mu\nu} f^{\mu\nu}$ and the time components of the tensor $P^{\alpha\beta}$ are expressed with the help of (F2) and (F3) through the vectors $\mathbf{C}$ and $\mathbf{I}$:

$$f_{\mu\nu} f^{\mu\nu} = -\frac{2}{c^2} (C^2 - c^2 I^2) ,$$

$$P^{00} = \frac{1}{8\pi\sigma} (C^2 + c^2 I^2) , \quad P^{0i} = \frac{c}{4\pi\sigma} [\mathbf{C} \times \mathbf{I}] . \qquad \text{(F5)}$$

The component P^{00} of the stress-energy tensor of pressure determines the pressure energy density inside the bodies, and the vector $\mathbf{F} = c P^{0i} = \frac{c^2}{4\pi\sigma} [\mathbf{C} \times \mathbf{I}]$ defines the density of the pressure energy flux.

We will now estimate the quantity $f_{i\sigma}J^{\sigma}$ with the index $i=1,2,3$. According to (31), this quantity determines the contribution of the pressure field into the total density of the force acting on the particle. In view of (F2), it turns out that the density of the pressure force has two components:

$$f_{i\sigma}J^{\sigma}=-\gamma\rho_0\left(\mathbf{C}+[\mathbf{v}\times\mathbf{I}]\right).$$

For comparison, the time component is the density of the pressure force capacity divided by the speed of light:

$$f_{0\sigma}J^{\sigma}=\frac{\gamma\rho_0\mathbf{v}\cdot\mathbf{C}}{c}.$$

The vector $\mathbf{C}$ has the dimension of acceleration and the vector $\mathbf{I}$ has the dimension of frequency. These vectors, with the help of (F1) and the definition of the four-potential of the pressure field $\pi_{\mu}=\frac{p_0}{\rho_0 c^2}u_{\mu}=\left(\frac{\wp}{c},-\mathbf{\Pi}\right)$ in Minkowski space, can be written as follows:

$$\mathbf{C}=-\nabla\wp-\frac{\partial\mathbf{\Pi}}{\partial t}=-\nabla\left(\frac{\gamma p_0}{\rho_0}\right)-\frac{\partial}{\partial t}\left(\frac{\gamma p_0\mathbf{v}}{\rho_0 c^2}\right),$$

$$\mathbf{I}=\nabla\times\mathbf{\Pi}=\nabla\times\left(\frac{\gamma p_0\mathbf{v}}{\rho_0 c^2}\right), \qquad \text{(F6)}$$

where u_{μ} denotes the four-velocity, p_0 is the pressure in the frame of reference associated with the particle, $\gamma=\frac{1}{\sqrt{1-v^2/c^2}}$ is the Lorentz factor and $\mathbf{v}$ is the particle velocity.

The vector $\mathbf{I}$, according to its properties, is similar to the magnetic induction vector, and the vector $\mathbf{C}$ is similar to the electric field strength. Motionless particles do not create the vector $\mathbf{I}$, and for the vanishing of the vector $\mathbf{C}$ it is also necessary that the relation $\gamma p_0/\rho_0$ would not depend on the coordinates. In this case, the contribution of the pressure field into the acceleration of the particles will be zero.

References:

[1] Misner, C.W., Thorne, K.S. and Wheeler, J.A., "Gravitation", (W.H. Freeman, San Francisco, CA, 1973).

[2] Poplawski, N.J., A Lagrangian description of interacting energy, arXiv:gr-qc/0608031v2.

[3] Fedosin, S.G., Hadronic Journal, 35(1) (2012) 35.

[4] Fedosin, S.G., Advances in Natural Science, 5(4) (2012) 55. doi: 10.3968%2Fj.ans.1715787020120504.2023.

[5] Hilbert, D., *Göttinger Nachrichten*, Math.-Phys., Kl (1915) 395.

[6] Weyl, H., "Raum, Zeit, Materie. Vorlesungen über allgemeine Relativitätstheorie", (J. Springer, Berlin, 1919).

[7] Fock, V.A., "The Theory of Space, Time and Gravitation", (Pergamon Press, London, 1959).

[8] Dirac, P.A.M., "General Theory of Relativity", (John Wiley & Sons, New-York, 1975).

[9] Pauli, W., "Theory of Relativity", (Dover Publications, New York, 1981).

[10] Born, M., *Annalen der Physik*, 333(3) (1909) 571.

[11] Fedosin, S.G., "Fizicheskie teorii i beskonechnaia vlozhennost' materii", (Perm, 2009).

[12] Утияма, Р., "Теория относительности", (Атомиздат, Москва, 1979).

[13] Landau, L.D. and Lifshitz, E.M., "The Classical Theory of Fields", Vol. 2, 4th ed. (Butterworth-Heinemann, 1975).

[14] Einstein, A., *Annalen der Physik*, 354(7) (1916) 769. doi: 10.1002/andp.19163540702.

Volume 9, Number 1, 2016. pp. 31-46

Jordan Journal of Physics

ARTICLE

Fine Particle Number Concentrations in Amman and Zarqa during Spring 2014

T. Hussein[a], **M. Halayaka**[a], **R. Abu Al-Ruz**[b], **H. Abdullah**[c], **B. Mølgaard**[d] and **T. Petäjä**[d]

[a] *Department of Physics, the University of Jordan, Amman 11942, Jordan.*
[b] *Department of Physics, Institute of Applied Technology, Abu Dhabi 107110, United Arab Emirates.*
[c] *Department of Mechanical Engineering, Osaka University, Suita 565-0871, Osaka, Japan.*
[d] *Division of Atmospheric Sciences, University of Helsinki, PL 48, FI-00014, Helsinki, Finland.*

Received on: 26/12/2015; Accepted on: 16/6/2016

Abstract: We measured the fine particle number concentrations at four sites in Amman and one site in Zarqa during March 6 – May 28, 2014. These were urban except for one, which was a sub-urban site. The highest number concentrations (24-hour median as high as 5.2×10^4 cm^{-3}) were observed at Hai Masoum; an urban site in Zarqa influenced by traffic and industrial activities. In Amman, the highest number concentrations were observed at the urban residential sites (Umm Summaq and Al-Hashmi Al-Shamali, 24-hour median as high as 4.6×10^4 cm^{-3}), whereas the lowest was at the sub-urban site (Shafa Badran, 24-hour median as high as 2.3×10^4 cm^{-3}). The daily pattern of the fine particle number concentrations was characterized by three peaks during the daytime. The first and last peaks are probably related to the morning and afternoon traffic rush hours, which are similar to those observed in the developed countries. The third peak was around midday, which is possibly related to increased traffic activities related to school buses. The lowest concentrations (~4600 cm^{-3}) at Shafa Badran were observed after midnight and before the morning rush hours. Different lowest values were observed at the five sites because of different population densities and nearby anthropogenic activities.
Keywords: Atmospheric aerosol particles, Spatial-temporal variation, Daily pattern, Background.

1. Introduction

Urban aerosols have a complex dynamic behavior, because they are a mixture of regionally transported aerosols and a wide range of locally emitted aerosols [1]. Besides being externally mixed, their composition can vary depending on the source type, geographical region, state of development and dynamic processes involved in their transformation.

While the urban aerosols impact the local air quality (e.g., loss of visibility), they also have a large spatial-scale effect, because they are not localized to the geographical location of the source area and are likely to be transported over large distances where they affect the air quality and the climate. Exposure to urban aerosols might lead to serious health effects [2–6]. As stated by the WHO, the health effects of urban aerosols are usually assessed by monitoring exposure to certain particulate matter classes (such as PM_{10} and $PM_{2.5}$), in addition to some gaseous pollutants (such as carbon oxides, nitrogen oxides, …etc.). Not long time ago, the WHO suggested that black carbon (BC, often

Corresponding Author: T. Hussein **Email**: t.hussein@ju.edu.jo

measured as elemental carbon, EC) may operate as a carrier of a wide variety of combustion-derived chemical constituents of varying toxicity. While the health effects occur at relatively low particle mass concentrations, the toxicity of inhaled particles is believed to be linked to other concentration metrics, such as the particle number or surface area concentrations [7].

As will be presented herein, the aerosol research activities in the Middle East have been limited to PM concentrations, some gaseous pollutants, chemical and elemental analysis and very few about particle number concentration. It is worth to mention two studies that presented an Enhanced Particulate Matter Surveillance Program. This program aimed at providing scientifically founded information on the physical and chemical properties of dust collected during a period of approximately 1 year in Djibouti, Afghanistan, Qatar, United Arab Emirates, Iraq and Kuwait [8–9]. The region has been under considerable development and urbanization, leading to a change in land use and surface geology. For example, dried soils and diminished vegetation cover in the Fertile Crescent have caused greater dust generation and increased dust days in the past years [10]. As it is expected, the eastern Mediterranean region will suffer warming and drying during this century leading to higher dust emissions and thus, exposure to ambient aerosols.

In Egypt, aerosol research has been the most extensive in the Arab world. It is dated back to the late 70's and early 80's of the past century [11–12]. Tadros et al. [13] reported the difference in the aerosol size distribution, which was indirectly calculated by means of the Mie theory, between agricultural and industrial sites in Egypt. More recently, Moustafa et al. [14] determined the mass size distributions of seven elemental composition aerosols at an industrial site. More about elemental and chemical analysis of aerosols can be found in Boman et al. [15], Hassan et al. [16] and El-Araby et al. [17]. Mahmoud et al. [18] utilized a box model to derive the origin and amount of emissions of black carbon in Cairo. It was also shown that the air quality of the coastal regions in North Egypt is affected by the flow bringing long-range transported anthropogenic air pollution from Europe towards North Africa, as well as the flow of desert dust from North Africa towards Europe [19]. This phenomenon was explained by certain weather conditions prevailing in the Mediterranean Sea. In another study, El-Askary and Kafatos [20] examined the influence of dust storms, dense haze and a smog-like phenomenon known as the 'black cloud' on the aerosol optical properties. The effect of meteorological conditions on air pollution and the optical properties of aerosols were examined by Elminir [21] and by El-Metwally and Alfaro [22].

In Saudi Arabia, for instance, about eleven studies focused on PM concentrations and some chemical and elemental analysis [1, 23–30]. In the United Arab Emirates, there is a very few number of articles focused on aerosols with most of them dedicated to the aerosol optical depth and its relation to the dust episodes [31–33]. In fact, airborne dust affects the aerosol optical depth on a large scale [33–35].

In Kuwait, the main focus of aerosol research was dated to the oil fire plumes in 1991 [36–41] and very few focused on aerosol dust episodes [42]. In Iraq, Dobrzhinsky et al. [43] and Engelbrecht and Jayanty [44] focused on mineral and road dust events, whereas Hamad et al. [45] presented a source apportionment analysis for $PM_{2.5}$ carbonaceous aerosols in Baghdad.

Researchers in Lebanon have given extensive attention to analyze the chemical composition of fine and coarse aerosols and its relation to certain dust outbreaks, long-range transport and local emissions [46–52]. Waked et al. [53] modeled the evolution of some air pollution parameters (O_3, CO, NO_x and $PM_{2.5}$) at a sub-urban site in Beirut. In another study, they reported the composition and source apportionment of organic aerosols in Beirut during winter 2012 [54].

To our knowledge, there is less than ten articles published on PM, some gaseous pollutants and limited chemical analysis in Jordan. For instance, Al-Momani et al. [55] and Gharaibeh et al. [56] focused on heavy metals and elemental analysis of aerosol samples in Al-Hashimya and Irbid, respectively. Soleiman et al. [57] indicated that emissions from the highly populated and industrialized Israel-Gaza coast are transported inland and lead to elevated levels of ozone over Jordan. Hamasha and Arnott [58] reported black carbon concentrations at six sites in Irbid city. Abu Allaban et al. [59] focused on dust re-suspension from limestone quarries nearby a town located north east of Amman and reported PM_{10} concentrations as high as 600 μg/m^3 with most of the airborne PM being in the coarse fraction. Schneidemesser et al. [60] determined sources and seasonal variation of organic carbon as well as the contribution to fine particulate matter ($PM_{2.5}$) in Palestine, Jordan and Israel. They recently presented an extensive analysis on the $PM_{2.5}$ to report its major chemical components including metals, ions, as well as organic and elemental carbon [61]. According to their study, the $PM_{2.5}$ varied from 20.6 to 40.3 μg/m^3 and was higher in summer compared to winter. The $PM_{2.5}$ concentrations in the spring were greatly impacted by regional dust storms. There was only one study that focused on fine particle number concentrations in Jordan, specifically in Amman city [62].

However, the previous studies mainly focused on regional aerosols (i.e., dust) and did not present information on the spatial-temporal variations of particle number concentrations within cities in the Middle East. The main objective of this study is to investigate the number concentrations of sub-micron particles at four sites within Amman and compare them with another site located in Zarqa city. The measurement campaign took place during three months: March 6 – May 28, 2014. We specifically focused on: (1) temporal variation (hourly, daily and weekly) and (2) spatial variation that covered an area confined within an equilateral triangle (9 km side length) inside Amman and extended to the location in Zarqa (at a distance of about 20 km from Amman).

2. Materials and Methods

2.1. Sites Description: the Hashemite Kingdom of Jordan

The Hashemite Kingdom of Jordan (29º–33º North and 37º–39º East) is located about 100 km east of the Mediterranean Sea. To its south is the Arabian desert and to its north is the Fertile Crescent part of Syria (Fig. 1a). It comprises a wide variety of topography: desert area (eastern and southern parts), high mountains (northern and western parts), as well as the Dead Sea and the Jordan Valley (at about 400 m below the sea level).

The population of Jordan is about 9.5 million people (by the end of 2016). One third of the population live in the capital city, Amman, which covers an area of about 50×35 km^2. The capital city itself is located in the north-western part and is comprised of a complex terrain of several mountains that makes it challenging to evaluate the air quality in the city. About 30 km north-east of Amman is located the second largest city (Zarqa) in Jordan. The topography of Zarqa is rather flat. Besides being large in population density, Zarqa accommodates a vast range of industrial activities and waste management sites.

Following our 2009 measurement campaign [61], we performed a more extensive measurement campaign in the spring season of the year 2014 to measure sub-micron particle number concentrations at four sites in Amman and one site in Zarqa (Fig. 1b). Following is a detailed description of each site. Table 1 lists the measurement sites along with the aerosol measurement period and site abbreviations, which are to be used throughout the article.

Campus of the University of Jordan – Amman: *urban-background site*

The campus of the University of Jordan (JU @ [32.0129N,35.8738E]) is a mixture of pine tree forest and buildings (3–4 floors). It can be classified as an urban-background site. It is located at about 10 km from the city center. The surrounding of the campus is mainly a populated residential area. One of the main highways is parallel to the western side of the campus.

Umm Summaq – Amman: *urban-residential site with major traffic influence*

Umm Summaq (US @ [31.9880N,35.8387E]) is located in the north-western part of Amman at about 11 km from the city center. It can be classified as an urban-residential site. The surrounding area mainly contains residential buildings, schools, two big malls and business centers. The area has developed and most of the buildings have been built just few years ago.

Shafa Badran – Amman: *suburban-residential site with minor traffic influence*

Shafa Badran (SB @ [32.0527N,35.8960E]) is located in the north-eastern part of Amman at about 13 km from the city center. It can be classified as an urban-residential site. The nature of the area is rocky landscape intersected by one of the main highways (Al-Urdon street), which links the capital Amman with the northern cities (Jarash, Ajloun, Irbid, …etc.). The residential area has been under continuous development with many multi-floor buildings rising every year.

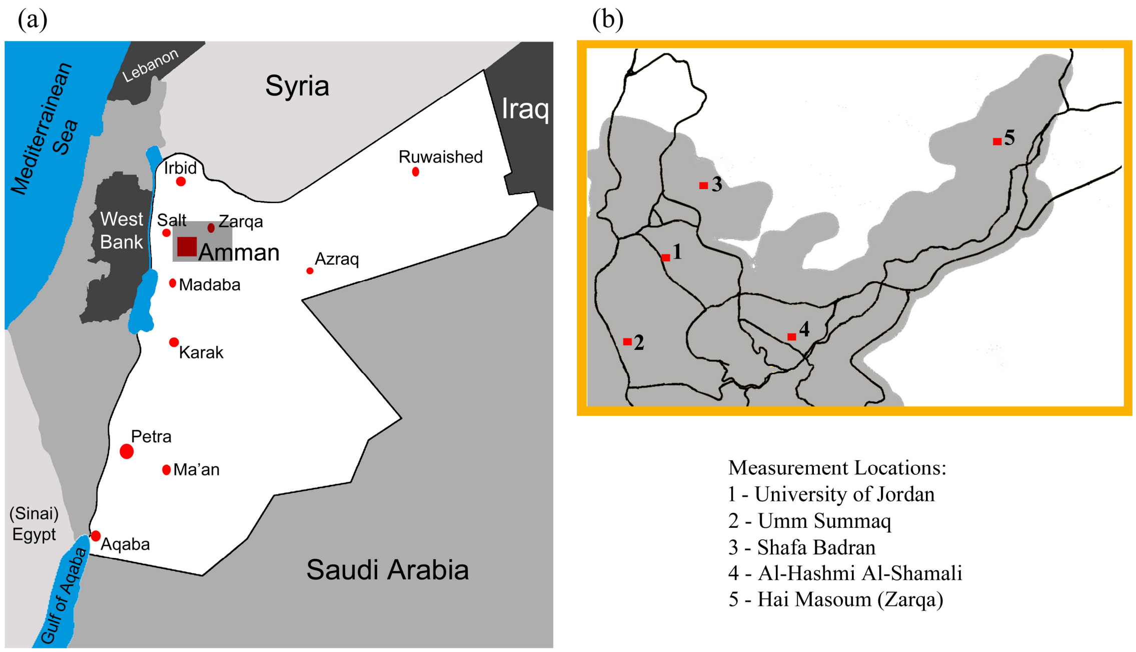

FIG. 1. (a) Map of Jordan showing the main cities and (b) A zoom in Amman and a part of Zarqa with a shade that indicates the land use. The numbers indicate the measurement site locations.

TABLE 1. Measurement sites.

Site Name	City	Classification			Period	Code
Campus of the University of Jordan	Amman	Urban	Background	--	March 6 – 18 April 14 – 30	JU1 JU2
Umm Summaq	Amman	Urban	Residential	Major traffic	March 18 – April 13	US
Shafa Badran	Amman	Sub-urban	Residential	Minor traffic	May 1 – 11	SB
Hai Masoum	Zarqa	Urban	Residential	Major traffic Minor industry	May 11 – 18	HM
Al-Hashmi Al-Shamali	Amman	Urban	Residential	Major traffic	May 19 – 26	HS

Al-Hashmi Al-Shamali – Amman: *urban-residential site with major traffic influence*

Al-Hashmi Al-Shamali (HS @ [31.9656N,35.9552E]) is located in the eastern part of Amman at about 2 km from the city center. It can be classified as an urban-residential site. The measurement location itself was situated on a slope of a mountain. Towards the south-west, there is a mountain on which the Royal Palaces are situated. Both mountains form a canyon, where one of the main roads (Al-Istiklal) connects the eastern parts to the western parts of the capital city.

Hai Ma'soum - Zarqa: *urban-residential site with major traffic and minor industry influence*

Zarqa is the second largest city in Jordan after Amman. It is located about 24 km northeast of Amman. The border between Amman and Zarqa is not well defined, because both cities have expanded toward each other over the past three decades. Zarqa accommodates densely packed residential areas mixed with military centers, small and large industrial facilities, waste management sites, as well as quarries and mines.

The measurement location at Hai Masoum (HM @ [32.0704N,36.0753E]) was chosen as close as possible to Amman, but still as far as possible from the potential sources other than local traffic. Therefore, this site can be classified as an urban-residential site with major traffic and minor industry influence.

2.2 Aerosol Measurement

The aerosol measurement was performed with a portable Condensation Particle Counter (CPC, TSI model 3007). This type of CPC is capable of recording the fine particle number concentration in the diameter range of 10 nm – 1 µm. We operated CPC with a 5-minute averaging time at each site. The sampling inlet was an about 1-meter copper tube (4–mm inner diameter). The use of a short sampling line would have minimal effects on the nominal flow rate, cut-off size and particle losses.

2.3 Weather Conditions

The Jordan Meteorological Department (JMD) provided the weather data during the measurement campaigns. The weather data used for this study was measured at the Amman Civil Airport, which is located in Marka. The airport itself is located at about 11.5 km south east of the central site in this study (the University of Jordan campus).

Records of the meteorological variables included hourly averages of the ambient temperature, relative humidity, wind direction and speed, precipitation and pressure.

According to this weather observation (Fig. 2), the wind speed was as high as 11.6 m/s, with a median of 2.7 m/s and an overall average of about 3 m/s. The overall average and median values of temperature were about 18.3 ºC, having a clear daily pattern with a maximum as high as 33 ºC (observed around midday) and a minimum as low as 4 ºC (registered around midnight). The relative humidity varied between 7% and 91% with an overall average value of about 40% (median 36%). The pressure varied between 917 mbar and 932 mbar with an average value around 925 mbar. During the whole measurement campaign, the prevailing wind direction was rarely from east; it was mainly (more than 65%) between -135° and +45°.

3. Results and Discussion

3.1 Spatial Variation

The fine particle number concentration showed a clear spatial variation within the capital city (Amman); see Tables 1–6 and Fig. 2. The lowest concentrations were observed at Shafa Badran (SB), which is a sub-urban residential site with minor traffic influence. As shown in Table 4, the daily median value varied between 1.0×10^4 and 2.3×10^4 cm^{-3} (average $1.1\times10^4 – 2.4\times10^4$ cm^{-3}). The urban background site (the University of Jordan campus, JU) had slightly higher daily median concentrations than those observed at SB (Tables 2 and 4); the daily median value varied between 1.3×10^4 and 4.0×10^4 cm^{-3} (average $1.5\times10^4 – 4.1\times10^4$ cm^{-3}).

The two urban sites (Umm Summaq and Al-Hashmi Al-Shamali) recorded somewhat higher daily median values of fine particle number concentrations (Tables 3–5). At Umm Summaq (US), the daily median value varied between 1.8×10^4 and 4.6×10^4 cm^{-3} (average 1.9×10^4 – 5.2×10^4 cm^{-3}), whereas at Al-Hashmi Al-Shamali (HS) it was $3.0\times10^4 – 4.6\times10^4$ cm^{-3} (average $3.0\times10^4 – 4.6\times10^4$ cm^{-3}). We attribute the higher concentrations at these two sites to the anthropogenic activities (mainly traffic emissions) nearby the measurement sites.

The site located in Zarqa city showed the highest concentrations with a daily median value between 2.0×10^4 and 5.2×10^4 cm^{-3} (average $2.2\times10^4 – 5.3\times10^4$ cm^{-3}); Table 6. We expect the number concentrations to be even higher in areas nearby the center of Zarqa city, because this city has high population density with industrial activities distributed within and around the city.

As illustrated in the introduction section, fine particle number concentrations in the Middle East, especially in Jordan, have not been reported with an exception for the study by Hussein et al. [61], who reported the fine particle number concentrations at JU and HS during spring 2009; about one week measurement period at each site. The observed concentrations in this study for HS (average $3.0\times10^4 – 4.6\times10^4$ cm^{-3}) agree with those previously reported by Hussein et al. [61] as $2.3\times10^4 – 6.9\times10^4$ cm^{-3}. The same can be found for the JU site; in this study, the average concentrations are 1.5×10^4 – 4.1×10^4 cm^{-3}, whereas those reported by Hussein et al. [61] were $2.5\times10^4 – 3.7\times10^4$ cm^{-3}.

In general, the observed number concentrations in Amman were higher than what is usually reported in some cities in the developed countries [63–73]. For example, Ruuskanen et al. [74] presented the number concentrations in three European cities; the average number concentrations were about 20300 cm^{-3}, 25900 cm^{-3} and 25800 cm^{-3} in Helsinki, Erfurt and Alkmaar, respectively. Recently, Reche et al. [75] reported the average particle number concentrations in the urban background of Barcelona (Spain), Lugano (Italy) and North Kensington (UK) as 16850 cm^{-3}, 14950 cm^{-3} and 12150 cm^{-3}, respectively. In the same study, the average number concentrations at road site in Bern (Switzerland) and Marylebone (UK) were 28000 and 22150 cm^{-3}, respectively. A sub-tropical urban site (Santa

Cruz Tenerife) influenced by shipping emissions had an average number concentration of about 12000 cm^{-3}, whereas at an industrial site at Huelva (Spain) it was 17900 cm^{-3}. Wehner and Wiedensohler [76] showed a seasonal trend in the particle number concentration at a moderately polluted site in Leipzig (Germany) with average concentration as 21400 cm^{-3} in winter and 11600 cm^{-3} in summer. Puustinen et al. [77] compared fine particle number concentrations between central and residential locations in four EU cities. At the central locations of Helsinki, Athens, Amsterdam and Birmingham, they were about 12500 cm^{-3}, 20300 cm^{-3}, 18100 cm^{-3} and 18800 cm^{-3}, respectively. At the residential sites, they were 4500 cm^{-3}, 15250 cm^{-3}, 26350 cm^{-3} and 16100 cm^{-3}, respectively. We, therefore, expect that the number concentrations in some locations in Amman are in line with the previous results obtained in various locations in Europe.

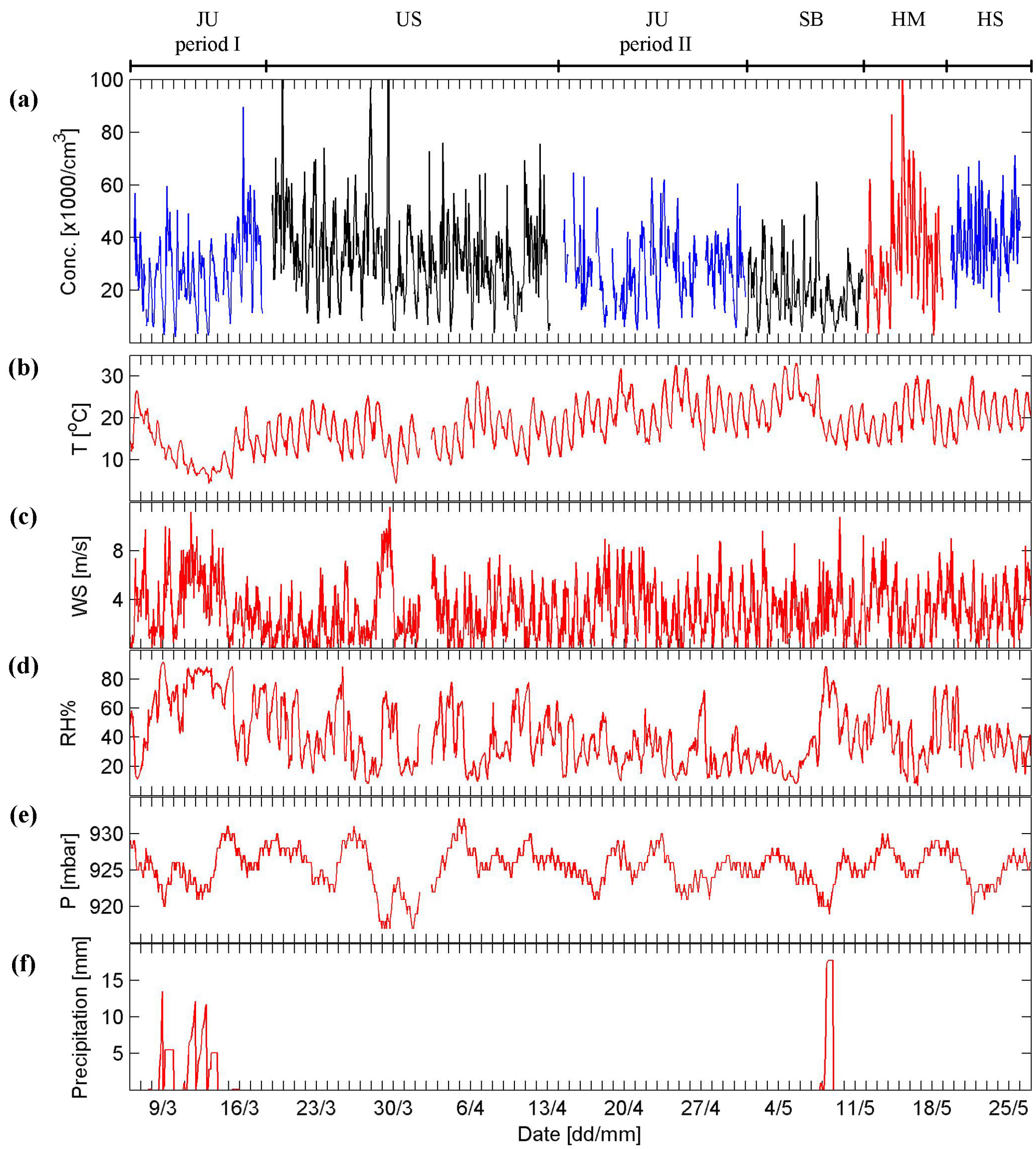

FIG. 2. Hourly average (a) fine particle number concentration, (b) ambient temperature, (c) wind speed, (d) relative humidity, (e) pressure and (f) precipitation during the whole measurement campaigns March 6 – May 28, 2015. *The abbreviations on top of the figure refer to the name of the site location as the campus of the University of Jordan (JU), Umm Summaq (US), Shafa Badran (SB) and Hai Masoum (HM).*

TABLE 2. 24-hour statistics of fine particle number concentrations at the University of Jordan campus (JU), which is an urban background site in Amman.

Date	Day	Mean	STD	25%	Median	75%
6 March	Thursday	32376	10449	23839	28829	39754
7 March	Friday	19090	8654	12031	19486	26082
8 March	Saturday	22133	10229	14226	24457	29056
9 March	Sunday	27721	16098	11395	31335	41351
10 March	Monday	22672	12489	10766	25193	28524
11 March	Tuesday	22112	7774	16937	19491	25990
12 March	Wednesday	20300	10891	10244	23877	29839
13 March	Thursday	21705	12292	8668	24050	32867
14 March	Friday	26632	7411	19027	25618	32205
15 March	Saturday	30911	13003	18057	34855	38462
16 March	Sunday	41123	16892	30147	39591	51179
17 March	Monday	34554	12896	24964	37533	43024
14 April	Monday	31852	7692	25021	31072	38339
15 April	Tuesday	33805	11829	26050	28603	43649
16 April	Wednesday	24104	10661	15661	22846	29543
17 April	Thursday	30874	10238	21398	30031	38091
18 April	Friday	14957	7619	9340	12768	21843
19 April	Saturday	15657	4866	12793	14383	19643
20 April	Sunday	25180	8901	15564	27597	29602
21 April	Monday	25839	14373	11077	25301	39698
22 April	Tuesday	34100	13901	22767	33069	42835
23 April	Wednesday	34635	17081	19900	32596	50521
24 April	Thursday	34059	9166	26932	32037	40572
25 April	Friday	20195	6232	15842	19843	23196
26 April	Saturday	25401	9551	17463	26061	33738
27 April	Sunday	31604	5468	27148	31697	36253
28 April	Monday	29938	8491	22208	29749	38027
29 April	Tuesday	27115	9566	17339	26700	36485
30 April	Wednesday	25839	14287	9798	24919	33908

TABLE 3. 24-hour statistics of fine particle number concentrations at Umm Summaq (US), which is an urban residential site with major traffic influence in Amman.

Date	Day	Mean	STD	25%	Median	75%
19 March	Wednesday	51613	27651	34945	46306	57965
20 March	Thursday	43544	11062	36168	42667	51589
21 March	Friday	35651	11749	26784	31529	41669
22 March	Saturday	36992	17475	22659	36693	50152
23 March	Sunday	32713	16335	20331	35175	40029
24 March	Monday	30540	13633	16333	31469	42103
25 March	Tuesday	32673	14250	22008	31788	45623
26 March	Wednesday	36193	11312	28673	34214	41279
27 March	Thursday	44989	24696	26289	41473	62581
28 March	Friday	37193	9874	31086	37822	43705
29 March	Saturday	36626	45626	16448	19343	35825
30 March	Sunday	19362	9924	11178	20308	24818
31 March	Monday	33176	12704	18995	34411	45214
1 April	Tuesday	26876	9703	19300	28034	35451
2 April	Wednesday	26913	12562	19857	25107	30858
3 April	Thursday	31968	17961	18163	28672	47663
4 April	Friday	28710	15392	12797	27596	40215
5 April	Saturday	33281	9393	27083	32256	37061
6 April	Sunday	27740	15216	15932	28210	38656
7 April	Monday	28586	11843	22286	26181	30932
8 April	Tuesday	27509	11934	23905	29167	37409
9 April	Wednesday	25067	10929	17040	25201	31788
10 April	Thursday	20083	15696	10818	18040	21926
11 April	Friday	36014	10427	27059	35239	43974
12 April	Saturday	37162	13033	28514	36032	41461
13 April	Sunday	6594	1626	5167	6413	7912

TABLE 4. 24-hour statistics of the particle number concentrations at Shafa Badran (SB), which is a sub-urban residential site with minor traffic influence in Amman.

Date	Day	Mean	STD	25%	Median	75%
1 May	Thursday	20840	11362	9615	23198	30409
2 May	Friday	21274	13781	7844	18677	32991
3 May	Saturday	19713	9964	13746	19976	23883
4 May	Sunday	20430	11436	12576	15994	27873
5 May	Monday	18151	8422	13520	16216	23561
6 May	Tuesday	19008	11753	10243	17829	23335
7 May	Wednesday	23834	16305	12299	17449	32216
8 May	Thursday	14415	6516	8973	14963	19052
9 May	Friday	11281	4914	7210	9990	14569
10 May	Saturday	20390	7537	14699	20170	25910
11 May	Sunday	16806	8242	7090	16700	24771

TABLE 5. 24-hour statistics of fine particle number concentrations at Al-Hashmi Al-Shamali (HS), which is an urban residential site with major traffic influence in Amman.

Date	Day	Mean	STD	25%	Median	75%
20 May	Tuesday	35609	12418	27490	34259	45474
21 May	Wednesday	37872	12934	26747	33198	48763
22 May	Thursday	38316	13242	28838	36061	45751
23 May	Friday	38717	10554	30934	36366	47197
24 May	Saturday	33688	13219	25684	30050	40669
25 May	Sunday	45317	11281	35877	45640	50898

TABLE 6. 24-hour statistics of fine particle number concentrations at Hai Masoum (HM), which is an urban residential site with major traffic and minor industry influence in Zarqa.

Date	Day	Mean	STD	25%	Median	75%
12 May	Monday	25639	15262	17718	21179	32314
13 May	Tuesday	22303	10466	15692	22173	30731
14 May	Wednesday	35103	19556	23141	36046	49287
15 May	Thursday	52847	27866	27846	48184	69366
16 May	Friday	41546	16820	29903	41084	51440
17 May	Saturday	33090	13889	18411	34342	42643
18 May	Sunday	26706	14501	15624	26259	36079

3.2 Temporal Variation – Daily Pattern

The temporal variation of fine particle number concentrations showed a clear daily pattern at each measurement site (Fig. 3). The average daily pattern of fine particle number concentrations at the urban background site (JU) was characterized by high concentrations during daytime (07:00–18:00) on all days. Dividing the dataset into workdays and weekends, we observed that on workdays, the daytime concentration was higher than 30000 cm^{-3}, while it was in the range of 20000–30000 cm^{-3} on weekends. The workdays had the highest concentrations (as high as 45000 cm^{-3}) during the morning traffic rush hours (between 06:00 and 09:00). The lowest concentrations (as low as 10000 cm^{-3}) were observed after midnight and before 06:00.

The sub-urban site (SB) showed rather a similar daily pattern to that of the urban background site (JU), but the concentrations were lower at the sub-urban site (Fig. 4). On both workdays and weekends, the average fine particle number concentrations were in the range of 20000–35000 cm^{-3} (Fig. 4a) on workdays and in the range of 20000–25000 cm^{-3} on weekends (Fig. 4b). On workdays, the effect of the morning traffic rush hours was also visible with the highest concentrations recorded at this site. Another peak in fine particle number concentrations was recorded around noon on workdays; that is most likely linked to increased traffic activities related to school buses, which are mainly operated by diesel engines. The lowest concentrations (as low as 4000 cm^{-3}) were observed after midnight and before 06:00.

The urban residential sites (Figs. 5 and 6), which were influenced by major traffic activities, showed similar daily patters, but the concentration values were higher at HS than at US. This is due to the fact that HS is a more populated area than US. Both workdays and weekends showed two main peaks during the daytime and a late evening peak. The first daytime peak was between 06:00 and 09:00 and represented the morning traffic rush hours, while the second daytime peak was around noon and represented the traffic activity of school buses, and the late evening peak was most likely due to late shopping activities. The workdays' daytime average concentration was 25000–55000 cm^{-3} at HS and 30000–42000 cm^{-3} at US. The late night peak observed on both workdays and weekends was as high as 45000 cm^{-3} at HS and as high as 42000 cm^{-3} at US. The lowest concentrations at both sites were recorded after midnight and before 06:00; at HS, the lowest concentration was as low as 20000 cm^{-3} and at US it was as low as 12000 cm^{-3}.

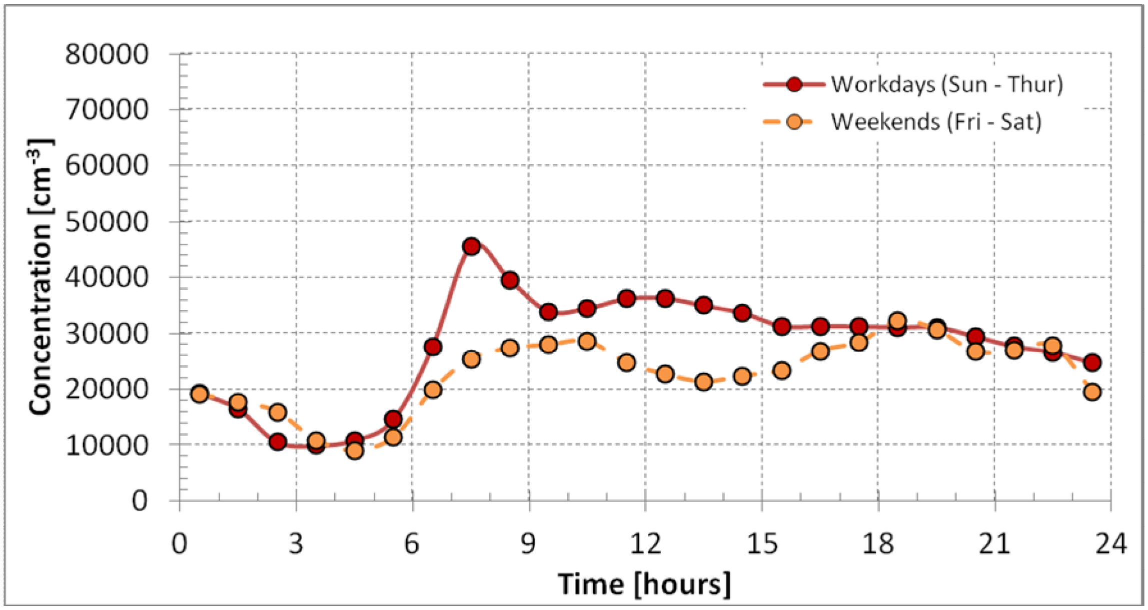

FIG. 3. Average daily patterns of fine particle number concentrations at the campus of the University of Jordan (JU, urban background) during March 6–18 and during April 14–30, 2014.

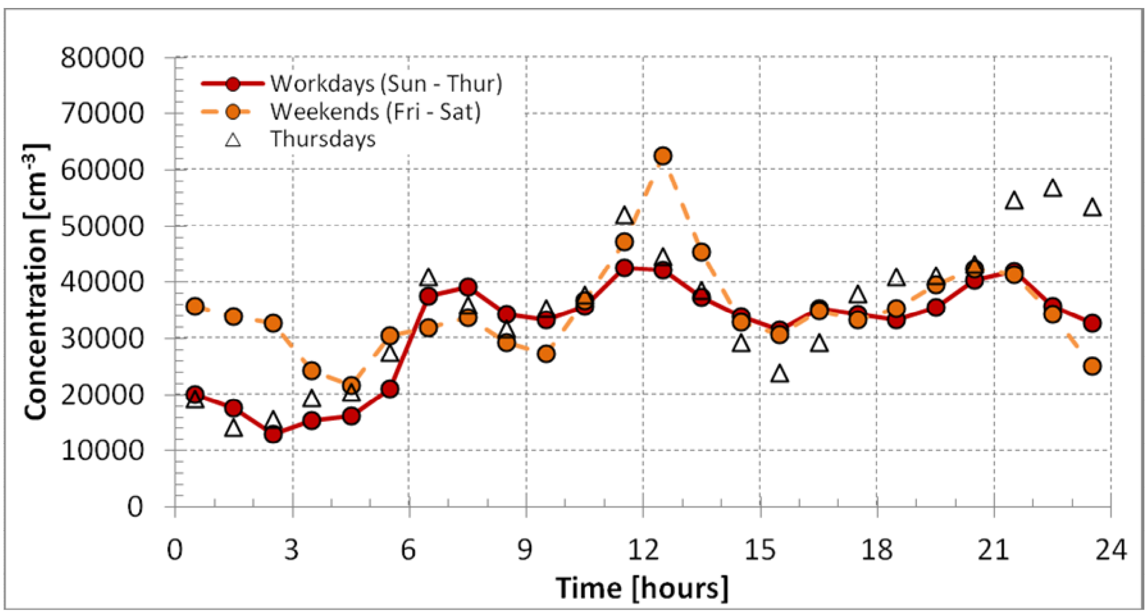

FIG. 4. Average daily patterns of fine particle number concentrations at Umm Summaq (US, urban residential with major traffic influence) during March 18 – April 13, 2014.

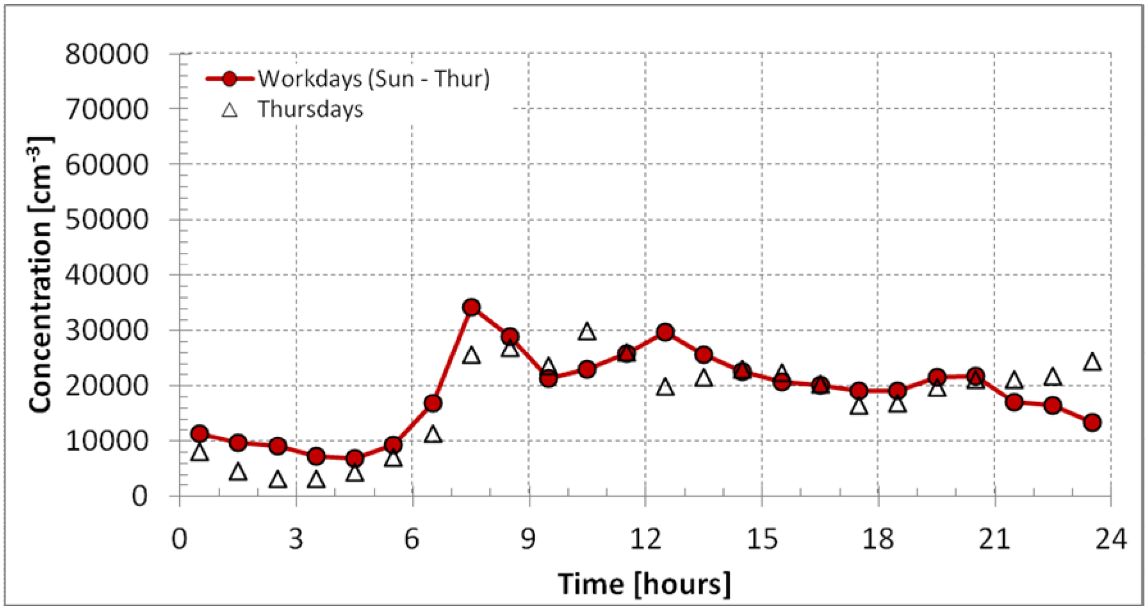

(a)

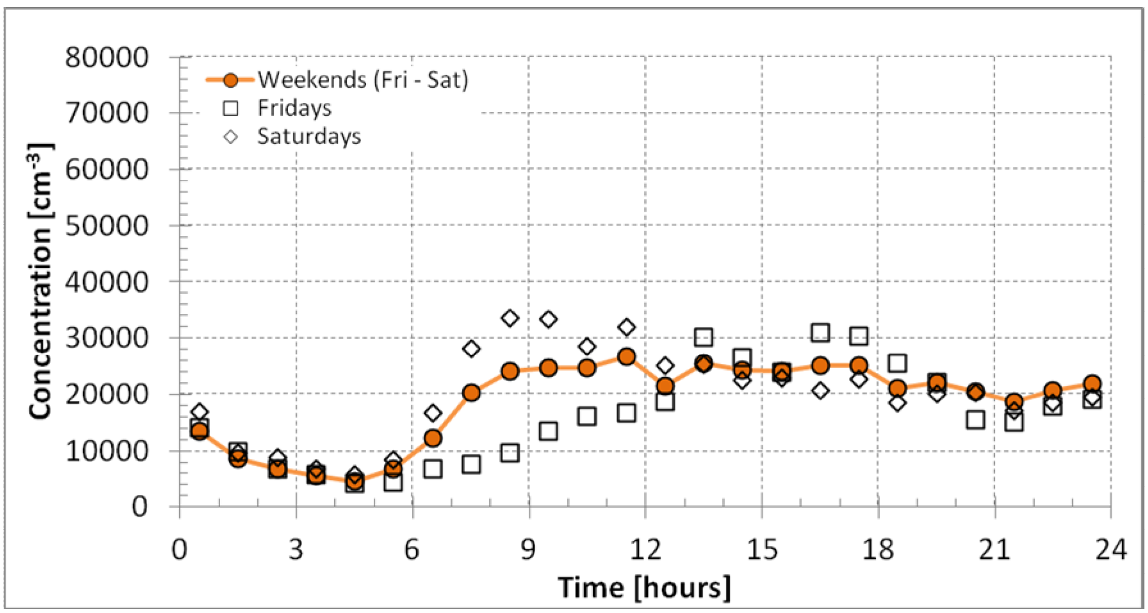

(b)

FIG. 5. Average daily patterns of fine particle number concentrations at Shafa Badran (SB, suburban residential with minor traffic influence) during May 1–11, 2014: (a) during workdays (Sunday - Thursday) and also showing Thursday separately and (b) on the weekend (Friday – Saturday) and also showing Friday and Saturday separately.

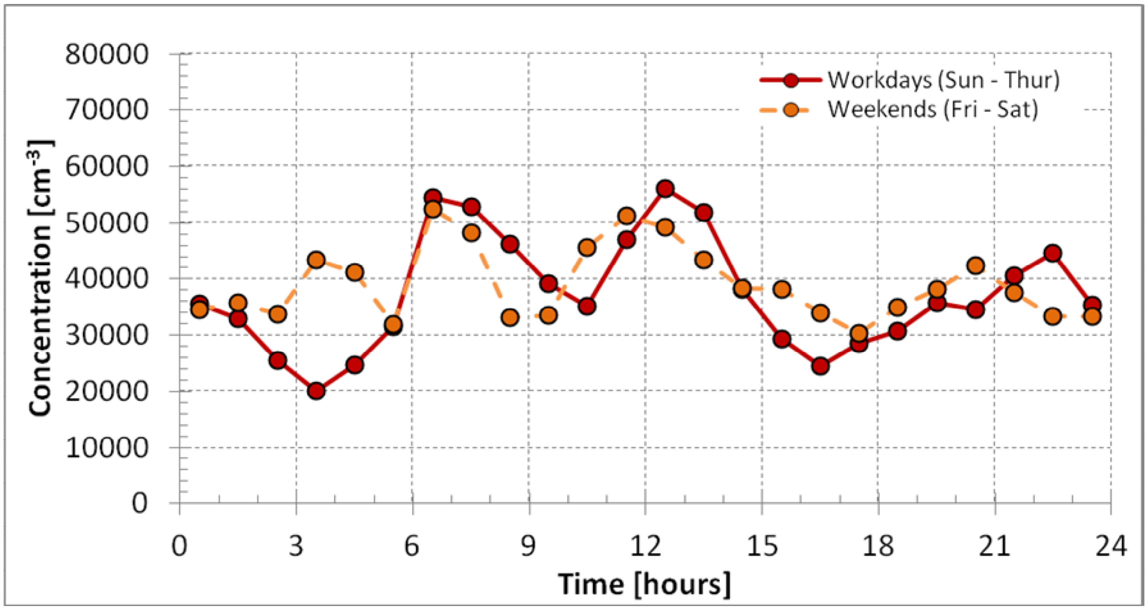

FIG. 6. Average daily patterns of fine particle number concentrations at Al-Hashmi Al-Shamali (HS, urban residential with major traffic influence) during May 26 – 29, 2014.

The urban site (HM) in Zarqa city also showed a similar daily pattern as those observed at HS and US (Fig. 7). The common thing between the three sites is that they are all urban residential with major traffic influences. However, the HM site had a minor influence of industrial activities. What is also interesting is that this site had a dominant morning peak in fine particle number concentrations that started around 05:00 and lasted until noon with a maximum concentration (higher than 60000 cm^{-3} around 07:00). Similar to the sites in Amman, the lowest concentration was recorded after midnight and before 06:00 and it was as low as 10000 cm^{-3}.

To sum up the findings about the daily patterns, all the urban residential sites showed a daily pattern for fine particle number concentrations that is characterized by three peaks (two during the daytime 06:00–18:00 and a late night peak); this daily pattern was similar for both workdays and weekends. The absolute value of the concentration was related to the population density and other anthropogenic activities. For example, HM and HS were more populated than US; and additionally, HM was influenced by industrial activities.

In the urban areas, the daily pattern of fine particle number concentrations is closely related to emissions from traffic and industry. For example, traffic activity on workdays is usually characterized by two main rush hours (morning and afternoon) that represent the times when people go to work and return back home [69]. Such daily patterns were reported in most cities in the developed countries [76, 78–79].

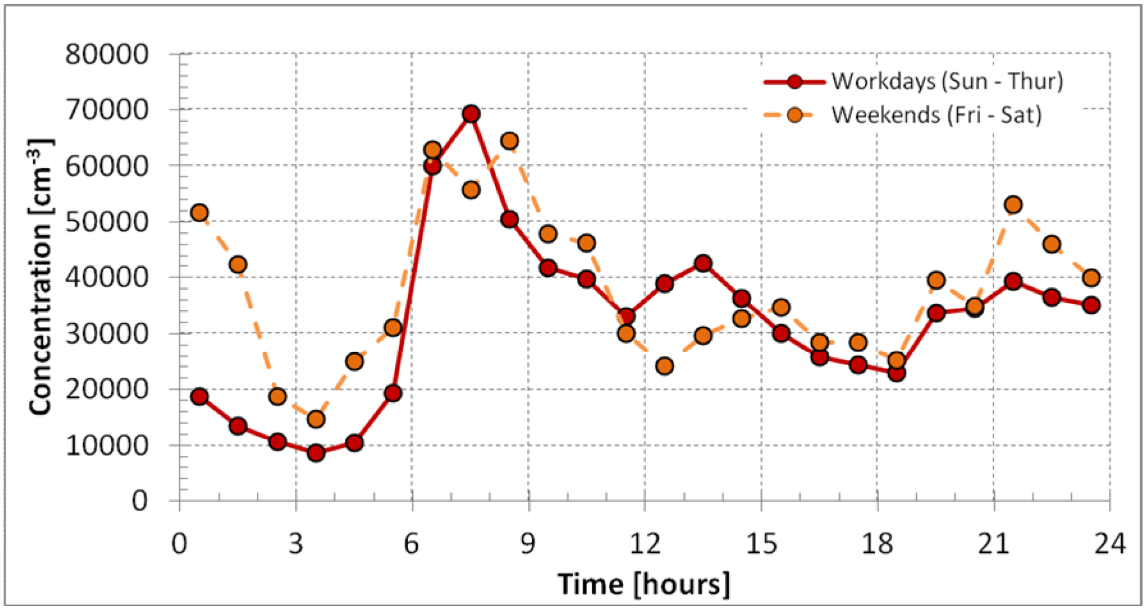

FIG. 7. Average daily patterns of fine particle number concentrations at Hai Masoum in Zarqa city (HM, urban residential with major traffic and minor industrial influence) during May 11–18, 2014.

4. Conclusions

We measured fine particle number concentrations in Jordan at four locations within the capital city, Amman. We additionally performed similar measurements at a single site in the second largest city in Jordan, Zarqa. The measurement campaign took place during March 6 – May 28, 2014. We specifically focused on the temporal-spatial variation (hourly, daily and weekly) of fine particle number concentrations. The measurement sites in Amman included an urban-background site (the University of Jordan campus), two urban-residential sites (Umm Summaq and Al-Hashmi Al-Shamali) and suburban-residential site (Shafa Badran). The site in Zarqa was an urban-residential site with minor industrial influence. All sites were influenced by traffic emissions.

There was a clear spatial and temporal variation of fine particle number concentrations within Amman. The highest concentrations were observed at the urban residential sites (Shafa Badran and Al-Hashmi Al-Shamali, 24-hour median value as high as 34.6×10^4 cm^{-3}) and the lowest were at the sub-urban site (Shafa Badran, 24-hour median value as high as 2.3×10^4 cm^{-3}). The highest concentrations among all sites were recorded at the urban-residential site in Zarqa (Hai Masoum); 24-hour median value being as high as 5.2×10^4 cm^{-3}.

The daily pattern at the residential sites was characterized by three peaks during the daytime. The first peak and last peak are related to the morning and afternoon traffic rush hours, which are similar to those observed in the developed countries. The third peak was around midday, which is possibly related to increased traffic activities related to school buses. During the day, the lowest fine particle number concentrations (~4600 cm^{-3}) were observed at the sub-urban residential site (Shafa Badran) after midnight and before the morning rush hours. This lowest value was different among the sites, and it was most likely related to population density. For example, at the urban sites, it was higher than that at the sub-urban site.

The spatial variation found in fine particle number concentrations agrees well with one of our studies about polycyclic aromatic hydrocarbons (PAHs) in collected floor dust within Amman city [80]. PAHs are usually accompanied with combustion processes and we presume that the main sources of fine particulate matter is also related to the same processes in Amman; hence, high fine particulate matter concentrations are expected to be in the same locations with high PAHs concentrations found in floor dust.

The limitations of this study are as follows: (1) It did not consider the particle number size distribution that can reveal the modal structure of aerosol particles and (2) The measurement campaign at some of the sites was very short that it might not be enough to make a strong conclusion about the fine particle characteristics. These features would require more comprehensive observations in Jordan.

Acknowledgments

This study was supported by the Deanship of Scientific Research at the University of Jordan and the Academy of Finland Center of Excellence (grant no. 272041). We would like to thank the crew at the Jordan Meteorological Department for providing the local weather information at the Amman Civil Airport. We especially thank Mr. Fathi Hussein for allowing the measurement at his house and also for participating in following up the measurements during nighttime.

References

[1] Hussein, T., Mølgaard, B., Hannuniemi, H., Martikainen, J., Järvi, L., Wegner, T., Ripamonti, G., Weber, S., Vesala, T. and Hämeri, K., Boreal Environ. Res., 19 (2014) 1.

[2] Peters, A., Wiclumann, H.E., Tuch, T., Heinrich, J. and Heyder, J., Am. J. Respir. Crit. Care Med., 155(4) (1997) 1376.

[3] Atkinson, R.W., Bremner, S.A., Anderson, H.R., Strachan, D.P., Bland, J.M. and de Leon, A.P., Arch. Environ. Health, 54 (1999) 398.

[4] Samet, J., Rappold, A., Graff, D., Cascio, W., Berntsen, J., Huang, Y.-C., Herbst, M., Bassett, M., Montilla I., Hazuch M., Bromberg, Ph. and Devlin R., Am. J. Respir. Crit. Care Med., 179 (2009) 1034.

[5] Pope, C.A., Burnett, R.T., Thun, M.J., Calle, E.E., Krewski, D., Ito, K. and Thurnston, G.D., Am. Med. Assoc., 287 (2002) 1132.

[6] Curtis, L., Rea, W., Smith-Willis, P., Fenyves, E. and Pan, Y., Environ. Intern., 32 (2006) 815.

[7] Osunsanya, T., Prescott, G. and Seaton, A., Occup. Environ. Medic., 58 (2001) 154.

[8] Engelbrecht, J.P., McDonald, E.V., Gillies, J.A., Jayanty, R.K.M., Casuccio, G. and Gertler, A.W., Inhalation Toxicology, 21 (2009a) 297.

[9] Engelbrecht, J.P., McDonald, E.V., Gillies, J.A., Jayanty, R.K.M., Casuccio, G. and Gertler, A.W., Inhalation Toxicology, 21 (2009b) 327.

[10] Notaro, M., Yu, Y. and Kalashnikova, O.V., J. Geophys. Res. – Atmos., 120 (2015) 10229.

[11] Ahmed, A.A., J. Aerosol Sci., 20 (1989) 1115.

[12] Hindy, K.T. and Farag, S.A., Environ. Pollution, Series B: Chem. and Phys., 5 (1983) 247.

[13] Tadros, M.T.Y., Madkour, M. and Elmetwally, M., Renew. Energ., 17 (1999) 339.

[14] Moustafa, M., Mohamed, A., Ahmed, A.-R. and Nazmy, H., J. Adv. Res., 6 (2015) 827.

[15] Boman, J., Shaltout, A.A., Abozied, A.M. and Hassan, S.K., X-Ray Spectros., 42 (2013) 276.

[16] Hassan, S.K., El-Abssawy, A.A., AbdEl-Maksoud, A.S., Abdou, M.H. and Khoder, M.I., Aerosol Air Qual. Res., 13 (2013) 1552.

[17] El-Araby, E.H., Abd El-Wahab, M., Diab, H.M., El-Desouky, T.M. and Mohsen, M., App. Rad. Isotopes, 69 (2011) 1506.

[18] Mahmoud, K.F., Alfaro, S.C., Favez, O., Abdel Wahab, M.M. and Sciare, J., Atmos. Res., 89 (2008) 161-169.

[19] El-Askary, H., Farouk, R., Ichoku, C. and Kafatos, M., Annales Geophysicae, 27 (2009) 2869.

[20] El-Askary, H. and Kafatos, M., Intern. J. Remote Sen., 29 (2008) 7199.

[21] Elminir, H.K., Sci. Total Environ., 350 (2005) 225.

[22] El-Metwally, M. and Alfaro, A.C., Atmos. Res., 132-133 (2013) 76.

[23] Alghamdi, M.A., Almazroui, M., Shamy, M., Redal, M.A., Alkhalaf, A.K., Hussein, M.A. and Khoder, M.I., Aerosol Air Qual. Res., 15 (2015) 440.

[24] Alghamdi, M.A., Khoder, M., Abdelmaksoud, A.S., Harrison, R.M., Hussein, T., Lihavainen, H., Al-Jeelani, H., Goknil, M.H., Shabbaj, I.I., Almehmadi, F.M., Hyvärinen, A.-P. and Hämeri, K., Air Qual. Atmos. Health, 7 (2014a) 467.

[25] Alghamdi, M.A., Khoder, M., Harrison, R.M., Hyvärinen, A.-P., Hussein, T., Al-Jeelani, H., Abdelmaksoud, A.S., Goknil, M.H., Shabbaj, I.I., Almehmadi, F.M., Lihavainen, H. and Hämeri, K., Atmos. Environ., 48 (2014b) 409.

[26] Habeebullah, T.M., Environ. Asia, 2 (2013) 11.

[27] Munir, S., Habeebullah, T.M., Seroji, A.R., Gabr, S.S., Mohammed, A.M.F. and Morsy, E.A., Atmos. Environ., 77 (2013a) 647.

[28] Munir, S., Habeebullah, T.M., Seroji, A.R., Morsy, E.A., Mohammed, A.M.F., Abu Saud, W., Abdou, A.E.A. and Awad, A.H., Aerosol Air Qual. Res., 13 (2013b) 901.

[29] Rushdi, A.I., Al-Mutlaq, K.F., Al-Otaibi, M., El-Mubarak, A.H. and Simoneit B.R.T., Arab J. Geosci., 6 (2013) 585.

[30] Khodeir, M., Shamy, M., Alghamdi, M., Zhong, M., Sun, H., Costa. M., Chen, L.-C. and Maciejczyk, P., Atmos. Pollut. Res., 3 (2012) 331.

[31] Basha, G., Phanikumar, D.V., Kumar, K.N., Ouarda, T.B.M.J. and Marpu, P.R., Remote Sen. Environ., 169 (2015) 404.

[32] Gherboudj, I. and Ghedira, H., Intern. J. Climat., 34 (2014) 3321.

[33] Reid, J.S., Reid, E.A., Walker, A., Piketh, S., Cliff, S., Al Mandoos, A., Tsay, S.-C. and Eck, T.F., J. Geophys. Res., 113 (2008) D14212.

[34] Satheesh, S.K., Deepshikha, S. and Srinivasan, J., Int. J. Remote Sens., 27 (2006) 1691.

[35] Alam, K., Trautmann, T., Blaschke, T. and Subhan, F., Remote Sens. Environ., 143 (2014) 216.

[36] Bonazza, A., Sabbioni, C., Ghedini, N., Hermosin, B., Jurado, V., Gonzalez, J.M. and Saiz-Jimenez, C., Environ. Sci. Tech., 41 (2007) 2378.

[37] Tazaki, K., Wakimoto, R., Minami, Y., Yamamoto, M., Miyata, K., Sato, K., Saji, I., Chaerun, S.K., Zhou, G., Morishita, T., Asada, R., Segawa, H., Imanishi, H., Kato, R., Otani, Y. and Watanabe, T., Atmos. Environ., 38 (2004) 2091.

[38] Rudich, Y., J. Geophys. Res., 108(D15) (2003) 4478.

[39] Herring, J.A., Ferek, R.J. and Hobbs, P.V., J. Geophys. Res., 101(D9) (1996) 14451.

[40] Daum, P.H., Al-Sunaid, A., Busness, K.M., Hales, J.M. and Mazurek, M., J. Geophys. Res., 98(D9) (1993) 16809.

[41] Lowenthal, D.H., Borys, R.D., Chow, J.C., Rogers, F., Shaw, G.E., J. Geophys. Res., 97(D13) (1992) 14573.

[42] Saeed, T.M., Al-Dashti, H. and Spyrou, C., Atmos. Chem. Phys., 14 (2014) 3751.

[43] Dobrzhinsky, N., Krugly, E., Kliucininkas, L., Prasauskas, T., Kireitseu, M., Zerrath, A. and Martuzevicius, D., Aerosol Air Qual. Res., 12 (2012) 1209.

[44] Engelbrecht, J.P. and Jayanty, R.K.M., Aeolian Res., 9 (2013) 153.

[45] Hamad, A.H., Schauer, J.J., Heo, J. and Kadhimd, A.K.H., Atmos. Res., 156 (2015) 80.

[46] Jaafar, M., Baalbaki, R., Mrad, R., Daher, N., Shihadeh, A., Sioutas, C. and Saliba, N.A., Sci. Tot. Environ., 496 (2014) 75.

[47] Dada, L., Mrad, R., Siffert, S. and Saliba, N.A., J. Aeros. Science, 66 (2013) 187.

[48] Daher, N., Saliba, N.A., Shihadeh, A.I., Jaafar, M., Baalbaki, R. and Sioutas, C., Atmos. Environ., 80 (2013) 96.

[49] Saliba, N.A., El Jam, F., El Tayar, G., Obeid, W. and Roumie, M., Atmos. Res., 97 (2010) 106.

[50] Saliba, N.A., Kouyoumdjian, H. and Roumie´, M., Atmos. Environ., 41 (2007) 6497.

[51] Kouyoumdjian, H. and Saliba, N.A., Atmos. Chem. Phys., 6 (2006) 1865.

[52] Shaka', H. and Saliba, N. A., Atmos. Environ. 38 (2004) 523.

[53] Waked, A., Seigneur, C., Couvidat, F., Kim, Y., Sartelet, K., Afif, C., Borbon, A., Formenti, P. and Sauvage, S., Atmos. Chem. Phys., 13 (2013b) 5873.

[54] Waked, A., Afif, C., Brioude, J., Formenti, P., Chevaillier, S., El Haddad, I., Doussin, J.-F., Borbon, A. and Seigneur, C., Aerosol Sci. Tech., 47 (2013a) 1258.

[55] Al-Momani, F., Daradkeh, A., Haj-Hussein, A., Yousef, Y., Jaradat, K. and Momani, K., Atmos. Res., 73 (2005) 87.

[56] Gharaibeh, A., El-Rjoob, A. and Harb, M., Environ. Monit. Assess., 160 (2010) 425.

[57] Soleiman, A., Abu-Allaban, M., Bornstein, B., Luria, M. and Gertler, A., 11th Conference on Atmospheric Chemistry (2009).

[58] Hamasha, K. and Arnott, W., Environ. Monitoring Assess., 166 (2010) 485.

[59] Abu Allaban, M., Hamasha, S. and Gertler, A., J. Air Waste Manag. Assoc., 56 (2006) 1440.

[60] Schneidemesser, E., Zhou, J., Stone, E., Schauer, J., Qasrawi, R., Abdeen, Z., Shapund, J., Vanger, A., Shraf, G., Moise, T., Brenner, S., Nassar, K., Al-Mahasneh, Q. and Sarnat, J., Atmos. Environ., 44 (2010) 3669.

[61] Abdeen, Z., Qasrawi, R., Heo, J., Wu, B., Shpund, J., Vanger, A., Sharf, G., Moise, T., Brenner, S., Nassar, K., Saleh, R., Al-Mahasneh, Q., Sarnat, J. and Schauer, J., Sci. World J., (2014) ID 878704.

[62] Hussein, T., Abu Al-Ruz, R., Petaja, T., Junninen, H., Arafah, D., Hämeri, K. and Kulmala, M., Aerosol Air Qual. Res., 11 (2011) 109.

[63] Mølgaard, B., Birmili, W., Clifford, S., Massling, A., Eleftheriadis, K., Norman, M., Vratolis, S., Wehner, B., Corander, J., Hämeri, K. and Hussein, T., J. Aerosol Sci., 66 (2013) 96.

[64] Mølgaard, B., Hussein, T., Corander, J. and Hämeri, K., Atmos. Environ., 46 (2012) 155.

[65] Salma, I., Borsós, T., Weidinger, T., Aalto, P., Hussein, T. and Kulmala, M., Atmos. Chem. Phys., 11 (2011) 1339.

[66] Birmili, W., Alaviippola, B., Hinneburg, D., Knoth, O., Tuch, T., Borken-Kleefeld, J. and Schacht, A., Atmos. Chem. Phys., 9 (2009) 2355.

[67] Hussein, T., Kukkonen, J., Korhonen, H., Pohjola, M., Pirjola, L., Wriath, D., Härkönen, J., Teinilä, K., Koponen, I.K., Karppinen, A., Hillamo, R. and Kulmala, M., Atmos. Chem. Phys., 7 (2007) 4081.

[68] Hussein, T., Hämeri, K., Aalto, P.P. and Kulmala, M., Atmos. Environ., 39 (2005) 1655.

[69] Hussein, T., Puustinen, A., Aalto, P.P., Mäkelä, J.M., Hämeri, K. and Kulmala, M., Atmos. Chem. Phys., 4 (2004) 391.

[70] Hussein, T., Hämeri, K. and Kulmala, M., Boreal Environ. Res., 7 (2002) 141.

[71] Dingenena, R.A., Raes, F., Putaud, J.-P., Baltensperger, U., Charron, A., Facchini, M.-C., Decesari, S., Fuzzi, S., Gehrige, R., Hansson, H.-C., Harrison, R.M., Hüglin, C.H., Jones, A.M., Laj, P., Lorbeer, G., Maenhaut, W., Palmgren, F., Querol, X., Rodriguez, S., Schneider, J., Ten Brink, H., Tunved, P., Torseth, K., Wehner, B., Weingartner, E., Wiedensohler, A. and Wåhlin, P., Atmos. Environ., 38 (2004) 2561.

[72] Buzorius, G., Hämeri, K., Pekkanen, J. and Kulmala, M., Atmos. Environ., 33 (1999) 553.

[73] Väkevä, M., Hämeri, K., Kulmala, M., Lahdes, R., Ruuskanen, J. and Laitinen, T., Atmos. Environ., 33 (1999) 1385.

[74] Ruuskanen, J., Tuch, Th., Ten Brink, H., Peters, A., Khlystov, A., Mirme, A., Kos, G.P.A., Brunekreef, B., Wichmann, H.E., Buzorius, G., Vallius, M., Kreyling, W.G. and Pekkanen, J., Atmos. Environ., 35 (2001) 3729.

[75] Reche, C., Querol, X., Alastuey, A., Viana, M., Pey, J., Moreno, T., Rodriguez, S., Gonzalez, Y., Fernandez-Camacho, R., Sanchez, de la Campa, A.M., de la Rosa, J., Dall'Osto, M., Prevot, A.S.H., Hueglin, C., Harrison, R.M. and Quincey, P., Atmos. Chem. Phys., 11 (2011) 6207.

[76] Wehner, B. and Wiedensohler, A., Atmos. Chem. Phys., 3 (2003) 867.

[77] Puustinen, A., Hämeri, K., Pekkanen, J., Kulmala, M., de Hartog, J., Meliefste, K., Ten Brink, H., Kos, G., Katsouyanni, K., Karakatsani, A., Kotronarouh, A., Kavouras, I., Meddings, C., Thomas, S., Harrison, R., Ayres, J.G., van der Zee, S. and Hoek, G., Atmos. Environ., 41 (2007) 6622.

[78] Olivares, G., Johansson, C., Ström, J. and Hansson, H.-C., Atmos. Environ., 41 (2007) 2145.

[79] Wehner, B., Wiedensohler, A., Tuch, T.M., Wu, Z.J., Hu, M., Slanina, J. and Kiang, C.S., Geophys. Res. Lett., 31 (2004) L22108.

[80] Maragkidou, A., Ma, Y., Jaghbeir, O., Faouri, D., Harrad, S., Al-Hunaiti, A., Arar, S., Hämeri, K. and Hussein, T., J. Chem. Eng. Proc. Technol., 7 (2016) 290.

Volume 9, Number 1, 2016. pp. 47-54

Jordan Journal of Physics

ARTICLE

Influence of Current Density on Morphology of Electrochemically Formed Porous Silicon

Ammar M. Al-Husseini

Department of Physics, The University of Jordan, Amman 11942, Jordan.

Received on: 14/1/2016; Accepted on: 6/4/2016

Abstract: Porous silicon samples were prepared by electrochemical anodic etching of p–type silicon wafer in hydrofluoric (HF) acid-based solution. The electrochemical process allowed precise control of porous silicon properties, such as average pore diameter, average pore depth and porosity. The effect of current density on physical properties of porous silicon was investigated by Scanning Electron Microscopy (SEM), I-V characteristics and Fourier Transform Infrared (FTIR) spectroscopy. The average pore diameter and average pore depth were found to increase with the increase in current density. The average pore diameter varied from (10 to 28) nm and the average pore depth varied from (470 to 2200) nm, when the current density was changed from (5 to 36) mA/cm^2 for 10 minutes. In addition, Al/porous/crystalline silicon sandwich showed a good rectification device.
Keywords: Porous silicon, Electrochemical etching, Current density, SEM, FTIR, I-V characteristics.

Introduction

Porous silicon is an important material for applications in microelectronics. Since Uhlir and Tumer [1, 2] first reported in the late 1950s that silicon surface can be covered with a brown film during anodization in HF solutions [3], porous silicon was found to form by electrochemical etching of p or n doped mono-crystalline silicon in hydrofluoric acid (HF) [4]. The microstructural and physical characteristics of porous silicon, such as thickness, pore diameter, pore distribution and specific surface area are critically dependent on various processing conditions, etching solution composition, current density, etching time, illumination and properties of the silicon substrate, such as doping level and crystal orientation [4-8]. In general, porous silicon (PS) obtained by anodization of a silicon wafer is a versatile material which can display different morphologies by varying the doping density of the wafer as well as the formation parameters. Nanoporous silicon (2–4 nm) can be generally achieved by using p-type as well as n-type silicon of low and moderate doping density. Mesoporous silicon with pore diameters from 5 to 50 nm is generally formed utilizing highly doped silicon as substrate, and for macropore (>50 nm up to a few µm) formation moderately doped silicon is usually employed [9]. All these different types of porous silicon are used in basic research studies, but are also appropriate for potential applications.

Porous silicon; a versatile material with various morphological natures, is compatible to today's microtechnology and is of interest for a great variety of applications. The high surface area of this material (nanoporous silicon ~1,000 m^2 /cm^3, mesoporous silicon ~100 m^2 /cm^3 and macroporous silicon ~1 m^2 /cm^3) makes it suitable to fill the pores with one or more guest materials, which results in a drastic change of the physical properties [10].

In order to form porous silicon, the current at the silicon side of the silicon/electrolyte interface must be carried by holes, injected from the bulk

Corresponding Author: Ammar M. Al-Husseini **Email**: a.taha@ju.edu.jo

towards the interface. Several different mechanisms regarding the solution chemistry of silicon have been proposed, but it is generally accepted that holes are required for pore formation [11]. The global anodic semi-reaction can be written during pore formation as:

$$Si + 2HF + 2h^+ \rightarrow SiF_2 + 2H^+ , \quad (1)$$

$$SiF_2 + 4HF \rightarrow H_2 + H_2SiF_6 . \quad (2)$$

The etching rate is determined by holes (h^+) accumulating in the adjacent regions of the HF electrolyte and Si atoms [3, 6, 7 and 12]. Porous silicon is a promising material due to excellent optical, mechanical and thermal properties, compatibility with silicon-based microelectronics [13] and low cost [14]. All these features have led to many applications of porous silicon, such as solar cells, gas sensors, pressure sensors, bio-sensors, photovoltaic devices, …etc. [15-19]. The interest in porous silicon has increased greatly over the past decades, mainly due to its photoluminescence properties and the potential applications arising from these [20]. Technological application of porous silicon (PS) as a light emitter would have a significant impact on numerous technologies, such as light emitting devices [21], micro-cavities[22], wave guides and solar cells[23,24]. Porous silicon (PS) is an interesting material for gas sensing applications [25, 26].

In this paper, scanning electron microscopy (SEM) is used to study the influence of etching current density on pore diameter and pore depth for mesoporous silicon.

Experimental Details

The experiment setup of electrochemical etching is illustrated in Fig. 1. A constant current is supplied between two electrodes immersed in Teflon cell (highly acid-resistant material) containing an aqueous solution of hydrofluoric acid HF (49%), ethanol C_2H_5OH (99%) and deionized water H_2O. Adding ethanol to the electrolyte produces more homogenous structures. Ethanol removes hydrogen bubbles induced during the electrochemical reaction, making the porous structures more uniform [6].

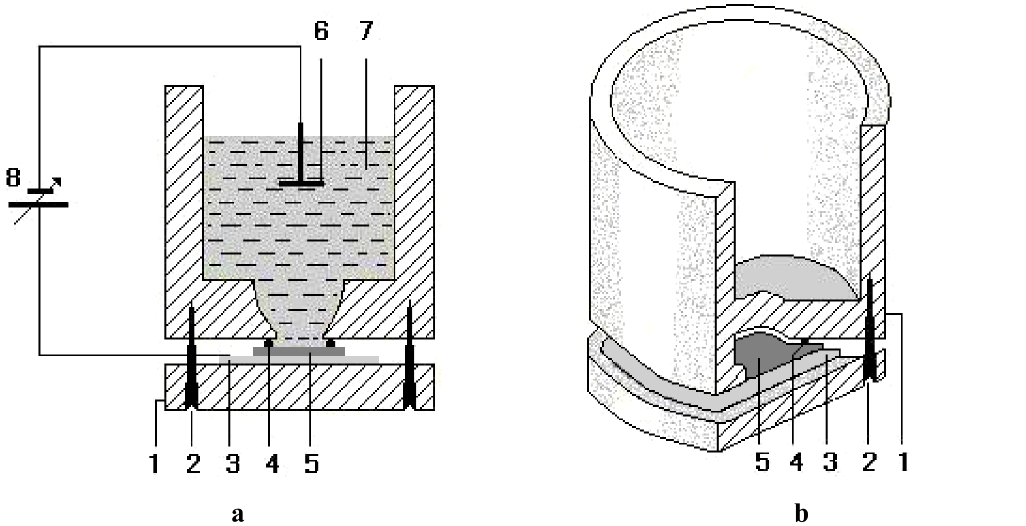

FIG. 1. Electrochemical etching experimental setup: (a) schematic view, (b) cross-section of the electrochemical etching tank. 1- Teflon container, 2- screw, 3- aluminum anode, 4- O-ring, 5- silicon wafer, 6- platinum cathode, 7- electrolyte, 8- variable power supply.

The substrate used was mono-crystalline p-type silicon (100) oriented, with 3-30 Ωcm resistivity and a thickness of 675 ± 25 μm. The silicon wafers were cleaved into 4cm squares (few mm larger that the O-ring used in the etching container) to ensure a leak-free seal. The silicon samples were placed at the bottom of the cylindrical Teflon container and fixed by an aluminum plate as backing material, so that the current required for the etching process could pass from the bottom surface to the top of the polished surface via the electrolyte. Platinum plate represents the cathode which was placed perpendicular to the silicon surface at a distance of 2cm. The porous layers on the surface of these samples were prepared at current densities of 5, 10, 20 and 36 mA/cm^2 for 10 min etching time. After etching, the samples were thoroughly rinsed with ethanol (twice or more) to remove any HF trace. Finally, the samples were examined using FIE Scanning Electron Microscope (SEM), Keithly electrometer I-V characteristics and Thermo Nicolet Fourier Transform Infra-Red (FTIR) spectroscopy in order to verify precisely pore formations on the silicon membrane.

Results and Discussion

Fig. 2 shows the top view and cross-section SEM images of the porous silicon, prepared by electrochemical etching of p-type silicon wafers for 10 minutes. The electrolyte consists of 1(49%) HF: 2(99%) C_2H_5OH:2 H_2O, using different current densities of 5, 10, 20 and 36 mA/cm^2. With the help of the surface images of the samples, the dark spots on the images are attributed to the pores formed, whereas the white area corresponds to the remaining silicon. The pores are spherical and irregular in shape and are randomly distributed on the porous silicon surface. Porous silicon formed at different current densities has different pore sizes. At a current density of 5 mA/cm^2, pores were 9-11 nm in diameter and 420-500 nm in depth (Fig. 2 a). For current density of 10 mA/cm^2, the pore diameter was 15-17 nm, while pores were 630-710 nm in depth (Fig.2 b). The use of 20 mA/cm^2 current density resulted in pore diameter of 18.4 -20.0 nm and pore depth of 1260-1400 nm (Fig. 2c). Finally, at a current density of 36 mA/cm^2, the pore diameter became 27-29 nm and the pore depth was 2130-2300 nm (Fig. 2d).

Fig. 3 shows the distribution of pore sizes for a sample prepared using a current density of 10 mA/cm^2, for which the average pore diameter was 16 nm with a standard deviation of 0.6 nm.

The variation in the average pore diameter of porous silicon with etching current density is illustrated in Fig. 4. As can be seen, the pore diameter increases exponentially with current density [27]. The current density was changed from 5 mA/cm^2 to 36 mA/cm^2 and the average pore diameter increased from 10 nm to 28 nm. The average pore diameters were determined via manual measurement of at least twenty pores randomly selected from two different SEM images. The average pore diameters appear to be in good agreement with what is expected for meso-pore layer [9,10]. The variation in the average pore depth of porous silicon with etching current density is illustrated in Fig. 5. The average pore depths were determined via manual measurement of at least ten pores randomly selected from two different SEM images. When the current density was changed from 5 mA/cm^2 to 36 mA/cm^2, the average pore depth increased from 470 nm to 2200 nm. Pore depth generally increases with increasing current density, because increasing current density produces excess electron-hole pairs and subsequently enhances the porous silicon thickness layer [11, 28]. In fact, the relation between pore depth and current density has been predicted to be of the form:

$$d_{pore} = (1.2)(J)^{0.8} , \tag{3}$$

where d_{pore} is the pore depth and J is the current density.

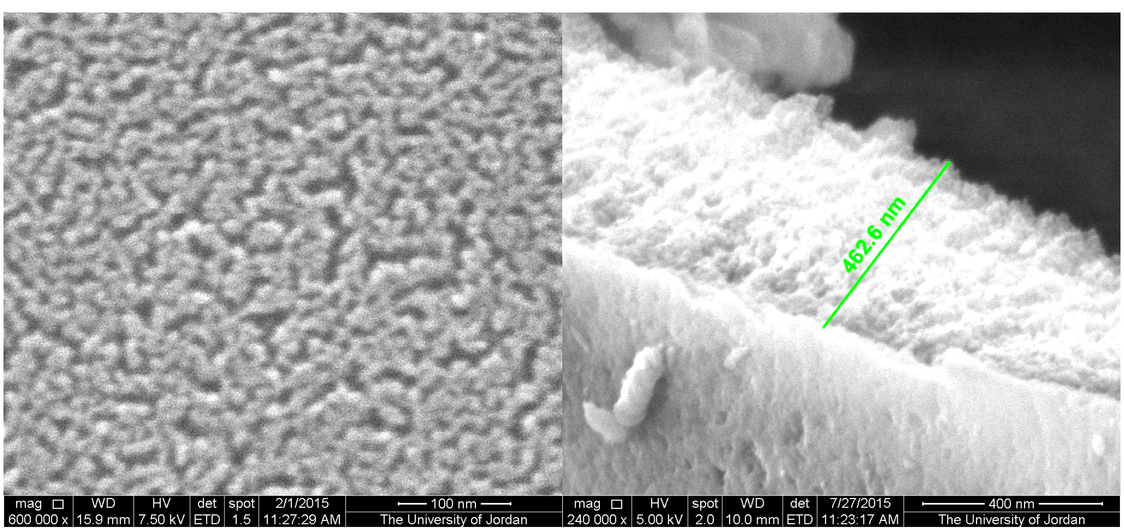

(a)

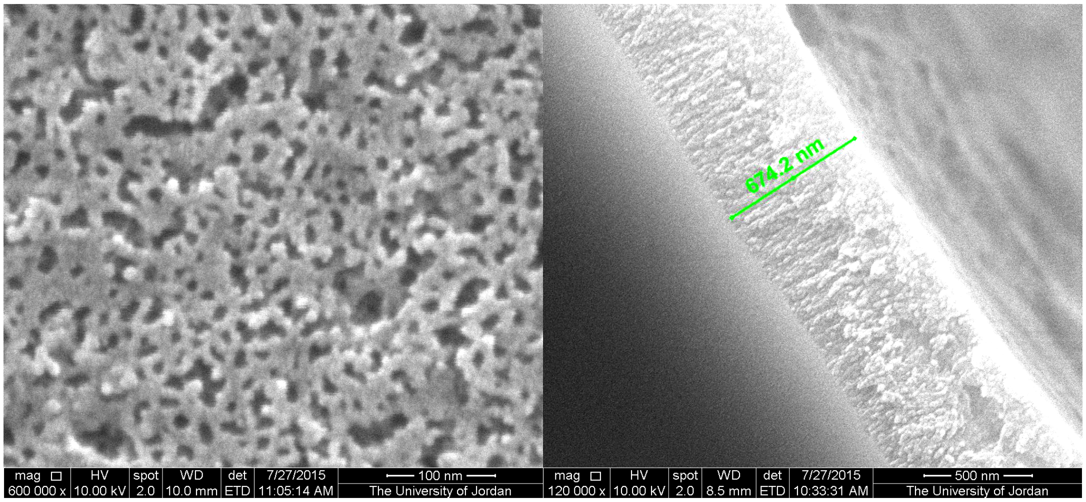

(b)

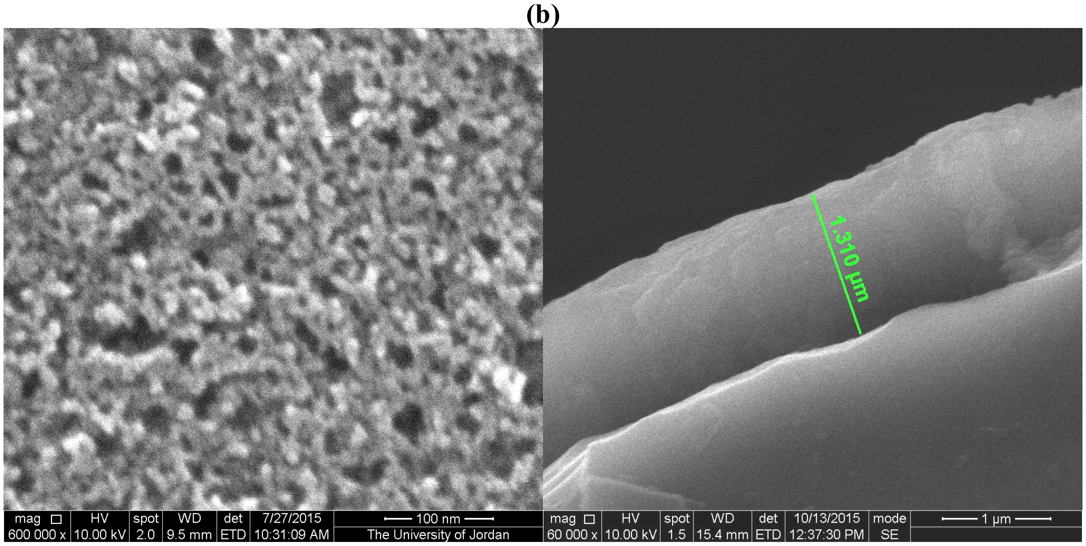

(c)

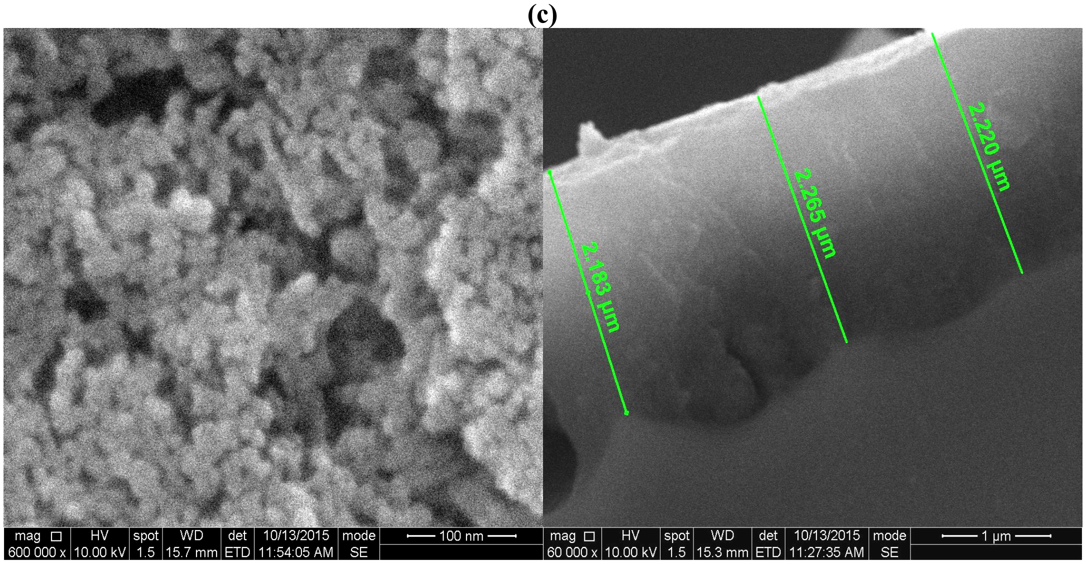

(d)

FIG. 2. Top view and cross-section SEM images of the porous silicon samples. The samples were prepared by p-type (100) orientation in electrolyte consisting of $HF:C_2H_5OH:H_2O$ in the ratio of (1:2:2) by volume with an etching time of 10 minutes, (a) current density = 5 mA/cm^2, (b) current density = 10 mA/cm^2, (c) current density = 20 mA/cm^2, (d) current density =36 mA/cm^2.

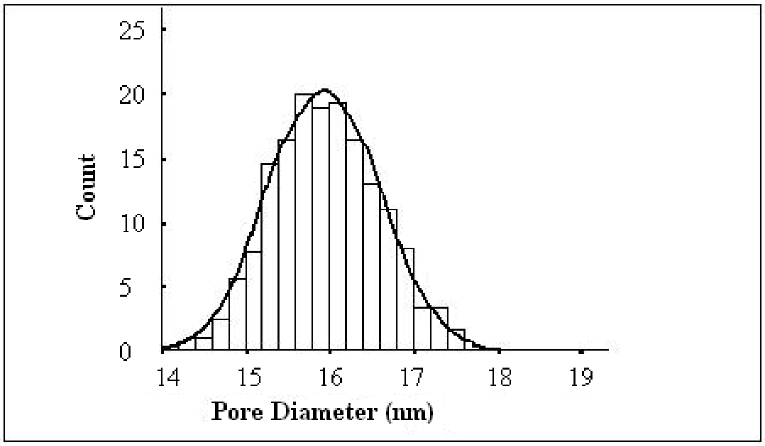

FIG. 3. Pore size distribution for a porous silicon sample formed at a current density of 10 mA/cm^2. Data from tow different SEM images was used.

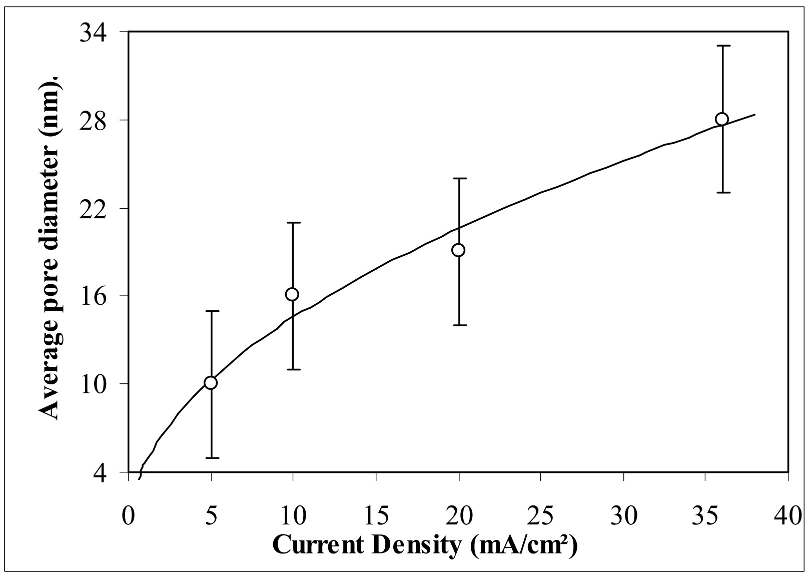

FIG. 4. Average pore diameter as a function of current density.

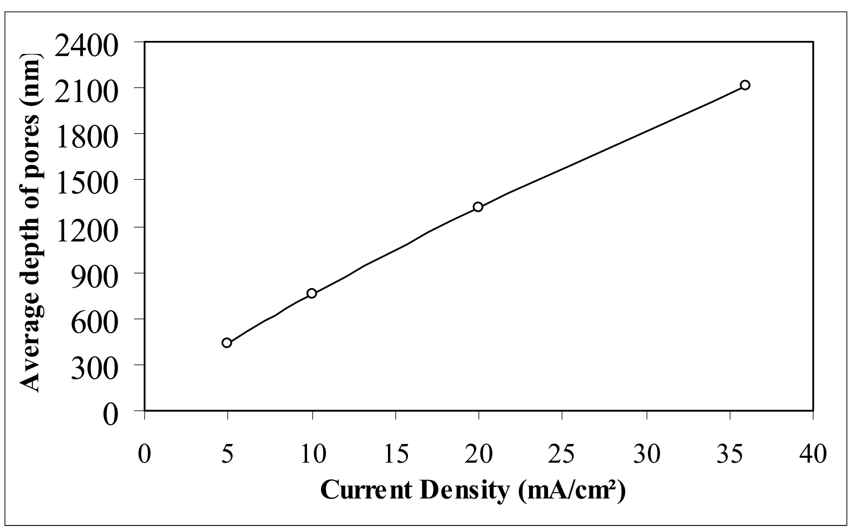

FIG. 5: Average depth of pores as a function of current density.

I-V Characteristics

Fig. 6 shows current-voltage (I-V) characteristics for Al/ porous silicon/ crystalline/ Al sandwich structure device. These were measured under illumination conditions as a function of different etching current densities (5mA/cm^2 and 20mA/cm^2) and 10 minutes etching time. Keithly electrometer (model 6517A) was used to measure the current-voltage (I-V) characteristics. The (I-V) curves were obtained by applying a varying bias voltage (from -5V to +5V). The variation in forward bias characterization is controlled by porous silicon layer resistance. This result explains the reduction of flow current in forward bias with increasing the etching current density [29]. The pore diameter increases as etching current density increases and hence the resistance of porous silicon layer becomes too high. This will reduce the forward current density. When the pore diameter increases, the pore wall which acts as a carriers' trap will increase to form a high resistive region which decreases the current passing through the porous silicon layer. Also, increasing the etching current density from 5 mA/cm^2 to 20 mA/cm^2 will lead to increase the thicknesses of the porous silicon layer. Increasing the thickness of the porous silicon layer will lead to increase its resistivity due to reduced mobility in it [30-33].

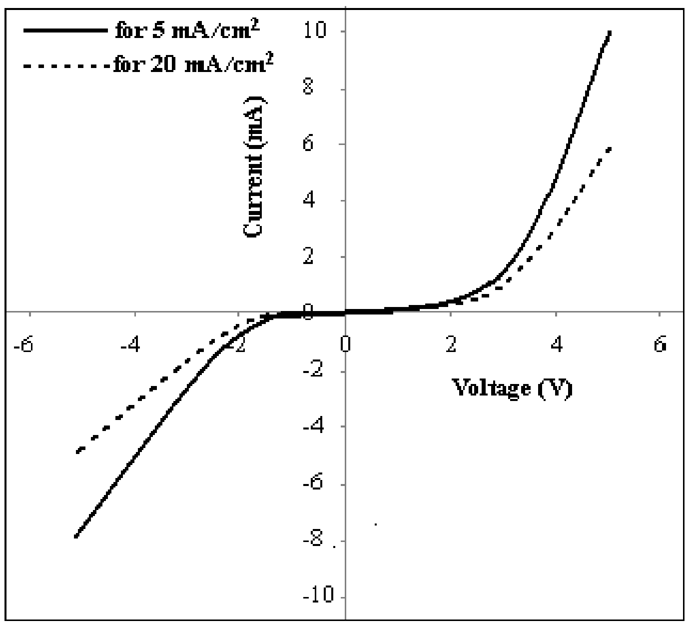

FIG. 6. I-V characteristics of Al/porous silicon/crystalline silicon/Al sandwich structure device.

Fourier Transform Infra-Red (FTIR) Study

Fourier Transform Infrared (FTIR) spectroscopy has been widely used as a tool for characterization of chemical bonding, especially extensively in porous silicon. Thermo Nicolet 670 FT-IR spectroscopy was utilized in this study to characterize the active vibrational bonds in the porous silicon sample. The system covers the range (500-4000 cm^{-1}) at room temperature. When infrared radiation interacts with the sample, the chemical bonds will stretch, contract and bend. As a result, the bonds will tend to absorb the infrared radiation at different wavelengths.

Fig. 7 shows the FTIR absorbance spectrum of porous silicon at a current density of 10 mA/cm^2 and an etching time of 10 minutes. The peaks are: 624.94 cm^{-1} Si-Si bonds vibration, 837.62 cm^{-1} Si-H_2 wagging mode and 940.21 cm^{-1} Si-H_2 scissor mode. The peaks around 1051.22 cm^{-1} and 1144.45 cm^{-1} are related to Si–O–Si stretching modes. The peaks at 2120.74 cm^{-1} and 2903.27 cm^{-1} are, respectively, related to Si–H stretch and C-H stretch. Chemical bonds and their IR resonance positions detected in porous silicon are shown in Table (1). The FTIR peaks are in good agreement with other reported results [34, 35].

TABLE 1. Bonds in porous silicon spectrum at a current density of 10 mA/cm^2 and an etching time of 10 min.

Wave number (cm^{-1})	Bonds	Vibration modes
634.50	Si-Si	Stretching
837.62	Si-H_2	Wagging
940.21	Si-H_2	Scissor
1051.22	Si-O-Si	Stretching
1144.45	Si-O-Si	Stretching
2120.74	Si-H	Stretching
2903.27	C-H	Stretching

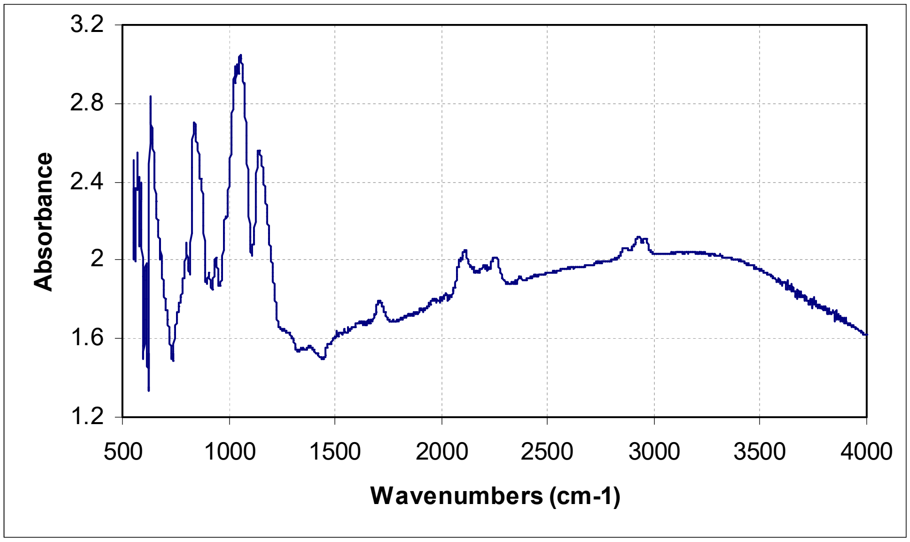

FIG. 7. FTIR spectrum of porous silicon at a current density of 10 mA/cm^2 and an etching time of 10 min.

Conclusions

Porous silicon samples were prepared by electrochemical etching method at various current densities. The results show that the diameter and depth of the pores were substantially affected by the etching current density. The Scanning Electron Microscopy (SEM) investigation shows that the average pore diameter and depth are increasing with the increase of etching current density. I-V characteristics of Al/porous silicon/crystalline silicon/Al sandwich structure device showed good rectification characteristics. Finally, Fourier Transform Infrared (FTIR) spectroscopy studies revealed vibration, symmetrical stretching, wagging and stretch/bend bonds. These results indicate that the porous silicon is a good candidate for photonic devices.

Acknowledgment

The author would like to thank both Dr. Walid Hamoudi and Dr. Bashar Lahlouh for their helpful discussion.

References

[1] Uhlir, A., The Bell Syst. Tech. J., 35 (1956) 333.

[2] Turner, D.R., J. Electrochem. Soc., 105 (1958) 402.

[3] Zhang, G.X., "Modern Aspects of Electrochemistiy", Number 39, edited by C. Vayenas et al., Springer, (New York, 2005) 65-69,155.

[4] Smith, R.L. and Collins, S.D., J. Appl. Phys., 71 (1992) R1.

[5] Zangooie, S., Jansson, R. and Arwin, H., Applied Surface Science, 136(1-2) (1998) 123.

[6] Sailor, M.J., Wiley-VCH Verlag and Co. KGaA, Boschstr. 12, 69469, (Weinheim, Germany, 2012) 5-12.

[7] Kumar, P. and Huber, P., Journal of Nanomaterials, (2007) 1.

[8] Peckham, J. and Andrews, G.T., Semicond. Sci. Technol., 28 (2013) 105027.

[9] Chazalviel, J.-N., Ozanam, F., Gabouze, N., Fellah, S. and Wehrspohn, R.B., J. Electrochem. Soc., 149 (2002) C511.

[10] Granitzer, P. and Rumpf, K., Materials, 3 (2010) 943, doi:10.3390/ma3020943.

[11] Pérez, E.X., Design, Fabrication and Characterization of Porous Silicon Multilayer Optical Devices, ISBN: 978-84-691-0362-3/DL: T.2181, (Universitat Rovira I Virgili, 2007).

[12] Zhang, X.G., Journal of the Electrochemical Society, 151(1) (2004) C69.

[13] Hirschman, K.D., Tsybeslcov, L., Duttaguola, S.P. and Fauchet, P.M., Nature, 384 (1996) 338.

[14] Behzad, K., Yunus, W.M.M., Talib, Z., Zakaria, A. and Bahrami, A., Int. J. Electrochem. Sci., 7 (2012) 8266.

[15] Dubey, R. and Gautum, D., Opt. Quant. Electron., 41 (2009) 189.

[16] De Stefano, L., Moretti, L., Lamberti, A., Longo, O., Rocchia, M., Rossi, A.M., Arcari, P. and Rendina, I., IEEE Transactions on Nanotechnology, 3(1) (2004).

[17] Singh, P., Sharma, S.N. and Ravindra, N.M., JOM, 62(6) (2010) 15.

[18] De Stefano, L. et al., Sensors, 7 (2007) 214.

[19] Mathew, F.P. and Alocilja, E.C., Biosensors Bioelctron., 20 (2005) 1656.

[20] Kawasaki, K.K., Material Science and Engineering, 69(70) (2000) 132.

[21] Adawiya, J.H., Iraq J. of Appl. Phys., 4(1) (2008) 37.

[22] Pavesi, L., Rivista Del Nuovo Cimento, 20 (1997) 1.

[23] Lin, T.L. Chen, S.C., Kao, Y.C., Wang, K.L. and Iyer, S., Applied Physics Letters, 48(26) (1986) 1793.

[24] Bilyalov, R.R. et al., Sol. Eng. Mater. Sol. Cells, 65 (2001) 477.

[25] Canham, L., “Porous Silicon Application Survey”, IEE Inspec., (London, U.K., 1997) 364.

[26] Alwan, A.M., Haider, A.J. and Jabbar, A.A., Surface and Coating Technology, 283 (2015) 22.

[27] Haldar, S., De, A., Chakraborty, S., Ghosh, S. and Ghanta, U., Procedia Materials Science, 5 (2014) 764.

[28] Foll, H., Carstensen, J. and Frey, S., Journal of Nanomaterials, (2006) 10.

[29] Arce, R.D., Koropecki, R.R., Olmos, G., Gennaro, A.M. and Schmidt, J.A., Thin Solid Films, 510 (2006) 169.

[30] Algun, G. and Arikan, M.C., Tr. J. of Physics, 23 (1999) 789.

[31] Chorin, M.B., Moller, F. and Koch, F., J. Appl. Phys., 77(9) (1995) 4482.

[32] Algun, G. and Arikan, M.G., J. Phys., 23 (1999) 789.

[33] Abd, H.R., Al-Douri, Y., Ahmed, N.M. and Hashim, U., Int. J. Electrochem. Sci., 8 (2013) 11461.

[34] Prokes, S.M. and Glembocki, O.J., Phys. Today, 83 (1997).

[35] Mawhinney, D.B. and Yales, J.T., Jr. J. Phys. Chem. B, 101 (1997) 1202.

Volume 9, Number 1, 2016. pp. 55-64

Jordan Journal of Physics

ARTICLE

Radionuclides Measurements in Some Rock Samples Collected from the Environment of Hebron Governorate -Palestine

K. M. Thabayneh[a], **L. A. Mashal**[a], **K. M. Awawdeh**[b] and **M. M. Abu-Samreh**[c]

[a] *Faculty of Sciences and Technology, Hebron University, P.O. Box 40, Hebron, Palestine.*
[b] *Faculty of Sciences and Arts, Palestine Technical University, Kadoorie, Tulkarem, Palestine*
[c] *Faculty of Arts and Sciences, Arab American University, Jenin, Palestine.*

Received on: 29/5/2015; Accepted on: 25/2/2016

Abstract: Using high-resolution γ- ray spectroscopy, the activity concentrations of some radioactive isotopes such as ^{238}U, ^{232}Th and ^{40}K in different rock samples, collected from 31 quarries in Hebron Governorate, Palestine were measured. For this purpose, 62 rock samples were gathered from different quarries of the region under investigation. The measured activities of ^{238}U, ^{232}Th and ^{40}K were found to range from 21.3 to 100.5, 1.3 to 11.6 and 13 to 583 $Bqkg^{-1}$, with average values of 47.6, 4.2 and 100 $Bqkg^{-1}$, respectively. For all samples, the radium equivalent activity (Ra_{eq}), as well as other radiological effects were estimated and found to be below the recommended levels. Therefore, the results indicate that the investigated materials can be used as building construction materials without radiation threat. This study can be used as a baseline for natural radioactivity mapping in the region under investigation. The results may also be used as reference data for monitoring possible radioactivity pollution in the future.

Keywords: Natural radioactivity, Effective dose rate, Rocks, Hazard index, Palestine.

Introduction

Human beings are continuously exposed to ionizing radiations of natural origin, and life on earth has developed under the ubiquitous presence of environmental gamma and charged-particle radiation. Radiation may be one of the effects for life and biological development. It is also, however, well established that ionizing radiation may harm life and biological systems. Measurement of natural radiation background is very important to determine the environmental hazards on human health and is essential to set the standard radiation levels and national guidelines according to international recommendations [1, 2].

Natural radioactivity in geological materials, mainly rocks and soil, comes from ^{232}Th and ^{238}U series and natural ^{40}K [3]. These radionuclides have a half-life comparable to the age of the earth. Gamma radiation from these radionuclides represents the main external source of irradiation of the human body. The knowledge of radionuclides distribution and radiation levels in the environment is important for assessing the effects of radiation exposure due to both terrestrial and extraterrestrial sources. Terrestrial radiation results from radioactive nuclides present in varying amounts in soils, building materials, water, rocks and the atmosphere. Some of the radionuclides from these sources are transferred to man through the food chain or inhalation, while extraterrestrial radiation originates from outer space as primary cosmic rays [4].

Corresponding Author: Khalil M. Thabayneh **Email**: khalilt@hebron.edu

As many know, building materials are comprised of rocks, thus containing radioactive nuclides. The knowledge of the natural radioactivity of building materials is important for the determination of a population's exposure to radiations, as most of the residents spend about 80% of their time indoors [5]. The presence of radioisotopes in building materials causes external exposure for those who live in buildings. ^{226}Ra and ^{232}Th can also increase the concentration of ^{222}Rn and ^{220}Rn, as well as its isotopic daughters in buildings. ^{40}K and part of the above-mentioned radionuclides cause external exposure, while the inhalation of ^{222}Rn, ^{220}Rn and their short lived progeny leads to internal exposure of the respiratory tract to alpha particles [5, 6].

In Palestine, our laboratory previously conducted a series of studies, with the objective to determine radioactivity levels and associated dose rates from surface soils, building materials, plants and some imported granites and ceramics [7-14]. For this study, we extend our measurements to systematically cover nearly all rock samples used as primary (raw) materials in the building and construction industry in Palestine. For this purpose, the activity concentrations and radiological effects of those naturally occurring radionuclides were measured in 62 representative samples, by means of high-resolution gamma-ray spectroscopy. The results obtained were compared with the world median values and the accepted upper limits.

Materials and Methods

The Study Area

Hebron Governorate (Latitude: 31° 32' 0" N, Longitude: 35° 5' 42" E) is located in the south of the West Bank, 30 km south of Jerusalem (Fig. 1). It is the largest governorate in the West Bank in terms of size and population. Its area is about 1068 km^2, which is about 19% of the West Bank total area. The population of Hebron Governorate is 650,000 people according to the estimates of the Palestinian Central Bureau of Statistics [15]. The number of Palestinian communities in the governorate is 158, the largest of which is Hebron city, located on the Hebron Mountains. The governorate lies between 400 and 1013 meters above sea level. Hebron is a busy hub of West Bank trade, responsible for roughly a third of the areas gross domestic product, largely due to the sale of rocks from quarries. In addition to sale of rocks, local economy relies on handicraft, different industries and construction [16]. The area mainly consists of Cenomanian, Eocene, Turonian and Senonian limestones. Whilst the Cenomanian and Turonian limestones are mostly very hard and resemble marble, the Senonian and Eocene limestones are generally of soft and chalky nature [17]. The main soil type is "terra rossa". This is the most typical soil of the mountains in the governorate and soil formation on hard limestone. Its soil reaction is generally neutral to moderately alkaline, and its soil has a high content of soluble salts. Both the high iron content and the low organic matter are responsible for the red color. They are mainly of loamy texture. In addition to the "terra rossa" soils, mountain marl soils and alluvial soils are also present in considerable areas. Mountain marl soils are formed from the chalky marls of Senonian and Eocene ages [17]. Agricultural areas surround the region, where the farmers in the region usually cultivate fruits, such as grapes, figs and plums [16]. The climate is of Mediterranean type with a long hot and dry summer and a short cool and rainy winter. Accordingly, the climate of Palestine is classified as an eastern Mediterranean one. Temperatures increase to the south and towards the Jordan Valley (east) [17].

Sampling and Sample Preparation

According to the map of Palestine shown in Fig. 1, a total of 62 rock samples have been collected randomly from 32 main quarries (two samples from each site) at the area under examination. Rock samples were crushed to small pieces and ground to powder. Each sample was dried in an oven at 105 ^{0}C and sieved through a 100 mesh, which is the optimum size enriched in heavy minerals. The samples were sealed in standard 1000 ml Marinelli beakers, dry weighed and stored for a minimum period of one month in order to allow daughter products to come into radioactive secular equilibrium with their parents ^{226}Ra and ^{232}Th. Then radionuclides were counted for 1200-1440 minutes, depending on the concentration of the radionuclides.

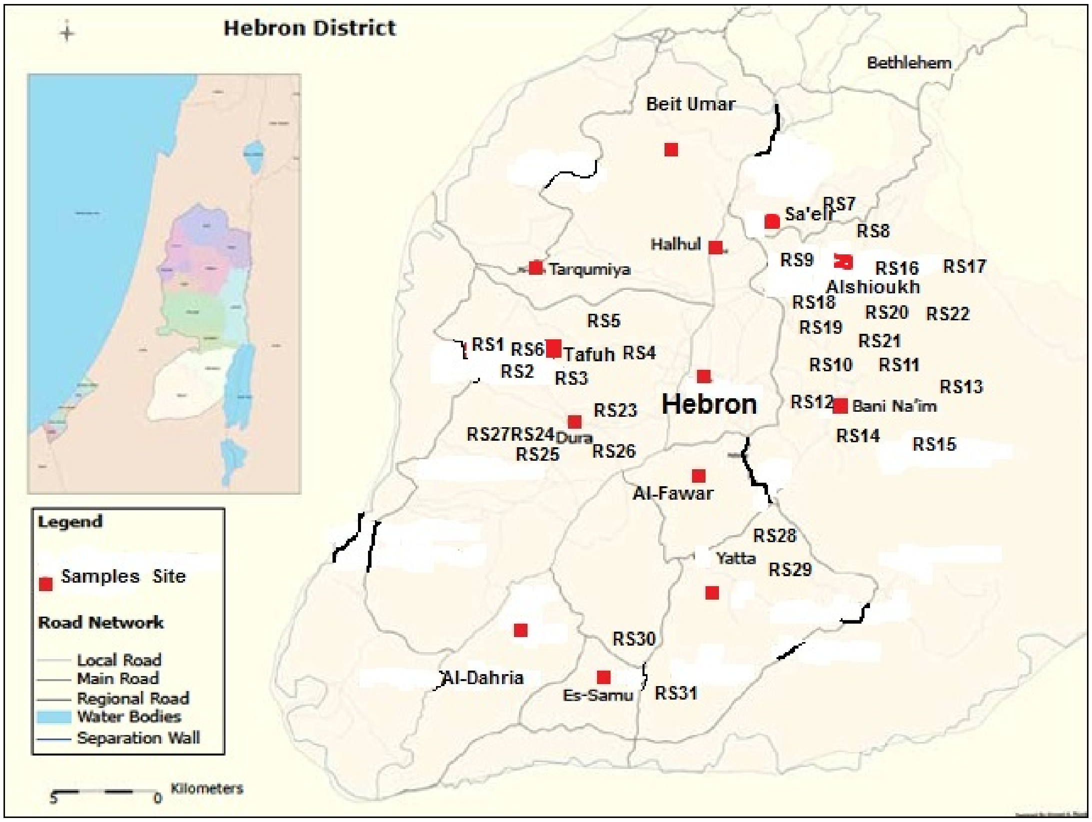

FIG.1. West Bank geographical map and sample location of the Hebron region.

Radioactivity Measurement

The concentrations of the natural radionuclides, such as ^{226}Ra, ^{238}U, ^{232}Th and ^{40}K were measured using gamma spectroscopy with an n-type HPGe detector with 15 % relative efficiency and 1.85 keV resolution (FWHM) for the 1332 keV photons of ^{60}Co and MCA with 8000 channel. The efficiency calibrated for the spectrometry system was designed by using a mixture of radioactive sources: ^{139}Ce (166 keV), ^{203}Hg (279 keV), ^{85}Sr (514 keV), ^{137}Cs (662 keV), ^{88}Y (898 and 1836 keV) and ^{60}Co (1173 and 1333 keV) in the energy range (186–1850) keV. The calibration efficiency curve beyond 1850 keV was constructed using different energy peaks of ^{226}Ra series (^{214}Bi has peaks at 2204 and 2448 keV) in order to cover the range from 60 up to 2500 keV (16). The standard source packed in the Marinelli beaker had the same geometry as that used for measured samples. The efficiency curve for HPGe detector is shown in figure 2.

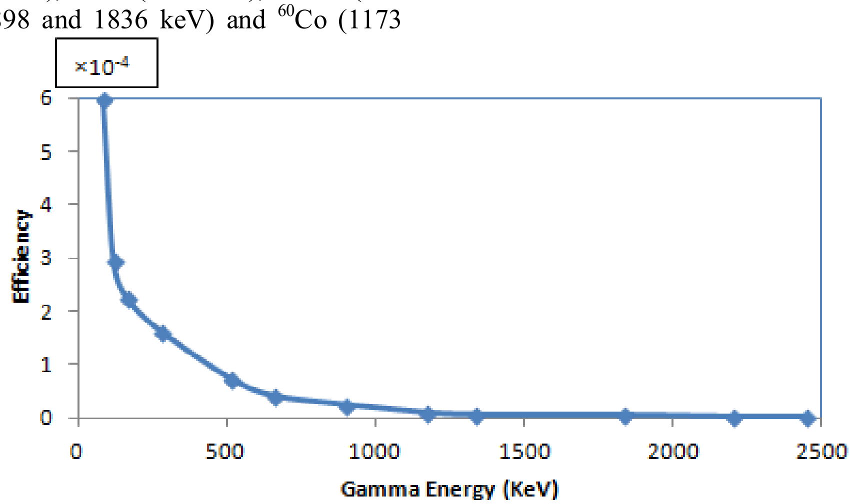

FIG.2. The photo peak efficiency curve of HPGe detector.

The activity concentrations of ^{40}K were measured using the gamma lines of 1460.8 keV. ^{238}U concentration was determined by means of its progeny full energy peak of gamma-ray lines: ^{226}Ra (186.2 keV), ^{214}Pb (295.21 keV, 352 keV) and ^{214}Bi (609 KeV, 1120.29 keV and 1764.8 keV). ^{232}Th was determined through its progeny full energy peak of gamma-ray lines: ^{228}Ac (338.6 keV, 911.2 keV and 968.9 keV),^{212}Pb (238.6 keV), ^{208}Tl (583.3 keV and 2614 keV) [11]. The software Personnel Computer Analyzer was used for the collection of the spectra. The net count rates under the most prominent full energy peak of all radionuclide daughter peaks were calculated by subtracting the background spectrum from the respective count rate obtained for the same counting time. Then, the activity of the radionuclide was calculated from the net area of prominent gamma ray energies.

Since the counting rate is proportional to the amount of the radioactivity in the samples, the activity concentration (C) can be calculated from the following equation [9]:

$$C\left(Bq/kg\right)=\frac{C_{net}}{I_{\gamma}\times\varepsilon_{ff}\times M}\ , \qquad (1)$$

where C_{net} is the net peak count rate, I_γ is the absolute gamma decay intensity for the specific energy photo peak (including the decay branching ratio information), E_{ff} is the absolute efficiency of the Germanium detector at this energy and M is the mass of the sample in kg.

Results and Discussion

Activity Concentrations of ^{238}U,^{232}Th and ^{40}K

The activity concentrations of natural radionuclides (^{238}U, ^{232}Th and ^{40}K) for all rock samples are determined and shown in (Table 1). The average activity concentrations of ^{238}U, ^{232}Th and ^{40}K are in the range of 21.3- 100.5 Bqkg^{-1}, 1.3 - 11.6 Bqkg^{-1} and 13.0 - 583 Bqkg^{-1}, respectively, with total average values of 47.6, 4.2 and 100 Bqkg^{-1}, respectively. The measured activity concentrations of ^{238}U, ^{232}Th and ^{40}K were compared with the values reported worldwide, as shown in Table 2. The study determined that the measured average activity concentrations of ^{238}U in this study are higher than most of the reported values from other countries, as well as the world's average value (35 Bqkg^{-1}) [18], while the average activity concentrations of ^{232}Th and ^{40}K are lower than most of the reported values from other countries, as well as the world's average values (30 Bqkg^{-1} for ^{232}Th and 400 Bqkg^{-1} for ^{40}K) [18]. The highest levels of ^{238}U radionuclides were recorded in the samples RS_1, RS_2, RS_3, RS_4 and RS_5 at the Tafuh site and in the samples RS_{23}, RS_{24}, RS_{25} and RS_{26} at the Dura site, knowing that the two sites are geographically adjacent. For ^{40}K radionuclides, the highest levels were recorded in the samples RS_1, RS_2 and RS_6 at the Tafuh site. In the present study, higher values of ^{238}U could be due to the presence of higher amounts of accessory minerals and may be the result of the presence of radioactive-rich granite, phosphate, sandstone and quartzite. The variations of radioactivity levels at different measurement locations are due to the variation of concentrations of these radioactive nuclides in the geological formations.

In all sampling sites, mean activity concentration is of the order ^{232}Th < ^{238}U < ^{40}K. Actually, the activity concentration of ^{232}Th is much lower than those of ^{238}U and ^{40}K, since ^{232}Th is more soluble in rain water. ^{238}U concentration is found to be higher than that of ^{232}Th in all the sampling sites. This may be due to the low geochemical mobility and insoluble nature in water of uranium. The ^{40}K activity dominates over ^{232}Th isotope activities, which may be due to the presence of feldspar minerals that are more concentrated in ^{40}K.

TABLE 1. The average activity concentrations of radionuclides in rock samples at different locations in Hebron region- Palestine.

Sample code	Site	Density	The activity concentrations (Bqkg^{-1})		
		kg/m^3	^{238}U	^{232}Th	^{40}K
RS_1	Tafuh	1890	51.8	7.7	548.6
RS_2	Tafuh	1610	59.3	9.9	462.4
RS_3	Tafuh	1940	58.7	7.5	242.6
RS_4	Tafuh	1810	57.5	4.3	74.1
RS_5	Tafuh	1530	100.5	4.7	24.4
RS_6	Tafuh	1960	44.9	7.3	583.0
RS_7	Sa'eir	1950	35.6	4.2	63.0
RS_8	Sa'eir	1880	38.9	3.0	48.0
RS_9	Sa'eir	1620	22.5	1.4	17.5
RS_{10}	Bani Na'im	1250	44.2	4.5	51.5
RS_{11}	Bani Na'im	1450	38.7	2.6	36.8
RS_{12}	Bani Na'im	1750	31.8	2.0	24.9
RS_{13}	Bani Na'im	1740	43.0	2.9	31.5
RS_{14}	Bani Na'im	1790	72.2	4.1	45.7
RS_{15}	Bani Na'im	1840	37.3	2.0	15.7
RS_{16}	Alshioukh	1510	35.0	3.0	40.7
RS_{17}	Alshioukh	1560	42.4	2.1	19.8
RS_{18}	Alshioukh	1620	35.6	2.8	39.4
RS_{19}	Alshioukh	1460	46.6	2.7	33.7
RS_{20}	Alshioukh	1920	25.6	1.3	18.1
RS_{21}	Alshioukh	1925	44.0	2.9	32.1
RS_{22}	Alshioukh	1360	21.3	3.0	32.8
RS_{23}	Dura City	1880	77.2	2.5	39.0
RS_{24}	Karma/ Dura	1810	79.6	3.7	30.6
RS_{25}	Karma/ Dura	1940	59.1	8.7	13.0
RS_{26}	Tabaka/ Dura	1810	87.7	5.3	68.8
RS_{27}	Kraseh/ Dura	1490	33.0	11.6	271.9
RS_{28}	Yatta	1360	37.8	2.8	41.1
RS_{29}	Yatta	1350	39.6	2.7	45.2
RS_{30}	Samou	1660	44.0	3.3	51.4
RS_{31}	Samou	1710	30.0	3.4	31.9
Range	-------	1250 - 1960	21.3- 100.5	1.3 - 11.6	13.0 - 583.0
Total average	-------	1690	47.6	4.2	100

TABLE 2. Comparison of activity concentrations of rock samples at the area under investigation with other areas of the world.

Country	^{238}U (Bqkg^{-1})	^{232}Th (Bqkg^{-1})	^{40}K (Bqkg^{-1})	References
Nigeria	39.7	62.6	604	[4]
Cyprus	1.0 - 588	1.0 – 906	50 - 1606	[19]
Brazil	31.0	73.0	1648	[20]
Germany	5.1 – 76.0	3.4 – 70.0	10 - 2070	[21]
Kenya	43.1 - 360	38.6 - 271.7	245 - 1780	[22]
Turkey	19.7	35.1	386	[23]
Iran	7.5 - 178.1	6.5 - 172.2	557 - 1539	[24]
Iraq	29.0	3.0	361	[25]
Saudi Arabia	513.1	39.1	242	[26]
India	36.6	73.2	992	[27]
Egypt	12.0 – 19.3	10 – 17.7	298.6 – 955.8	[28]
Palestine	21.3- 100.5	1.3 - 11.6	13 – 583	Present study
	47.6	4.2	100	
World average	35	30	400	[18]

Absorbed Dose Rate Measurement

Based on the radioactivity levels of ^{238}U, ^{232}Th and ^{40}K, the absorbed dose rate in air (D_r) in nGy h^{-1} at 1 meter above ground level with have contribution of terrestrial gamma radiation was calculated using the following formula [29, 30]:

$$\left.\begin{array}{l} D_r\left(nGy/hr\right)= \\ 0.427C_U+0.662C_{Th}+0.043C_K \end{array}\right\}, \qquad (2)$$

where C_U, C_{Th} and C_K are activity concentrations (Bqkg^{-1}) of ^{238}U, ^{232}Th and ^{40}K, respectively, in the rock samples.

The calculated average absorbed dose rate varied from 11.2 to 50.8 nGyh^{-1} with a total average value of 27.4 nGyh^{-1} (Table 3). The high calculated absorbed dose rate may be due to elevated level of ^{238}U. Minimum dose rate may be due to lower amount of all the measured radionuclides. The average absorbed dose rate obtained is lower than 55 nGyh^{-1} which was reported by UNSCEAR [18].

TABLE 3. The radium equivalent (Ra_{eq}), the dose rate (Dr) and the annual effective dose (AED) in rock samples.

Sample Code	Ra_{eq} (Bqkg^{-1})	D_r (nGyh^{-1})	AED (μSvyr^{-1})
RS_1	105.0	50.8	62.3
RS_2	109	51.8	63.5
RS_3	88.1	40.5	49.7
RS_4	69.3	30.6	37.5
RS_5	109.1	47.1	57.8
RS_6	100.2	49.1	60.2
RS_7	46.4	20.7	25.4
RS_8	46.9	20.7	25.4
RS_9	25.8	11.2	13.8
RS_{10}	54.6	24.1	29.5
RS_{11}	45.2	19.8	24.3
RS_{12}	36.6	16.0	19.6
RS_{13}	49.6	21.6	26.5
RS_{14}	81.6	35.5	43.6
RS_{15}	41.4	17.9	23.0
RS_{16}	42.4	18.7	22.4
RS_{17}	46.9	20.3	24.9
RS_{18}	42.6	18.7	23.0
RS_{19}	53.0	23.1	28.4
RS_{20}	28.7	12.5	15.3
RS_{21}	50.6	22.1	27.1
RS_{22}	28.1	12.5	15.3
RS_{23}	83.8	36.3	44.5
RS_{24}	87.2	37.8	46.3
RS_{25}	72.5	31.6	38.7
RS_{26}	100.6	43.9	53.9
RS_{27}	70.5	33.5	41.1
RS_{28}	44.9	19.7	24.2
RS_{29}	46.9	20.6	25.3
RS_{30}	52.7	23.2	28.4
RS_{31}	37.3	16.4	20.2
Range	25.8 -109.1	11.2- 50.8	13.8 -63.5
Total average	61.2	27.4	33.6

Annual Effective Dose

In order to estimate the annual effective doses, one must take into account the conversion coefficient from absorbed dose in air into effective dose received by adults and the outdoor occupancy factor. In the UNSCEAR [18] report, a value of 0.7 SvGy^{-1} was used for the conversion coefficient from absorbed dose in air to effective dose received by adults, while a value of 0.2 was used for the outdoor occupancy factor. The annual effective dose (AED) was calculated from the following equation [4]:

$$AED\left(\mu Sv\ /\ yr\right)=\left[D_r\left(nGy\ /\ hr\right)\times 24(hr\ /day\ )\times 365.25(day\ /\ yr\times 0.2\times 0.7Sv\ /Gy\ \right]\times 10^3\ . \quad (3)$$

The results of the annual effective dose (*AED*) are presented in (Table 3). The highest annual effective dose rate value was found to be 63.5 μSvy^{-1}, while the lowest value was found to be 13.8 μSvy^{-1}. The total average value of *AED* is 33.6 μSvy^{-1}.The world average annual effective dose equivalent (*AED*) from outdoor terrestrial gamma radiation is 70 μSvy^{-1} [18]. Therefore, the obtained values from this preliminary study are all lower than the accepted average worldwide value.

Radium Equivalent Activity

It is important to assess gamma radiation hazards to persons associated with the use of rocks in building materials. The activities due to ^{238}U, ^{232}Th and ^{40}K are represented by a single quantity, which takes into account the radiation hazards that may be caused by a common index. This is called the radium equivalent (Ra_{eq}), and has been written as shown in the following equation [11, 30]:

$$Ra_{eq}\ =\ C_U+\left(C_{Th}\times 1.43\right)+\left(C_k\times 0.077\right). \quad (4)$$

This formula is based on the estimation that 1 Bqkg^{-1} of ^{238}U, 0.7 Bqkg^{-1} of ^{232}Th and 13 Bqkg^{-1} of ^{40}K produce the same γ-ray dose rates [2, 31]. The values of radium equivalent for different rock samples in the area under investigation were calculated using the equation above, and these values are presented in (Table 3). The produced values range from 25. 8 to 109.1 Bqkg^{-1}, with a total average value of 61.2 Bqkg^{-1}, which is lower than the recommended maximum value of 370 Bqkg^{-1} [31].

Indices for External and Internal Gamma Radiation

The external hazard index (H_{ex}) – resulting from emitted γ-rays of the soil samples – is calculated and examined according to the following criterion [29]:

$$H_{ex}=\frac{C_U}{370}+\frac{C_{Th}}{259}+\frac{C_K}{4810}\leq 1\ . \quad (5)$$

The value of H_{ex} must be lower than unity in order to keep the radiation hazard insignificant. The maximum value of H_{ex} must be equal to unity to correspond to the upper limit of Ra_{eq} (370 Bq kg^{-1}).

The calculated values of H_{ex} for the rock samples studied range from 0.07 to 0.29, with an average value of 0.17 (Table 4). Since these values are lower than unity, then, according to the Radiation Protection 112 report [32], rocks from these regions can be used as construction material, without posing any significant radiological threat to the population.

The internal radiation hazard index (H_{in}) provides an estimation of the exposure to radon and its daughter products and is defined as follows [29]:

$$H_{in}=\frac{C_U}{185}+\frac{C_{Th}}{259}+\frac{C_K}{4810}\leq 1\ . \quad (6)$$

The internal hazard index is defined so as to reduce the acceptable maximum concentration of ^{238}U to half the value appropriate to external exposures alone. Like the external hazard index, the construction materials would be safe if $H_{in}\leq 1$ [2]. As shown in (Table 4), internal hazard indices for the rock samples in this study varied from 0.13 to 0.57, with an average value of 0.30. The internal hazard index for the studied rock samples is less than unity, which indicates that the investigated materials can be used as building construction materials without radiation threat.

Gamma Index Level

The European Commission has suggested a gamma index level (I_γ) for defining radiation risk from excessive gamma exposure by the following equation [33]:

$$I_\gamma=\frac{C_U}{150}+\frac{C_{Th}}{100}+\frac{C_K}{1500}\ . \quad (7)$$

Values of index $I_\gamma\leq 2$ correspond to a dose rate criterion of 0.3 mSvy^{-1}, whereas $2\leq I_\gamma\leq 6$ correspond to a criterion of 1 mSvy^{-1} [34]. Thus, materials with $I_\gamma > 6$ should be avoided as building materials, because these values correspond to dose rates higher than 1 mSvy^{-1}; the dose rate which was recommended by UNSCEAR [18]. In the current study, I_γ was calculated using equation (7). The gamma index value ranged from 0.18 to 0.80, with an average value of 0.43 (Table 4). For all measured samples used in this study, $I_\gamma\leq 1$. This corresponds to an absorbed gamma dose rate of 0.3 mSvy^{-1} [32]. The gamma index calculated for all assessed samples was less than the gamma index limit.

TABLE 4. The external hazard index (H_{ex}), the internal hazard index (H_{in}), the gamma index level (I_γ) and the alpha index (I_α) in rock samples.

Sample Code	H_{ex}	H_{in}	I_γ	I_α
RS_1	0.28	0.42	0.79	0.26
RS_2	0.29	0.45	0.80	0.30
RS_3	0.24	0.40	0.63	0.29
RS_4	0.19	0.34	0.48	0.29
RS_5	0.29	0.57	0.73	0.50
RS_6	0.27	0.39	0.76	0.22
RS_7	0.13	0.22	0.32	0.18
RS_8	0.13	0.23	0.32	0.19
RS_9	0.07	0.13	0.18	0.11
RS_{10}	0.15	0.27	0.37	0.22
RS_{11}	0.12	0.23	0.31	0.19
RS_{12}	0.10	0.18	0.25	0.16
RS_{13}	0.13	0.25	0.34	0.22
RS_{14}	0.22	0.42	0.55	0.36
RS_{15}	0.11	0.21	0.28	0.19
RS_{16}	0.11	0.21	0.29	0.18
RS_{17}	0.13	0.24	0.32	0.21
RS_{18}	0.12	0.21	0.29	0.18
RS_{19}	0.14	0.27	0.36	0.23
RS_{20}	0.08	0.15	0.19	0.13
RS_{21}	0.14	0.26	0.34	0.22
RS_{22}	0.08	0.13	0.19	0.11
RS_{23}	0.23	0.44	0.57	0.39
RS_{24}	0.24	0.45	0.59	0.34
RS_{25}	0.20	0.36	0.49	0.30
RS_{26}	0.27	0.51	0.68	0.44
RS_{27}	0.19	0.28	0.52	0.17
RS_{28}	0.12	0.22	0.31	0.19
RS_{29}	0.13	0.23	0.32	0.20
RS_{30}	0.14	0.26	0.36	0.22
RS_{31}	0.10	0.18	0.26	0.15
Range	0.07- 0.29	0.13- 0.57	0.18- 0.80	0.11- 0.50
Total average	0.17	0.30	0.43	0.24

Hazard Indices for Alpha Radiation

The index dealing with the assessment of excess alpha radiation, due to radon inhalation originating from rock materials, is called alpha index or internal index (I_α) and has been developed in the following equation [3, 35]:

$$I_\alpha = \frac{C_U}{200} \,. \tag{8}$$

When the ^{238}U activity concentration of rock samples exceeds the value of 200 $Bqkg^{-1}$, it is possible that radon inhalation from this material could cause indoor radon concentrations exceeding 200 Bqm^{-3}. The recommended values of I_α, like I_γ, are below 0.5 and 1 [32]. The values of I_α ranged from 0.11- 0.50, with an average value of 0.24 (Table 4).These observed values are less than unity, showing that the rock materials are safe from the point of view of environmental radiation hazards.

Conclusions

The activity concentrations of ^{238}U, ^{232}Th and ^{40}K, as well as radium equivalent activity and gamma indices, were evaluated in rock samples in the Hebron region of Palestine, in order to assess the potential radiological hazards associated with building materials that are manufactured from those rocks. Such data is of value in determining the radioactivity content of buildings and the possible radiological risks associated with these structures. The variations and the spread in the data measured are a reflection of the different geological origins of the raw materials.

The results of the presented study show that the activity concentrations of ^{238}U, ^{232}Th and ^{40}K

in several samples are within the range of limit values, except some samples collected from the Tafuh and Dura sites. The average Ra_{eq} values of the studied samples are below the internationally accepted value (370 $Bqkg^{-1}$). The calculated total annual effective dose of all rock samples was lower than 70 μSvy^{-1}. As such, this study shows that the analyzed rocks (except some samples collected from Tafuh and Dura sites) do not pose any significant source of radiation hazard and are safe for use in the construction of dwellings.

Finally, one can conclude that rock materials in the Hebron region of Palestine are safe and that no health hazard effects exist to people living in the region under investigation.

References

[1] Arman, E., Turk. J. Med. Sci., 37 (2007) 199.

[2] Laith, A., Nada, F. and Fouzey, H., Australian J. of Basic and Applied Sci., 7 (2013) 56.

[3] Simin, M., Reza, F. and Sedigheh, S., NUKLEONIKA, 56 (2011) 363.

[4] Okedeyi, A., Gbadebo, A., Arowolo, T., Mustapha, A. and Tchokossa, P., J. of Appl. Sci., 12 (2012) 2178.

[5] Ferdoas, S. Al–Saleh and Al-Berzan, B., J. of Nuclei. and Radia. Phys., 2 (2007) 25.

[6] Savidou, A., Raptis, C. and Kritidis, P., Environ. Radioactivity, 31 (1996) 21.

[7] Thabayneh, K., Arab J. of Nuclear Sci. and Applic., 40 (2007) 207.

[8] Thabayneh, K., Sroor, A. and Abdel-Haleem, S., Al-Quds Univ. J. for Research and Studies, 12 (2008) 23.

[9] Thabayneh, K., Mashal, L. and Hasan, F., Rad. Prot. Dos., 131 (2008) 265.

[10] Thabayneh, K., Hebron University Research J. A (Natural Science), 3 (2008) 49.

[11] Thabayneh, K. and Jazzar, M., Open J. of Soil Science, 2 (2012) 7.

[12] Abu Samreh, M., Thabayneh, K. and Khrais, F., Turkish J. Eng. Env. Sci., 38 (2014) 113.

[13] Thabayneh, K. and Jazzar M., Rad. Prot. Dos., 153 (2013) 467. doi:10.1093/rpd/ncs122.

[14] Thabayneh, K., Arab J. Sci. Eng., 38 (2013) 201.

[15] Palestinian Central Bureau of Statistics (PCBS). Population, Housing and Establishment Census 2011. Ramallah – Palestine (2012).

[16] Applied Research Institute – Jerusalem (ARIJ). GIS Database. Spanish Cooperation and Azahar Program, Palestinian Localities Study-Hebron Governorate (2009).

[17] Dudeen, B., Bari: CIHEAM., 34 (2001) 203.

[18] UNSCEAR (2000). Sources and effects of ionizing radiation. Report to General Assembly, with Scientific Annexes. United Nations, New York (2000).

[19] Michalis, T., Haralabos, T., Stelios, C. and George, C., J. of Environ. Radio. 70 (2003) 223.

[20] Anjos, R. et al., Eur. J. Phys., 25 (2004) 133.

[21] Ahmed, N., Abbady, A., El Arabi, A., Michel, R., Kamel, A. and Abbady, A.G., Indian J. of Pure and Applied Physics, 44 (2006) 209.

[22] Kinyua, R., Atambo, V. and Ongeri, R., African J. of Environ. Sci. and Tech., 5 (2011) 682.

[23] Keser, R., Korkmaz, F., Alp, İ. and Okumusoğlu, N., Int. J. Radiat. Res., 1 (2013) 155.

[24] Abbasi, A. and Mirekhtiary, F., World Academy of Science, Engineering and Technology, 52 (2001) 667.

[25] Ali, A. Ahmed, Mohammed, I. and Hussein, A., World Academy of Science, Engineering and Technology, 74 (2011) 132.

[26] Al–Zahrani, J., Al-Harbi, W. and Abbady, G., Australian J. of Basic and Applied Sciences, 5 (2011) 683.

[27] Manjunatha, S., Jayasheelan, A. and Venkataramanaiah, P., Int. J. Radiat. Res., 11(2013) 183.

[28] Harb, S., El-Kamel, A., Abd El-Mageed, A., Abbady, A. and Rashed, W., IOSR J. of Applied Phys. (IOSR-JAP), 6 (2014) 40.

[29] Harb, S., El-Kamel, A., Zahran, A., Abbady, A. and Ahmed, F., IOSR J. of Applied Phys. (IOSR-JAP), 5(2014) 39.

[30] Manigandan, P. and Natrajan, K., International J. of Students Research in Technology and Management, 2 (2014) 103. http://www.giapjournals.org/ijsrtm.html

[31] Beretka, J. and Mathew, P., Health Phys., 48 (1985) 87.

[32] European Commission (EC) (199. Radiation Protection 112). Brussels, European Commission (1999).

[33] Rafique, M., Rehman, H., Matiullah, M.F., Rajput, M., Rahman, S. and Rathore, M., Iran. J. Radiat. Res., 9 (2011) 77.

[34] Anjos, R. et al., Radiation Measurement, 39 (2005) 245.

[35] Stoulos, S., Manolopoulou, M. and Papastefanou, C., J. Environ. Radioactivity, 69 (2003) 225.

Volume 9, Number 1, 2016. pp. 65-70

Jordan Journal of Physics

ARTICLE

The Study of Zero-Spin Isotopes with the Modified Manning-Rosen Potential by Relativistic Cluster Models

Mohammad Reza Shojaei

Department of Physics, Shahrood University of Technology, P.O. Box 36155-316, Shahrood, Iran.

Received on: 29/3/2016; Accepted on: 26/5/2016

Abstract: In this paper, we studied the zero-spin isotopes with N=Z and A=4n in relativistic cluster models as a system which can be considered to be composed of α-particles. For interaction between the clusters, we use modified Manning-Rosen potentials and solve the relativistic Klein-Gordon (KG) equation using the Nikiforov-Uvarov (NU) method to calculate the energy spectrum. We found the ground state energy and the first excited energy. Finally, the calculated results are compared with the experimental data for light nuclei, such as ^{8}Be, ^{12}C and ^{16}O. The results show that the modified Manning-Rosen (MR) potential is adaptable for cluster interactions.

PACS codes: 21.60.Gx.

Keywords: Zero-spin isotopes, Modified MR potential, KG equation, Cluster model.

1. Introduction

One of the fundamental models of nuclear structure is the cluster model which has a long history [1]. Cluster interpretation is a suitable model to describe nuclear states and has been successful in reproducing energy spectra and other nuclear properties, such as electro-magnetic properties, α-emission widths and α-particle elastic scattering data in nuclei near the double closed shell. In 1936, when Bethe predicted that nuclei are made of alpha particles and proposed a geometrical arrangement of alpha particles inside nuclei, the cluster model was introduced [2]. In 1937, Wheeler [3] extended this work, and similar models were suggested concurrently by Wefelmeier [4], Weizsacker [5] and Fano [6]. Freer and Merchant, in 1997, studied the role of clustering and cluster models in nuclear reactions and examined the evidence for α-cluster chain configurations in the light even - even nuclei from ^{8}Be to ^{28}Si [7]. Recently, several systems of even-even nuclei were studied with a cluster model and their results were reasonably compared to the experimental spectra for ground state and some excited states [7-12]. The alpha particle, ^{4}He nucleus, is the most common cluster which is exceptionally stable (its first excited state is 20.2 MeV [13]), and its binding energy is 7.07 MeV/nucleon. It is also very compact (a charge radius of 1.673fm [14]), and has zero-spin for all quantum numbers (spin and isospin), which makes it easy to combine into larger systems. Also, it is the first doubly magic nucleus with the first closed shell $1S_{1/2}$, which accounts for its exceptional stability. Also, in nuclear and high energy physics, particles are in a strong potential field, and for studying the internal structure of any quantum mechanical systems, such as nuclei, the relativistic effect must be considered. In relativistic quantum mechanics, one can apply the KN equation to the treatment of a zero-spin particle, such as the alpha particle and the Dirac equation for the spin half particle. The KN equation is frequently used to describe the particle dynamics, and in recent years, many studies have been carried out to explore the relativistic energy Eigen-values and

Corresponding Author: Mohammad Reza Shojaei **Email**: shojaei.ph@gmail.com

corresponding wave functions of the KN equation [15-18]. Hence, in this article, we study the light nuclei in the relativistic cluster model and solve the KN equation for the isotopes with N=Z and A=4n (n=2, 3, 4 …) as a system which can be considered to be composed of α-particles.

Modeling the effective interaction among clusters is very important. The cluster-core interaction leads to the identification of clustering in the nuclear matter and the description of clustering phenomenon in various nuclei. In 1960s, Ali and Bodmer used the experimental data on alpha-alpha scattering and obtained potentials which were fitted to the scattering phase shifts [19, 20]. During the past decade, the modified phenomenological Saxon-Woods plus Cubic Saxon-Woods cluster potential has successfully described various phenomena related to alpha clustering in light as well as even-even heavy nuclei [21, 22]. Prior to the development of the Saxon-Woods plus Cubic Saxon-Woods potential form, such a microscopic interaction has been employed in various forms to describe cluster bound states in light nuclei [23] and exotic decays in heavy nuclei [22]. Despite its success, the modified Saxon-Woods potential model tells us very little about the microscopic nature of clustering in closed shell nuclei.

The MR potential is one of the most useful and convenient models for studying the energy Eigen-values. It also gives an excellent description of the interaction between the two atoms in a diatomic molecule and constitutes a convenient model for other physical situations in term of their bound states and scattering properties. So, in our work, we offer the modified Manning-Rosen potential as a reasonable potential to study nuclear structure in cluster model, due to some similarity of multi-atomic molecules to multi-alpha-cluster nuclei. The short range Manning-Rosen potential is given by [24-29]:

$$V(r)=\frac{-A\hbar^2}{2\mu b^2}\frac{e^{-r/b}}{1-e^{-r/b}}+\frac{\alpha(\alpha-1)\hbar^2}{2\mu b}\left[\frac{e^{-r/b}}{1-e^{-r/b}}\right]^2, \quad (1)$$

where A and α are dimensionless parameters, while b is the screening parameter which has the dimension of length. Our modified Manning-Rosen potential is:

$$\left.\begin{aligned} V_{M.}(r)=&\frac{-A\hbar^2}{2\mu b^2}\frac{e^{-r/b}}{1-e^{-r/b}}\\ &+\frac{\alpha(\alpha-1)\hbar^2}{2\mu b}\left[\frac{e^{-r/b}}{1-e^{-r/b}}\right]^2+\frac{k}{r^2}\end{aligned}\right\}, \quad (2)$$

where k is the coulomb repulsion potential coefficient between the clusters.

In section two, we solve the KN equation to find the Eigen-values and Eigen-functions with the modified Manning-Rosen Potential. Then, in section three, we examine the results for some isotopes. At the end, conclusions are given in section four.

2. The Eigen-values and Eigen-Functions with the Manning-Rosen Potential for Nα–Body System

The many-body forces are more easily introduced and treated within the hyperspherical harmonics formalism. Now, we consider a system of identical α particles. The D-dimensional time-independent arbitrary l-state radial KN equation with scalar and vector potentials S(r) and V (r), respectively, where r = |r| describing a spinless particle, such as α-particle, takes the general form [30-32]:

$$\left.\begin{aligned}&\nabla_D^2\psi_{l_1\ldots l_{D-2}}^{(l_{D-1}=l)}(r)\\ &+\frac{1}{\hbar^2c^2}\left\{\begin{aligned}&\left[E_{nl}-V(r)\right]^2-\\ &\left[Mc^2+S(r)\right]^2\end{aligned}\right\}\psi_{l_1\ldots l_{D-2}}^{(l_{D-1}=l)}(r)\\ &=0,\end{aligned}\right\} \quad (3)$$

where E_{nl}, M and ∇_D^2 denote the KG energy, the mass and the D-dimensional Laplacian, respectively. If the scalar and vector potentials S (r_{ij}) and V (r_{ij}) are a two-body potential of interaction, so we can expand them in the hyperspherical harmonics formalism. We define a set of the Jacobi coordinates for r_{ij}, where $\vec{r}_{ij}=\vec{r}_i-\vec{r}_j$ [34]:

$$x^2=\sum_{i=1}^{N-1}(r_i-R)^2=\frac{2}{N-1}\sum_{k,l>k}r_{kl}^2, \; R=\frac{1}{N}\sum_i^N r_i. \quad (4)$$

The center of mass R eliminates using the Jacobi coordinates. In addition, x is a D-dimensional position vector in Jacobi coordinates. Therefore, by choosing a common ansatz for the wave function in the form:

$$R_l(x)=x^{-(D-1)/2}u_l(x), \tag{5}$$

Eq. (3) reduces to the form shown below and KG equation turns into a Schrödinger-like equation. Thus, the bound state solutions are very easily obtained with the NU method [35-37]:

$$\left.\begin{array}{l}\dfrac{d^2u_l(x)}{dx^2}+\\ \dfrac{1}{\hbar^2c^2}\left\{\begin{array}{l}\left[E_{nl}-V(x)\right]^2-\\ \left[Mc^2+S(x)\right]^2-\\ \dfrac{(D+2l-1)(D+2l-3)}{4x^2}\end{array}\right\}u_l(x)\\ =0.\end{array}\right\} \tag{6}$$

By replacing C = A and $D=-A-\alpha(\alpha-1)$, the modified MR potential can be written in the following simple form:

$$V_{M.}(x)=-\frac{Ce^{-x/b}+De^{-2x/b}}{(1-e^{-x/b})^2}+\frac{k}{x^2}\ . \tag{7}$$

Under the equally mixed potentials *S(r)* = *V(r)* and using Eq. (7), we obtain:

$$\left.\begin{array}{l}\dfrac{d^2u_l(x)}{dx^2}+\\ \dfrac{1}{\hbar^2c^2}\left(\begin{array}{l}E_{nl}^2-m^2c^4-\\ 2(E_{nl}-mc^2)(-\dfrac{\hbar^2}{2\mu b^2}(\dfrac{Ce^{-x/b}+De^{-2x/b}}{(1-e^{-x/b})^2}))\\ -\dfrac{(D+2l-1)(D+2l-3)-4k}{4x^2}\end{array}\right)u_l(x)\\ =0.\end{array}\right\} \tag{8}$$

The good approximation for the kinetic energy term $((D+2l-1)(D+2l-3)-4k)/4x^2$ in the centrifugal barrier is taken as [37-39]:

$$\frac{1}{x^2}\approx\frac{1}{b^2}\frac{e^{-x/b}}{(1-e^{-x/b})^2}\ . \tag{9}$$

To obtain the following hypergeometric equation, we substitute Eq. (9) into Eq. (8) and make change of the variables $x\rightarrow z$, $z=e^{-x/b}$, through the mapping function $x=f(z)$:

$$\left.\begin{array}{l}\dfrac{d^2R(z)}{dz^2}+\\ \dfrac{(1-z)}{z(1-z)}\dfrac{d}{dz}+\\ \dfrac{b^2}{\hbar^2c^2}\left[\dfrac{\left\{\begin{array}{l}(E_{nl}^2-m^2c^4)(1-z^2)\\ -2(E_{nl}-mc^2)(Cz+Dz^2)\end{array}\right\}}{z^2(1-z)^2}\right]R(z)\\ -\dfrac{1}{4\hbar^2c^2}\left[\dfrac{(D+2l-1)(D+2l-3)-4k}{z^2(1-z)^2}\right]R(z)\\ =0.\end{array}\right\} \tag{10}$$

By using Nikiforov-Uvarov method, we obtain the Eigen-values and Eigen-functions as follows [35-37]:

$$\left.\begin{array}{l}n+(2n+1)\left(\dfrac{0.5+\sqrt{\xi_3}+}{\sqrt{1/4+\xi_1+\xi_3-\xi_2}}\right)\\ +n(n-1)-\xi_2+2\xi_3\\ +2\sqrt{\xi_3(1/4+\xi_1+\xi_3-\xi_2)}\\ =0,\end{array}\right\} \tag{11}$$

and:

$$\left.\begin{array}{l}R(z)=\\ \quad z^{\sqrt{\xi_3}}\times(1-z)^{0.5+\sqrt{1/4+\xi_1+\xi_3-\xi_2}}\times\\ \quad P_n^{(2\sqrt{\xi_3},1+\sqrt{\xi_3}+\sqrt{1/4+\xi_1+\xi_3-\xi_2})}\times(1-2z)\end{array}\right\}, \tag{12}$$

where:

$$\xi_1=\frac{b^2}{\hbar^2c^2}\left[m^2c^4-E_{nl}^2+2(mc^2-E_{nl})D\right] \tag{13}$$

$$\xi_2=\frac{-b^2}{\hbar^2c^2}\left[\begin{array}{l}2(E_{nl}^2-m^2c^4)\\ +2(mc^2-E_{nl})C\\ -\dfrac{1}{4b^2}[(D+2l-1)(D+2l-3)\\ -4k]\end{array}\right] \tag{14}$$

$$\xi_3 = \frac{b^2}{\hbar^2 c^2}(m^2c^4 - E_{nl}^2). \tag{15}$$

The wave function that is obtained by Eq.12 is according to the boundary conditions for all the isotopes in the alpha cluster model. In the next section, we study ground state and first excited state energy for various combinations of light α- cluster nuclei.

3. Examples of Clustering

3.1. Example ^{8}Be

In our study, the simplest case is that of the two α-particle system ^{8}Be which would have a dumbbell shape and be a two-body system. Ikeda predicted that cluster structures are most obvious at an excitation which coincides with a particular decay threshold [40]. Experiments show that alpha + alpha cluster structure is found in the ground state of ^{8}Be, because it has a lifetime of ~ 10^{-16} s. The binding energy of ^{8}Be is -57.75 MeV and its ground state is unbound to 2α decay by 92 keV. It has a first excited 2^+ state at -53.27 MeV with a width of 1.51 MeV, as well as a 4^+ state at -46.6 MeV with a width of 3.5 MeV. These three states have an energy separation which is consistent with a rotational behavior given by $\hbar^2 j(j+1)/2\boldsymbol{I}$, where $\boldsymbol{I}$ is the moment of inertia. The calculated value for the moment of inertia is consistent with the picture of two touching α–particles; an essentially super-deformed nucleus [9-41].

With the picture of two touching α-particles and the use of the modified Manning-Rosen potential between them, we reproduce the spectrum of the ground state and the first excited state by Eq.11. Results are shown in Table 1 and compared with experimental data. It appears that our result have good agreement with the experimental results.

TABLE 1. The spectrum of the energy levels in ^{8}Be.

Levels	E_{cal}(MeV)	E_{exp}(MeV)
Ground state	-57.75	-56.50
First excited state	-53.27	-53.47

3.2. Example ^{12}C

The structure of "Hoyle" state; the first excited 0^+ state at -84.51 MeV in ^{12}C isotope is influenced by clustering or by symmetries thereof. So, the system can be constructed from a variety of geometric arrangements of three-alpha particles. It might be expected that the compact equilateral-triangle arrangement is the lowest energy configuration [8-42].

In the case of ^{12}C, the structure of the ground state is influenced by clustering or by symmetries thereof. So, the system can be constructed from a variety of geometric arrangements of three-alpha particles. It might be expected that the compact equilateral-triangle arrangement is the lowest energy configuration [43]. Hence, three identical body forces of the internal particle motion are described in terms of the Jacobi relative coordinates ρ, λ and R; center of mass. In the theory of many-particle systems, Jacobi coordinates often are used to simplify the mathematical formulation. Now, we can introduce the hyper-radius quantity x and the hyper-angle ξ as follows [33- 43]:

$$x = \sqrt{\rho^2 + \lambda^2} \quad \xi = \tan\left(\frac{\rho}{\lambda}\right), \tag{16}$$

where:

$$\rho = \frac{\vec{r}_1 - \vec{r}_2}{\sqrt{2}}, \; \lambda = \frac{\vec{r}_1 + \vec{r}_2 - 2\vec{r}_3}{\sqrt{6}}, \; R = \frac{\vec{r}_1 + \vec{r}_2 + \vec{r}_3}{\sqrt{3}}. \tag{17}$$

$\vec{r}_1$, $\vec{r}_2$ and $\vec{r}_3$ are the relative positions of the three particles. We solved the KN equation in new coordinates, similar to the previous ones. We found the best values of **b**, **α**, **A** and **k** by fitting to the experimental data at Hoyle state that has the cluster structure. Then, we calculated the approximate ground state energy and the first excited energy (in MeV). The results are shown in Table 2 for the ^{12}C isotope.

TABLE 2. The spectrum of the energy levels in ^{12}C.

Levels	E_{cal}(MeV)	E_{exp}(MeV)
Ground state	-92.61	-92.16
First excited state	-88.01	-87.72

The binding energy of ^{12}C is -92.16 MeV and in our model, we obtain a value of -92.61MeV. For the first excited state, our result is -88.01 MeV which is near to the experimental data.

3.3. Example ^{16}O

The ^{16}O isotope possesses the second closed shell $1P_{1/2}$, but not quite the degree of inertness of the α- particle. The Ikeda diagram suggests that ^{16}O has a ^{12}C + alpha structure at an excitation energy of around -120.46 MeV and a four-alpha particle structure at an excitation energy of around -113.18 MeV [40]. The experimental evidence supports the Ikeda model too. The experimental moments of inertia can be related back to shapes and alpha cluster configurations suggested by the moment of inertia calculations. These calculations do not rule out the possibility that the nucleus maintains a homogeneous composition throughout the deformed shape. However, the subsequent decay into two ^{8}Be, believed to have a 2α–cluster structure, and from there into four ^{4}He, supports the idea of four-alpha clusters [44].

TABLE 3. The spectrum of the energy levels ^{16}O

Levels	E_{cal}(MeV)	E_{exp}(MeV)
Ground state	-127.89	-127.62
First excited state	-121.84	-121.57

Now, we give in Table 3 a summary of our results for cluster states in ^{16}O nuclei obtained using our potential of Eq.6 in Jacobi coordinates.

The values of the ground state energy and the first excited energy are -127.62 MeV and -121.57 MeV, respectively, while we calculated them to be -127.89 MeV and -121.84 MeV, respectively.

4. Conclusions

In the present paper, we studied the light – α cluster (N=Z) nucleus. We selected the modified Manning – Rosen potential between the alpha clusters regardless of the internal structure of them. By solving the Klein Gordon equation in D-dimensions space using the Jacobi coordinates and NU method for our potential, we found the Eigen-values and Eigen-functions, generally. Then, we examined the results for ^{8}Be, ^{12}C and ^{16}O. Results for the ground state and the first excited state in the studied isotopes showed good agreement with the experimental data.

Acknowledgement

This research was supported by the research grant of Shahrood University of technology.

References

[1] Brink, D.M., J. Phys. Conf. Ser., 111 (2008) 012001.

[2] Bethe, H.A., Phys. Rev., 53 (1938) 842.

[3] Wheeler, J.A., Phys. Rev., 52 (1937) 1083.

[4] Wefelmeier, W.Z., Physik, 107 (1937) 332.

[5] Von Weizsäcker, C.F., Naturwiss., 26 (1938) 209.

[6] Fano, U., Naturwiss., 25 (1937) 602.

[7] Freer, M. et al., J. Phys. G, 23 (1997) 206.

[8] Freer, M., Scholarpedia, 5 (2010) 9652.

[9] Freer, M. et al., Phys. Rev. C, 83 (2011) 034314.

[10] Y'epez-Mart'nez, H. et al., Phys. Rev. C, 86 (2012) 034309.

[11] Y'epez-Mart'nez, H. et al., Phys. Rev. C, 85 (2012) 014316.

[12] Fraser, P.R. et al., Phys. Rev. C, 85 (2012) 014317.

[13] Tilley, D.R., Weller, H.R. and Hale, G.M., Nucl. Phys. A, 541 (1992) 1.

[14] Borie, E. and Rinker, G.A., Phys. Rev. A, 18 (1978) 324.

[15] Ikot, A.N., Akpabio, L.E. and Uwah, E.J., E. J. T. P., 8 (2011) 225.

[16] Chen, G., Diao, Y.F. and Jia, C.S., Phys. Scr., 79 (2009) 065014.

[17] Yasuk, F., Durmus, A. and Boztosun, I., J. Maths. Phys., 47 (2006) 082302.

[18] Ikot, A.N., Udoimuk, A.B. and Akpabio, L.E., Am. J. Sci. Ind. Res., 2 (2011) 179.

[19] Kanada-En'yo, Y., Prog. Theor. Phys., 117 (2007) 655.

[20] Ali, S. et al., Nucl. Phys., 80 (1966) 99.

[21] Wyngaardt, S.M. et al., J. Phys. Conf. Ser., 205 (2010) 012013.

[22] Buck, B. et al., Phys. Rev. C, 39 (1989) 2097.

[23] Buck, B. et al., Phys. Rev. C, 11 (1975) 1803.

[24] Qiang, W.C. and Dong, S.H., Phys. Lett. A, 368 (2007) 13.

[25] Diaf, A., Chouchaoni, A. and Lombard, R.L., Ann. Phys. (Paris), 317 (2005) 354.

[26] Qiang, W.C., Li, K. and Chen, W.L., J. Phys. A: Math. Theor., 42 (2009) 205306.

[27] Manning, M.F. and Rosen, N., Phys. Rev., 44 (1933) 953.

[28] Pekeris, C.L., Phys. Rev., 45 (1934) 98.

[29] Bayrak, O. and Boztosun, I., J. Phys. A: Math. Gen., 39 (2006) 6955.

[30] Qiang, W.C. and Dong, S.H., Phys. Lett. A, 363 (2007) 169.

[31] Ikhdair, S.M., J. Q. I. Sci., 1 (2006) 73.

[32] Rajabi, A.A. and Shojaei, M.R., Int. J. Phys. Sci., 6 (2011) 33.

[33] Rjabi, A.A., Few-Body Syst., 37 (2006) 267.

[34] Miranda, M.G., Sun, G.H. and Dong, S.H., Int. J. Mod. Phys. E, 19 (2010) 123.

[35] Sever, T.C., R. Int. J. Theor. Phys., 48 (2009) 337.

[36] Shojaei, M.R. and Mousavi, M., Int. J. Phys. Sci., 10 (2015) 324.

[37] Greene, R.L. and Aldrich, C., Phys. Rev. A, 14 (1976) 2363.

[38] Qiang, W.C. and Dong, S.H., Phys. Lett. A, 368 (2007) 13.

[39] Ikhdair, S.M. and Sever, R., Ann. Phys., 17 (2008) 897.

[40] Ikeda, K., Tagikawa, N. and Horiuchi, H., Prog. Theor. Phys., 464 (1968).

[41] Freer, M. et al., Phys. Rev. C, 86 (2012) 034320.

[42] Freer, M. et al., Phys. Rev. C, 76 (2007) 034320.

[43] Shojaei, M.R. et al., Mod. Phys. Lett. A, 23 (2008) 267.

[44] Freer, M. et al., Phys. Rev. C, 70 (2004) 064311.

Authors Index

Subject Index

المراجع: يجب طباعة المراجع بأسطر مزدوجة ومرقمة حسب تسلسلها في النص. وتكتب المراجع في النص بين قوسين مربعين. ويتم اعتماد اختصارات الدوريات حسب نظام Wordlist of Scientific Reviewers.

الجداول: تعطى الجداول أرقاما متسلسلة يشار إليها في النص. ويجب طباعة كل جدول على صفحة منفصلة مع عنوان فوق الجدول. أما الحواشي التفسيرية، التي يشار إليها بحرف فوقي، فتكتب أسفل الجدول.

الرسوم التوضيحية: يتم ترقيم الأشكال والرسومات والرسومات البيانية (المخططات) والصور، بصورة متسلسلة كما وردت في النص.

تقبل الرسوم التوضيحية المستخرجة من الحاسوب والصور الرقمية ذات النوعية الجيدة بالأبيض والأسود، على ان تكون أصيلة وليست نسخة عنها، وكل منها على ورقة منفصلة ومعرفة برقمها بالمقابل. ويجب تزويد المجلة بالرسومات بحجمها الأصلي بحيث لا تحتاج إلى معالجة لاحقة، وألا تقل الحروف عن الحجم 8 من نوع Times New Roman، وألا تقل سماكة الخطوط عن 0.5 وبكثافة متجانسة. ويجب إزالة جميع الألوان من الرسومات ما عدا تلك التي ستنشر ملونة. وفي حالة إرسال الرسومات بصورة رقمية، يجب أن تتوافق مع متطلبات الحد الأدنى من التمايز (1200 dpi Resolution) لرسومات الأبيض والأسود الخطية، و 600 dpi للرسومات باللون الرمادي، و300 dpi للرسومات الملونة. ويجب تخزين جميع ملفات الرسومات على شكل (jpg)، وأن ترسل الرسوم التوضيحية بالحجم الفعلي الذي سيظهر في المجلة. وسواء أرسل المخطوط بالبريد أو عن طريق الشبكة (Online)، يجب أرسال نسخة ورقية أصلية ذات نوعية جيدة للرسومات التوضيحية.

مواد إضافية: تشجع المجلة الباحثين على إرفاق جميع المواد الإضافية التي يمكن أن تسهل عملية التحكيم. وتشمل المواد الإضافية أي اشتقاقات رياضية مفصلة لا تظهر في المخطوط.

المخطوط المنقح (المعدَل) والأقراص المدمجة: بعد قبول البحث للنشر وإجراء جميع التعديلات المطلوبة، فعلى الباحثين تقديم نسخة أصلية ونسخة أخرى مطابقة للأصلية مطبوعة بأسطر مزدوجة، وكذلك تقديم نسخة إلكترونية تحتوي على المخطوط كاملا مكتوبا على Microsoft Word for Windows 2000 أو ما هو استجد منه. ويجب إرفاق الأشكال الأصلية مع المخطوط النهائي المعدل حتى لو تم تقديم الأشكال إلكترونيا. وتخزن جميع ملفات الرسومات على شكل (jpg)، وتقدم جميع الرسومات التوضيحية بالحجم الحقيقي الذي ستظهر به في المجلة. ويجب إرفاق قائمة ببرامج الحاسوب التي استعملت في كتابة النص، وأسماء الملفات على قرص مدمج، حيث يعلَم القرص بالاسم الأخير للباحث، وبالرقم المرجعي للمخطوط للمراسلة، وعنوان المقالة، والتاريخ. ويحفظ في مغلف واقٍ.

الفهرسة: تقوم المجلة الأردنية للفيزياء بالإجراءات اللازمة لفهرستها وتلخيصها في جميع الخدمات الدولية المعنية.

حقوق الطبع

يُشكِّل تقديم مخطوط البحث للمجلة اعترافاً صريحاً من الباحثين بأنَ مخطوط البحث لم يُنْشَر ولم يُقَدَّم للنشر لدى أي جهَة أخرى كانت وبأي صيغة ورقية أو إلكترونية أو غيرها. ويُشترط على الباحثين ملء أنموذج يَنُصُ على نقْل حقوق الطبع لتُصبح ملكاً لجامعة اليرموك قبل الموافقة على نشر المخطوط. ويقوم رئيس التحرير بتزويد الباحثين بإنموذج نقْل حقوق الطبع مع النسخة المُرْسَلَة للتنقيح. كما ويُمنع إعادة إنتاج أيِّ جزء من الأعمال المنشورة في المجلَة من دون إذن خَطِّيٍّ مُسْبَق من رئيس التحرير.

إخلاء المسؤولية

إن ما ورد في هذه المجلة يعبر عن آراء المؤلفين، ولا يعكس بالضرورة آراء هيئة التحرير أو الجامعة أو سياسة اللجنة العليا للبحث العلمي أو وزارة التعليم العالي والبحث العلمي. ولا يتحمل ناشر المجلة أي تبعات مادية أو معنوية أو مسؤوليات عن استعمال المعلومات المنشورة في المجلة أو سوء استعمالها.

معلومات عامة

المجلة الأردنية للفيزياء هي مجلة بحوث علميّة عالمية متخصصة مُحكمة تصدر بدعم من صندوق دعم البحث العلمي، وزارة التعليم العالي والبحث العلمي، عمان، الأردن. وتقوم بنشر المجلة عمادة البحث العلمي والدراسات العليا في جامعة اليرموك، إربد، الأردن. وتنشر البحوث العلمية الأصيلة، إضافة إلى المراسلات القصيرة Short Communications، والملاحظات الفنية Technical Notes، والمقالات الخاصّة Feature Articles، ومقالات المراجعة Review Articles، في مجالات الفيزياء النظرية والتجريبية، باللغتين العربية والإنجليزية.

تقديم مخطوط البحث

تقدم البحوث عن طريق إرسالها إلى البريد الإلكتروني : jjp@yu.edu.jo

تقديم المخطوطات إلكترونيًا: اتبع التعليمات في موقع المجلة على الشبكة العنكبوتية.

ويجري تحكيمُ البحوثِ الأصيلة والمراسلات القصيرة والملاحظات الفنية من جانب مُحكِّمين اثنين في الأقل من ذوي الاختصاص والخبرة. وتُشَجِّع المجلة الباحثين على اقتراح أسماء المحكمين. أما نشر المقالات الخاصّة في المجالات الفيزيائية النَشِطَة، فيتم بدعوة من هيئة التحرير، ويُشار إليها كذلك عند النشر. ويُطْلَب من كاتب المقال الخاص تقديم تقرير واضح يتَسم بالدقة والإيجاز عن مجال البحث تمهيداً للمقال. وتنشر المجلةُ أيضاً مقالات المراجعة في الحقول الفيزيائية النشطة سريعة التغيُر، وتُشَجَع كاتبي مقالات المراجعة أو مُستَكتبيها على إرسال مقترحٍ من صفحتين إلى رئيس التحرير. ويُرْفَق مع البحث المكتوب باللغة العربية ملخص (Abstract) وكلمات دالة (Keywords) باللغة الإنجليزية.

ترتيب مخطوط البحث

يجب أن تتم طباعة مخطوط البحث ببنط 12 نوعه Times New Roman، وبسطر مزدوج، على وجه واحد من ورق A4 (21.6 × 27.9 سم) مع حواشي 3.71 سم ، باستخدام معالج كلمات ميكروسوفت وورد 2000 أو ما استَجَد منه. ويجري تنظيم أجزاء المخطوط وفق الترتيب التالي: صفحة العنوان، الملخص، رموز التصنيف (PACS)، المقدّمة، طرق البحث، النتائج، المناقشة، الخلاصة، الشكر والعرفان، المراجع، الجداول، قائمة بدليل الأشكال والصور والإيضاحات، ثَمَّ الأشكال والصور والإيضاحات. وتُكْتَب العناوين الرئيسة بخطٍ **غامق**، بينما تُكْتَب العناوين الفرعية بخطٍ *مائل*.

صفحة العنوان: وتشمل عنوان المقالة، أسماء الباحثين الكاملة وعناوين العمل كاملة. ويكتب الباحث المسؤول عن المراسلات اسمه مشارا إليه بنجمة، والبريد الإلكتروني الخاص به. ويجب أن يكون عنوان المقالة موجزا وواضحا ومعبرا عن فحوى (محتوى) المخطوط، وذلك لأهمية هذا العنوان لأغراض استرجاع المعلومات.

الملخص: المطلوب كتابة فقرة واحدة لا تزيد على مائتي كلمة، موضحة هدف البحث، والمنهج المتبع فيه والنتائج وأهم ما توصل إليه الباحثون.

الكلمات الدالة: يجب أن يلي الملخص قائمة من 4-6 كلمات دالة تعبر عن المحتوى الدقيق للمخطوط لأغراض الفهرسة.

PACS: يجب إرفاق الرموز التصنيفية، وهي متوافرة في الموقع http://www.aip.org/pacs/pacs06/pacs06-toc.html.

المقدمة: يجب أن توضّح الهدف من الدراسة وعلاقتها بالأعمال السابقة في المجال، لا أن تكون مراجعة مكثفة لما نشر (لا تزيد المقدمة عن صفحة ونصف الصفحة مطبوعة).

طرائق البحث (التجريبية / النظرية): يجب أن تكون هذه الطرائق موضحة بتفصيل كاف لإتاحة إعادة إجرائها بكفاءة، ولكن باختصار مناسب، حتى لا تكون تكرارا للطرائق المنشورة سابقا.

النتائج: يستحسن عرض النتائج على صورة جداول وأشكال حيثما أمكن، مع شرح قليل في النص ومن دون مناقشة تفصيلية.

المناقشة: يجب أن تكون موجزة وتركز على تفسير النتائج.

الاستنتاج: يجب أن يكون وصفا موجزا لأهم ما توصلت إليه الدراسة ولا يزيد عن صفحة مطبوعة واحدة.

الشكر والعرفان: الشكر والإشارة إلى مصدر المنح والدعم المالي يكتبان في فقرة واحدة تسبق المراجع مباشرة.

Subscription Form

Jordan Journal of

PHYSICS

An International Peer-Reviewed Research Journal issued by the Support of the Scientific Research Support Fund

Published by the Deanship of Research & Graduate Studies, Yarmouk University, Irbid, Jordan

Name: .... :الأسم

Specialty:... :التخصص

Address: .... :العنوان

P.O. Box:.. : صندوق البريد

City & Postal Code: .... :المدينة/الرمز البريدي

Country: .... :الدولة

Phone: .... :رقم الهاتف

Fax No:.. :رقم الفاكس

E-mail:.. :البريد الإلكتروني

No. of Subscription: .... :عدد الإشتراكات

Method of Payment:... :طريقة الدفع

Amount Enclosed:.. :المبلغ المرفق

Signature: .... :التوقيع

Cheques should be paid to Deanship of Research and Graduate Studies - Yarmouk University.

I would like to subscribe to the Journal
For

- One Year
- Two Years
- Three Years

One Year Subscription Rates

	Inside Jordan	Outside Jordan
Individuals	JD 8	€ 40
Students	JD 4	€ 20
Institutions	JD 12	€ 60

Correspondence

Subscriptions and Sales:

Prof. Nehad M. Tashtosh
Deanship of Research and Graduate Studies
Yarmouk University
Irbid – Jordan
Telephone: 00 962 2 711111 Ext. 2075
Fax No.: 00 962 2 7211121

المملكة الأردنية الهاشمية
جامعة اليرموك

المجلة الأردنية للفيزياء

مجلة بحوث علمية عالمية متخصصة محكّمة

تصدر بدعم من صندوق دعم البحث العلمي

المجلد (9)، العدد (1)، 2016م / 1437هـ

المجلة الأردنية

للفيزياء

مجلة بحوث علمية عالمية محكّمة

المجلد (9)، العدد (1)، 2016م / 1437هـ

المجلة الأردنية للفيزياء: مجلة علمية عالمية متخصصة محكَمة تصدر بدعم من صندوق دعم البحث العلمي، وزارة التعليم العالي والبحث العلمي، الأردن، وتصدر عن عمادة البحث العلمي والدراسات العليا، جامعة اليرموك، إربد، الأردن.

ترسل البحوث إلى العنوان التالي:

الأستاذ الدكتور نهاد محمد طشطوش
رئيس تحرير المجلة الأردنية للفيزياء
عمادة البحث العلمي والدراسات العليا، جامعة اليرموك
إربد ، الأردن
هاتف 00 962 2 7211111 **فرعي** 2075
E-mail: *jjp@yu.edu.jo* **Website**: *http://Journals.yu.edu.jo/jjp*